

Microbiome and ecology of a hot spring-microbialite system on the Trans-Himalayan Plateau

Chayan Roy¹, Moidu Jameela Rameez¹, Prabir Kumar Haldar¹, Aditya Peketi², Nibendu Mondal¹, Utpal Bakshi³, Tarunendu Mapder⁴, Prosenjit Pyne¹, Svetlana Fernandes², Sabyasachi Bhattacharya¹, Rimi Roy^{1,s}, Subhrangshu Mandal¹, William Kenneth O'Neill⁵, Aninda Mazumdar², Subhra Kanti Mukhopadhyay⁶, Ambarish Mukherjee⁷, Ranadhir Chakraborty⁸, John Edward Hallsworth⁵ and Wriddhiman Ghosh^{1*}

Addresses:

- ¹ Department of Microbiology, Bose Institute, P-1/12 CIT Scheme VIIM, Kolkata 700054, India.
- ² Gas Hydrate Research Group, Geological Oceanography, CSIR-National Institute of Oceanography, Dona Paula, Goa - 403004, India.
- ³ Microbiome Program, Center for Individualized Medicine, Mayo Clinic, Rochester, MN-55905, USA.
- ⁴ ARC CoE for Mathematical and Statistical Frontiers, School of Mathematical Sciences, Queensland University of Technology, Brisbane, QLD 4000, Australia.
- ⁵ Institute for Global Food Security, School of Biological Sciences, Queen's University Belfast, 19 Chlorine Gardens, Belfast, BT9 5DL, Northern Ireland.
- ⁶ Department of Microbiology, University of Burdwan, Burdwan, West Bengal 713104, India.
- ⁷ Department of Botany, University of Burdwan, Burdwan, West Bengal 713104, India.
- ⁸ Department of Biotechnology, University of North Bengal, Siliguri, West Bengal 734013, India.

Present Addresses:

- ^s Department of Botany, Jagannath Kishore College, Purulia - 723101, West Bengal, India.

* Correspondence: Email: wriman@jcbose.ac.in; Wriman@rediffmail.com

Phone: +91-33-25693246; Fax: +91-33-23553886

Abstract

Little is known about life in the boron-rich hot-springs of Trans-Himalayas. Here, we explore the geomicrobiology of a 4438-m-high spring which emanates ~70°C-water from a boratic microbialite called *Shivlinga*. Due to low atmospheric pressure, the vent-water is close to boiling-point and can entropically destabilize biomacromolecular systems. Starting from the vent, *Shivlinga*'s geomicrobiology was revealed along the thermal gradient of an outflow-channel, and a progressively-drying thermal gradient having no running-water; ecosystem constraints were then considered in relation to those of entropically-comparable environments. The spring-water chemistry and sinter mineralogy were dominated by borates, sodium, thiosulfate, sulfate, sulfite, sulfide, bicarbonate, and other macromolecule-stabilizing (kosmotropic) substances. Microbial diversity was high along both the hydrothermal gradients. Bacteria, Eukarya and Archaea constituted >98%, ~1% and <1% of *Shivlinga*'s microbiome, respectively. Temperature constrained the biodiversity at ~50°C and ~60°C, but not below 46°C. Along each water-transit, communities were dominated by *Aquificae/Deinococcus-Thermus*, then *Chlorobi/Chloroflexi/Cyanobacteria*, and finally *Bacteroidetes/Proteobacteria/Firmicutes*. Interestingly, sites of >45°C were inhabited by phylogenetic relatives of taxa for which laboratory grow this not known at >45°C. *Shivlinga*'s geomicrobiology highlights the possibility that the system's kosmotrope-dominated chemistry mitigates the biomacromolecule-disordering effects of the thermal-water via mechanisms analogous to kosmotrope-mediated mitigation of the chaotropy of MgCl₂-dominated brines.

Introduction

The microbial ecologies of habitats that are hydrothermal, or hypersaline, have been well-characterized, and can give insights into the origins of early life on Earth¹⁻³. Both chaotrope-rich hypersaline brines and high-temperature freshwater systems can entropically disorder the macromolecules of cellular systems, and are therefore analogous as microbial habitats⁴⁻⁷. Indeed, highly-chaotropic and hydrothermal habitats are comparable at various scales of biology: the biomacromolecule, cellular system, and functional ecosystem^{8,9}.

Chaotropic, hypersaline habitats include the MgCl₂-constrained ecosystems located at the interfaces of some of the stratified deep-sea hypersaline brines and their overlying seawater. Biophysical, culture-based, and metagenomic studies of the steep haloclines found at these interfaces have revealed that macromolecule-disordering (chaotropic) activities of MgCl₂ not only determine microbial community composition, but also limit Earth's functional biosphere^{5,7,10} in such locations, as *in situ* microbial communities stop functioning at 2.2-2.4 M MgCl₂ concentrations in the absence of any compensating ion (above these concentrations there is no evidence of cellular functions or life processes)⁵. While the biophysical activities of MgCl₂ (and other chaotropic solutes and hydrophobes) constrain the functionality of biomacromolecular systems (via mechanisms that are entropically analogous to the action of heat^{8,11,12}), a number of macromolecule-ordering (kosmotropic) solutes such as NaCl, proline, trehalose and ammonium sulfate, as well as low temperature, can stabilize, structure, and impart rigidity to biomacromolecules^{11,13-16}, and thereby mitigate against the inhibition of cellular systems by chaotropic agents^{5,7,17,18}. Accordingly, active microbial life thrives even in hypersaline brines of up to 2.50-3.03 M MgCl₂ when sodium or sulfate ions are also present^{5,7,10}. Likewise, for other macromolecule-disordering agents such as ethanol, diverse types of kosmotropic substance as well as low temperature have been reported to mitigate against the chaotropic stress¹⁷⁻¹⁹. Whereas chaotropy typically constrains cellular activity at temperatures > 10°C, chaotropes can promote metabolic activity at lower temperatures, thereby extending the growth windows for microbes under extreme cold^{6,19}.

Ecological studies of geographically distinct hydrothermal habitats²⁰⁻²⁶ have elucidated various aspects of *in situ* microbiology including diversity²⁷⁻³¹ and correlation of community structures/functions with temperature³²⁻³⁹. However, in relation to conditions which permit and/or constrain habitability, we currently know little about the geochemistry and biophysics of hot-spring systems, especially the ones discharging hot waters, which have neutral pH and are typically poor in sulfide, silicate and total dissolved solids but rich in sodium, boron, elemental sulfur and sulfate⁴⁰⁻⁴². The current study, based in the Puga geothermal area of eastern Ladakh (within the Trans-Himalayan

region, at the northern tip of India; see Supplementary Fig. 1 and Supplementary Note 1), focused on revealing the geomicrobiology of a sulfate- and boron-rich, silica-poor and neutral pH, hot spring originating from within a large chimney-shaped hydrothermal microbialite, known as *Shivlinga* (Fig. 1). This microbialite, which has formed via epithermal accretion of boratic and carbonatic hydrothermal minerals, is situated at an altitude of 4438 m, where the boiling point of water is approximately 85°C. The functional ecology of *Shivlinga*'s microbiome was elucidated via a sampling-microscopy-geochemistry-metagenomics-biophysics approach, which encompassed analyses of water from the vent, microbial mats along the spring-water transit/dissipation, and fresh mineral sinters precipitating on mat-portions growing near the margins of the water-flow. Microbial diversity, microbe-mineral assemblages, and geochemical and biophysical parameters were characterized along *Shivlinga*'s hydrothermal gradients (Fig. 1) so as to determine the factors constraining and promoting the microbiome. The chemical milieus of these hydrothermal gradients were found to be rich in kosmotropic (macromolecule-stabilizing) ions and so their ecology and biophysics were compared with those of the kosmotrope-compensated chaotropic haloclines.

Results

The boratic microbialite, *Shivlinga*

Shivlinga is a 35-cm tall microbialite that is several decades old according to residents of the closest village situated at the eastern end of the Puga valley (Fig. 1A, G). The abundance of microbial biomass on its surface and chemical composition of its mineral body (see below) suggest that *Shivlinga* has formed via precipitation of boratic minerals on lithifying microbial mats. Laminated, clotted or dendritic fabrics commonly found on stromatolites, thrombolites or dendrolites⁴³ were not encountered on *Shivlinga*'s mineral deposits. It is for this reason that *Shivlinga* was considered to be a microbialite, i.e. a microbe-mediated sedimentary rock-like mineral deposit with or without defined internal fabrics⁴³. The near-circular flat top of *Shivlinga*'s mineral body has a mean diameter of ~22 cm (Fig. 1C, I). Throughout the year, there is a gentle discharge of water (68-73°C, pH 7.0-7.5) from a 10-cm diameter vent at the summit of *Shivlinga*; this is accompanied by a weak emission of hydrothermal gases (a comprehensive characterization of the gaseous discharges of the geothermal vents of Puga valley had previously shown that they all emit steam, carbon dioxide and hydrogen sulfide⁴¹). *Shivlinga*'s discharge runs down the side of the microbialite (Fig. 1C, I) onto the bedrock surrounding its base (Fig. 1D, J). Beyond the slopes of the basement rock, the spring-water flows along several, shallow channels (the longest one running 3.3 m from *Shivlinga*'s base), and eventually percolates into the regolith of the surrounding apron (Fig. 1B, H). Temperature, pH and flow-rates of the vent-water and outflows were found to remain consistent during the 2008-2013

annual site visits (Table 1 and Supplementary Table 1); this stability was attributable to the physicochemical consistency of the underlying geothermal reservoir⁴⁴. The sizes and structures of the microbial mats growing along *Shivlinga*'s spring-water transit also remained largely unchanged from 2008-2013, indicating the microbiome's resilience to seasonal and annual variations in weather. This observation was consistent with reports for microbial mats at other geothermal sites^{22,25}; so *Shivlinga*'s ecosystem was considered suitable for studying microbial community dynamics along its hydrothermal gradients, and a comprehensive geomicrobiological exploration of the site was undertaken in July 2013.

Chemical characteristics of the vent-water

The chemical composition of *Shivlinga*'s vent-water was determined by collecting surficial discharges from the center of the vent's orifice. The vent-water, at the time of the current sampling (on 23 July 2013), had a neutral pH (7.0) and low total dissolved solids (2000 mg L⁻¹) compared with other neutral-pH hot springs located in distinct geographical areas of the world^{41,45,46}. *Shivlinga*'s vent-water was found to have high concentrations of boron (175 mg L⁻¹), sodium (550 mg L⁻¹), bicarbonate (620 mg L⁻¹) and chloride (360 mg L⁻¹), compared to the other solutes detected in the vent-water. There was also some silicon (60 mg L⁻¹), potassium (15 mg L⁻¹), calcium (10 mg L⁻¹), lithium (6 mg L⁻¹) and magnesium (3 mg L⁻¹) detected. Of the sulfur species present, thiosulfate (3 mM) and sulfate (1 mM) were the most abundant, but sulfite (225 μM) and sulfide (250 μM) were also present at significant concentrations. Collectively, the vent-water chemistry was consistent with that reported for other hot springs within the Puga region^{40,41}.

Distinct mineralogies of *Shivlinga*'s vent and body, bedrock slope, and apron

For each of the water-flows running in *Shivlinga*'s vent to apron trajectory, and starting from the surface of the vent-water, multi-colored microbial mats grow all along their transits, until the end of the flow near the edge of the apron. Depending on their thickness, the mats are either slightly submerged or stay just above the water-level. Segments of mats that lie at the interface of the spring-water and the regolith are typically dry at their surface but moist within. Every mat at the site is intermeshed with fresh mineral accretions that precipitate from the cooling spring-water and also condense from the gases that arise from the vent; but mineralization processes are at far more advanced stages in the less-hydrated segments of mats. For microbial biomass growing just beneath the water level, or protruding from the water surface by mm to cm, mineral dusts visible to the naked eye are present on the mat surfaces. For those mats or parts of mats that are situated at the margins of outflows, mm- to cm-sized, soft, white spherules and shrub-like bodies of accreted minerals cover

the mats (Fig.2A). In the latter cases, mineralization is very conspicuous: monitoring this process over a period of 21 days using close-up photography revealed that the microbial mats grow out from the top of the encrustations, and spread again over the surface of the spherules (Supplementary Fig.2). It was also evident that the fresh biomasses at the surface of such mats are covered by fresh mineral deposition; and so the process continues. Mineralization acts to solidify all the mat structures of the microbiome from the bottom upwards. The microbialite thereby grows in height as well as in girth, besides hardening from within [the height of *Shivlinga*, according to our field observations, increased by ~4 cm (and the vent orifice narrowed slightly) between 2008 and 2013]. Spherules and shrub-like structures form across the apron's dry surface, presumably due to condensation of *Shivlinga*'s fumarolic gases on the regolith (Fig. 1B, H). However, the salt accretions which form beyond a few cm from the banks of the water-flows are not associated with microbial mats, and are dry and brittle.

We analyzed fine mineral particles accreted on the mat samples taken from the middle of the water-flow, and also sinter-spherules precipitating on mat-portions growing near the margins of the water-flow. Sinter-spherules and shrub-like bodies that were soft, so had presumably formed within a few weeks before sampling, were collected from one top-edge of *Shivlinga*'s body (Sinter-Sample 1), one side-surface of the microbialite (Sinter-Sample 2), one point in the bedrock slope around *Shivlinga*'s base (Sinter-Sample 3), and one point of mat:regolith interface on the margin of the spring-water flow in the apron (Sinter-Sample 4) (Fig. 1B-D, H-J). Besides these four samples, older and harder sinter material was collected from *Shivlinga*'s interior by boring the microbialite's side-surface, using a small drill, to a depth of 5 cm at a point located 15 cm below the summit (Sinter-Sample 5) (Fig. 1C, I).

All the sinter samples were found to be rich in boron, sodium and calcium (Supplementary Table 2); kernite ($\text{Na}_2\text{B}_4\text{O}_7 \cdot 4\text{H}_2\text{O}$) was the major mineral in *Shivlinga*'s interior, while borax ($\text{Na}_2\text{B}_4\text{O}_7 \cdot 10\text{H}_2\text{O}$) and then tincalconite ($\text{Na}_2\text{B}_4\text{O}_7 \cdot 5\text{H}_2\text{O}$) were predominant in the soft, recently-formed sinters (data not shown). Calcite (CaCO_3), gypsum ($\text{CaSO}_4 \cdot 2\text{H}_2\text{O}$), elemental sulfur, and silica (SiO_2) were also identified within the boron-mineral matrices of all the five sinter samples. Minute quantities of aluminum, gold, iron, manganese, zinc, molybdenum, lead, silver, nickel and cobalt were also detected, regardless of the sinter samples (Supplementary Table 2). These mineralogical data are consistent with *Shivlinga*'s vent-water chemistry, and together they suggest that the microbialite has formed from the gradual precipitation and accretion of boratic-, carbonatic-, and sulfatic-minerals, a process that, in part at least, is facilitated by its microbial communities (see Fig. 2A).

The process of precipitation of boron minerals is common to *Shivlinga*'s vent and microbialite body, bedrock slope and apron; yet there is considerable variation in the proportions of oxides or carbonates of metals, alkali metals and alkaline earth metals which combine with the boron minerals in the three zones of this microbiome (Supplementary Table 2). The soft (fresh) sinters of the vent and microbialite body, and those of the sloping bedrock, contain greater proportions of aluminum and gold; sinters of the apron however contain greater proportions of iron and manganese. On a w/w basis, the percentages of zinc, molybdenum, lead, silver, nickel and cobalt etc are higher in the freshly-precipitated sinters precipitated in the apron than in the accretions on the vent and microbialite body, or the bedrock slopes (Supplementary Table 2).

Microbial characterizations along *Shivlinga*'s spring-water transit/dissipation: a wet, and a progressively-drying, thermal gradient

Microbiological investigations were carried out along two distinct axes of *Shivlinga*'s spring-water transit/dissipation. One of these represented a progressively-drying thermal gradient having no running-water on it (along this axis, the spring-water dissipated into the mineral sinters of the microbialite body); the other featured a wet thermal gradient along the outflow channel of the spring. Both of these gradients start from the vent and, besides the vent-water community (VW), share a common microbial mat community (VWM) that floats on the vent-water and anchors to the sintered rim of the vent (Fig. 1C, I). The drying thermal gradient traverses the moist sinters concentrically from the vent opening, ~15 cm towards the edge of *Shivlinga*'s flat-topped summit; two more, morphologically distinct but physically contiguous mat communities (DG3 and DG4) occur along this trajectory (Fig. 1C, I). On the other hand, the ~4-m-long, wet thermal gradient, at the time of sampling, laid along the longest and widest of the six prominent channels of *Shivlinga*'s spring-water transit; it ran from the vent, down one side of *Shivlinga*'s mineral body and base (Fig. 1C, D, I, J), and then along the outflow channel in the apron (Fig. 1B, H). Along the wet thermal gradient lies a continuum of multi-hued microbial mat communities, from within which five representative mats (WG3, WG4, WG5, WG6 and WG7) were chosen for investigation. In total, nine physically/morphologically distinctive microbial communities, including one in the vent-water (Table 1), were sampled across the two thermal gradients and subjected to analysis using microscopy and metagenomics. These microbiological data were collated with the mineralogical analyses of sinter materials (sediment-accretions) sampled and investigated from the five distinct depositional facies (physical and chemical conditions under which deposition takes place) existing in the *Shivlinga* territory. This revealed that the *Shivlinga* microbiome encompasses three distinct geomicrobiological zones (Fig. 1A, G) characterized by distinctive temperature- and pH-conditions, and topographical,

mineralogical and microbiological features. These are (i) the vent and the microbialite body, (ii) the microbialite's base (including the sloping bedrock) and (iii) the apron. Whilst the first geomicrobiological zone encompassed the VW, VWM, DG3, DG4 and WG3 communities (Fig. 1C, I), the second and the third included the communities WG4 and WG5 (Fig. 1D, J), and WG6 and WG7 (Fig. 1B, E, F, H, K, L), respectively. Further details of the geomicrobial features present along *Shivlinga*'s spring-water transit/dissipation are given in the Methods sub-section titled "Site Description".

Distinct mat morphologies of the vent surface, microbialite body, sloping bedrock-base, and apron

Microscopic examinations revealed four distinct patterns of organization of microbial cells in *Shivlinga*'s mat communities. The VWM and WG3 streamers are composed of rod-shaped bacterial cells (that lie end-to-end), interspersed with smaller coccoidal cells, within dense networks of a septate filaments of cyanobacteria that are long, straight, sheathed and semi-rigid (Fig. 3A, B). All the green, red and purple mats growing around the vent, on the microbialite body, and the bedrock slope, of *Shivlinga* (i.e. DG3, DG4, WG4 and WG5) are made up of spherical bodies ranging from 10-100 μm in diameter (Fig. 3C). Diatoms that appear to be members of Cymbellaceae form the margins of these spheres, and remain in immediate contact with adjacent spheres or other mineral structures (Fig. 3C, D). Cells, which have the dimensions and morphologies of prokaryotic cells, occur along the boundary of the spheres. Filamentous and coccoidal microorganisms, resembling *Chloroflexi* and Chroococcales respectively, occupy the internal core of the spheres; abundant hyphal structures that are a septate and white (some having stalked buds coming out of them), and resemble Phycomycetian fungi are also seen here (Fig. 3E-H). Notably, boron-mineral-encrusted forms of these spherical bodies were identified in SEM-EDS of Sinter Sample 5 (Fig. 2B, C). These microscopic data, together with the detection of small but definite proportions of fungus-affiliated reads in the subsequent metagenome analysis of the mat communities, indicated that specific amplification and sequencing of fungal DNA, in future investigations, may reveal even greater fungal diversity than shotgun metagenomics indicates.

The two morphologically distinct mat structures of the wet thermal gradient that are located within apron environment, i.e. WG6 and WG7, suggest processes by which mat formation had occurred. The former type appears to be formed by the nucleation of borax, extracellular organic matter, and traces of calcite and other minerals, on irregular aggregations of diatoms, cyanobacteria, red-pigmented *Chloroflexi*, and other cells having dimensions and morphologies akin to those of prokaryotes. The WG7 streamers, in contrast, exhibited a laminar organization. The top-most layer

of these stratified mats contained dense sheaths of filamentous bacteria resembling *Chloroflexi*, *Leptothrix* and *Sphaerotilus*. Embedded in complex mineral assemblages, these filamentous organisms are interspersed with large round-shaped cells that appear to be flagellates, according to their morphologies and 5-20 μm diameters (row A of Fig. 4). 1-2 mm beneath the top-layer (i.e. in the sub-surface layer 1), abundance of the filamentous bacteria decreases and the density of the eukaryotic cells increases; further more, at these depths, there were occasional cells of pennate diatom species (row B of Fig. 4). Diatoms are, however, much more abundant at subsequent depths up to the boratic substratum. At 3-4 mm from the mat surface (i.e. in the sub-surface layer 2), the diatoms co-exist with morphologically-diverse bacteria, many of which resemble purple sulfur and non-sulfur bacteria (row C of Fig. 4). At the deepest layer of WG7, 5-8 mm below the surface (i.e. in the sub-surface layer 3), diatom cells predominate and attach to borax crystals (row D of Fig. 4).

Bacteria-dominated vent-water community

PCR amplification (using Bacteria-/Archaea-specific oligonucleotide primers), followed by high throughput sequencing, of the V3 regions of all 16S rRNA genes present in the total environmental DNA extracted from the VW sample revealed the alpha diversity of the community. This is referred to hereafter as the metataxonomic composition⁴⁷ so as to distinguish the diversity reported for the VW community from those reported subsequently for the mat communities via shotgun metagenome sequencing and analysis. Notably, total environmental DNA yield from the VW sample was quantitatively insufficient for direct shotgun sequencing and metagenome analysis.

Bacteria-specific V3 primers generated PCR products of desired size (~200 bp) and therefore the amplification product was sequenced at high data throughput. Archaea-specific V3 primers did not yield any PCR product, suggesting that very low numbers of archaeal cells are present in *Shivlinga*'s vent-water. Reads of the Bacteria-specific V3 sequence dataset were clustered into operational taxonomic units (OTUs) or putative species-level entities unified at the level of 97% 16S rRNA gene sequence similarity (Supplementary Table 3 shows the summary results of OTU clustering). Rarefaction analysis of the dataset confirmed that the read-sampling level (data throughput) achieved was sufficient to reveal most of the diversity present in the sample (Supplementary Fig. 3).

64 bacterial OTUs - distributed over the phyla *Proteobacteria* (45), *Actinobacteria* (4), *Firmicutes* (4), *Deferribacteres* (2), *Deinococcus-Thermus* (2), *Ignavibacteriae* (2), *Armatimonadetes* (1), *Aquificae* (1), *Synergistetes* (1) - were identified in all (number of OTUs affiliated to each phylum is given in parenthesis); 2 OTUs belonged to unclassified Bacteria. Of the

64 OTUs, 19 could be classified at the genus level. The genera identified (number of affiliated OTUs given in parenthesis) were *Achromobacter* (2), *Alcaligenes* (1), *Aminicenantes* Incertae Sedis (1), *Armatimonadetes* gp5 (1), *Calditerrivibrio* (2), *Ignavibacterium* (2), *Paenibacillus* (1), *Propionibacterium* (1), *Sulfurihydrogenibium* (1), *Thermomonas* (4), *Thermus* (2) and *Thiofabia* (1). Notably, out of the 12 genera detected metataxonometrically in the 70°C VW, member strains of at least four have never been found to grow at >45°C *in vitro* (these are *Achromobacter*, *Alcaligenes*, *Paenibacillus* and *Propionibacterium*); and six are present in each of the mat communities studied (these are *Achromobacter*, *Calditerrivibrio*, *Paenibacillus*, *Propionibacterium*, *Sulfurihydrogenibium* and *Thermus*).

Microbiology of *Shivlinga*'s thermal gradients

Variations in the community composition of *Shivlinga*'s microbial mats were assessed via metagenome sequencing and analysis along each thermal gradient (Supplementary Tables 4 and 5 show the summary statistics plus domain-level classifications of the metagenomic data obtained from the mats of the drying and wet thermal gradients respectively). Although total number of metagenomic reads generated for the different samples varied, plateauing of rarefaction curves determined for the individual samples by plotting number of reads analyzed versus genera identified in searches against the non-redundant (nr) protein sequence database of National Center for Biotechnology Information (NCBI, USA) or the 16S rRNA gene sequence database of the Ribosomal Database Project (RDP) showed that the data throughput achieved was sufficient to reveal most of the diversity present in the sample. Furthermore, to avoid the risk of potential anomalies that may arise in the subsequent analyses due to differential read-count of the different samples, prevalence of taxa was quantified as the percentage of total metagenomic reads ascribed to them, i.e. relative abundance.

In searches against the nr protein database, unassigned and unclassified sequences made up 7-26% of the metagenomic readsets; Bacteria accounted for at least 72% of all these and Archaea constituted <1%, regardless of the sample. The highest relative abundance of Archaea was encountered in the distal (cooler) ends of the gradients, i.e. in DG4 (41°C), WG4 (46°C) and WG7 (33°C) communities. The genera *Archaeoglobus*, *Methanocaldococcus*, *Methanococcus*, *Methanosarcina*, *Methanospirillum*, *Methanothermobacter*, *Pyrococcus* and/or *Thermococcus* comprised the major archaeal component of every mat community. Eukarya accounted for <0.6% of the metagenomic readsets for VWM, WG3 and WG4; and ~1% for DG3, DG4; WG5, WG6, and WG7 (for at least one replicate). In other words, relative abundance of eukaryotes almost doubled along the drying, and wet thermal gradients at $\leq 52^\circ\text{C}$ and $\leq 38^\circ\text{C}$ (respectively), compared to those

observed at higher temperatures. Diverse types of virus are present *Shivlinga*'s mat communities and, remarkably their relative abundance is highest at 66°C (in VWM). Virus-affiliated reads made up 0.3% and 0.2% of the metagenomes obtained from the two VWM sample-replicates, but only 0.01-0.04% of those obtained from the other mat communities. Predominant members of the viral component of VWM metagenomes were temperate lactococcal phages, including r1t and *Listeria* phi-A118; notably, thermophilic phages that are commonly found in other hydrothermal ecosystems⁴⁸ were absent. Whereas the Bacteria are the dominant organisms in *Shivlinga*'s microbiome, the ecophysiological importance of eukaryotic microbes could be greater than suggested by their low number of metagenomic reads. Some indications of this are detailed below.

Microscopic analyses revealed dense but localized populations of diatoms in many of the mat communities, including those located at 52°C (Fig. 3C, D). Diatoms (Bacillariophyta) were also detected metagenomically in all of the microbial mats sampled, albeit in low numbers. Their relative abundance ranged from a minimum of 0.001%, for VWM, to a maximum of 0.05%, for DG3, along the drying thermal gradient and 0.6%, for WG5, along the wet thermal gradient (relative abundance values for diatoms were 0.2% for DG4, WG6 and WG7). The genera *Odontella*, *Phaeodactylum* and *Thalassiosira* consistently predominate diatom populations in all the eight mat communities, regardless of the hydrothermal gradient.

Microscopy revealed localized but dense populations of fungi in mat communities present at the 33-52°C sites. According to metagenomic analyses, fungi were also present in all of the other mat communities, albeit at low levels. Along the drying thermal gradient, their relative abundance ranged from a minimum of 0.02%, for VWM, to a maximum of 0.2%, for DG4, and along the wet thermal gradient from 0.02% (VWM) to 0.7%, for WG5. 63 fungal genera were present in VWM (66°C), and greater numbers of genera were detected in the communities growing at the distal ends of each gradient; e.g. 82 genera in DG4, 106 in WG5, and 142 in WG7. *Aspergillus*, *Gibberella*, *Neurospora*, *Saccharomyces*, *Schizosaccharomyces* and *Ustilago* constituted the major portions of the fungal populations across both the gradients.

Sequences matching Chlorophyta (green algae) were present in the metagenomes of all the mat communities, and their relative abundance ranged from 0.005% (for VWM) to a maximum of 0.1% (for DG4, WG5, WG6 and WG7). The genera *Chlamydomonas*, *Chlorella*, *Micromonas*, *Ostreococcus* and *Volvox* are the major green algal component of all the mat communities, whereas *Acetabularia*, *Bryopsis*, *Dunaliella*, *Nephroselmis*, *Pyramimonas* and *Scenedesmus*, sparse at high temperatures, increase towards the distal ends of the gradients. Remarkably, the eukaryotic components of each mat metagenome were not dominated by a microorganism, but by

the bryophyte *Physcomitrella* (spreading earthmoss) which has a simple life-cycle, and is considered to be the most-ancient of all land plants⁴⁹. It is an early colonizer of exposed mud/ sediment/soil around the edges of water bodies, and is widely distributed in temperate regions of the world. At the *Shivlinga* site, *Physcomitrella* is most abundant in VWM (66°C), where it constitutes 0.1% of the metagenomes. Notably, in the VWM metagenomes, known thermophilic genera such as *Archaeoglobus*, *Calditerrivibrio*, *Desulfotomaculum*, *Hydrogenivirga*, *Pyrococcus*, *Thermoanaerobacter* and *Thermocrinis*, each has <0.1% of reads ascribed to them. In the other mat communities, *Physcomitrella* constituted 0.02-0.04% of the metagenomes. In VWM, the most prevalent eukaryote after *Physcomitrella* is another photosynthetic organism, *Cyanidioschyzon* which is a unicellular, ~2µm-long red alga that often occurs in sulfur-containing, highly acidic hot springs at around 45°C⁵⁰. For all other mat communities, the second most prevalent eukaryote is the amoeba *Dictyostelium* which is found in soils, predates bacteria, and is commonly known as slime mold⁵¹. The other protists detected in *Shivlinga*'s mat communities included the flagellate cryptomonad alga *Guillardia*, the glaucophyte *Cyanophora*, and the chloroplast-bearing amoeba *Paulinella*. Notably, all these genera were present in sample sites of ≤ 46°C.

Along the drying, as well as the wet, thermal gradients (Fig. 5A; Supplementary Fig. 4 and Fig. 5B; Supplementary Fig. 5), mean relative abundances of the 26 major groups of Bacteria (i.e. 21 phyla and five proteobacterial classes) varied considerably. *Deinococcus-Thermus* and *Aquificae* dominate VWM, and are less prevalent in the communities located at the distal (cooler) ends of each gradient. Along the drying thermal gradient, this decline in the prevalence is very sharp for both phyla; relative abundance of *Deinococcus-Thermus* declined from 60% in VWM to ~2% in DG3 and DG4. In the drying thermal gradient, there was a concurrent increase of *Chloroflexi*; *Firmicutes*; *Alpha*, *Beta*, *Gamma* and *Delta* classes of *Proteobacteria*; *Actinobacteria*; *Acidobacteria* and *Planctomycetes*, which continues through DG3 and DG4. Notably, *Cyanobacteria*, *Chlorobi*, *Bacteroidetes*, *Spirochaetes* and *Verrucomicrobia* are more abundant in DG3 (relative to VWM), but declined in DG4 (relative to WG3). Contrary to the above trends, *Epsilonproteobacteria* and *Thermotogae* were low in DG3 (relative to their VWM levels) but increased again in DG4.

Phylum-level population fluctuations are more irregular along the wet thermal gradient; the relative abundances of *Alphaproteobacteria*, *Chlamydiae* and *Planctomycetes* continue to increase along the water transit, in the vent-to-apron direction. The frequencies of *Actinobacteria*, *Cyanobacteria* and *Spirochaetes* also increase up to the 38°C site. Similarly, *Acidobacteria*, *Bacteroidetes*, *Chlorobi*, *Deferribacteres*, *Deltaproteobacteria*, *Dictyoglomi*, *Firmicutes*, *Fusobacteria*, *Gemmatimonadetes*, *Nitrospirae*, *Synergistetes* and *Tenericutes* increase up to the

46°C site. By contrast, the frequencies of *Aquificae* and *Epsilonproteobacteria* continue to decrease along the gradient, down to the 38°C sample site, and *Deinococcus-Thermus* decreases down to the 36°C site. Frequencies of *Betaproteobacteria*, *Chloroflexi*, *Gammaproteobacteria* and *Verrucomicrobia* increase till the 56°C site. Remarkably, the relative abundance of *Thermotogae* does not vary with temperature along the wet thermal gradient. Consistent with these trends, only *Aquificae*, *Deinococcus-Thermus* and *Epsilonproteobacteria* exhibited significant positive correlation with both temperature and flow-rate of the spring-water (SupplementaryTable 6). Whereas correlation of these three phyla with pH was significantly negative, only *Aquificae* showed significantly negative correlation with distance from the vent. *Actinobacteria*, *Alphaproteobacteria*, *Chlamydiae*, *Firmicutes*, *Fusobacteria*, *Gammaproteobacteria*, *Gemmatimonadetes*, Other phyla, *Planctomycetes*, *Spirochaetes*, Unclassified Bacteria and Unclassified *Proteobacteria*, all exhibited significant negative correlations with both temperature and flow rate. All these groups, remarkably, had significant positive correlations with pH and distance from the vent. *Acidobacteria*, *Bacteroidetes*, *Betaproteobacteria*, *Chlorobi*, *Chloroflexi*, *Cyanobacteria*, *Deferribacteres*, *Deltaproteobacteria*, *Dictyoglomi*, *Nitrospirae*, *Synergistetes*, *Tenericutes*, *Thermotogae* and *Verrucomicrobia* showed no significant correlation with temperature, although *Acidobacteria*, *Betaproteobacteria*, *Deltaproteobacteria*, *Synergistetes* and *Verrucomicrobia* had positive correlations with pH as well as distance from the vent – of these, *Acidobacteria* and *Betaproteobacteria* additionally exhibited significant negative correlations with flow rate. *Tenericutes* had significant positive and negative correlations with pH and flow rate respectively. SupplementaryTables 7-12 shows the calculations for all the correlation coefficients and their Benjamini-Hochberg-corrected P values.

Thermodynamic constraints on microbial colonization

Thermodynamic constraints on the microbial colonization of *Shivlinga* sites were delineated based on relative abundance of taxa along the hydrothermal gradients. These, in turn, were derived from the percentage of metagenomic reads ascribed to individual taxa within each community. Diversity within *Shivlinga*'s microbial communities increases towards the distal ends of the thermal gradients, and community compositions change from being *Aquificae/Deinococcus-Thermus-* to *Chlorobi/Chloroflexi/Cyanobacteria*-dominated, and then being *Bacteroidetes/Proteobacteria/Firmicutes*-dominated (Fig. 5). Although the VWM community on *Shivlinga*'s vent-water is biomass-dense, its microbial diversity is lower than that of the mat communities located at the distal end of each thermal gradient. This is likely due to the habitability barrier imposed by the high vent-water-temperature that, in turn, is exacerbated by the low

atmospheric pressure. At an altitude of 4438 m, atmospheric pressure is ~6.4 KPa, which is close to the 2.5-5 KPa threshold that is known to prevent *in vitro* growth of bacteria adapted to atmospheric pressure at sea level (i.e. ~101.3 kPa)⁵². Low pressure not only lowers the boiling point of water but can also contribute to the entropic destabilization of biomacromolecular systems (conversely, high pressures appear to, in part at least, mitigate against the chaotropicity of MgCl₂ in deep-sea brine systems⁵). Conditions at the *Shivlinga* site, therefore, destabilize biomacromolecules, and elicit cellular stress responses which impose high energetic cost on microbial systems and/or can ultimately cause cell-system failure^{53,54}. For VW and VWM (the communities at the highest temperatures) an environment-driven selection for thermotolerant/thermophilic taxa would be expected. Accordingly, relative abundance of 19 out of the 26 major bacterial phyla/proteobacterial classes present along the wet thermal gradient was lower in VWM (66°C) than in WG3 (56°C). Only *Aquificae*, *Deferribacteres*, *Deinococcus-Thermus*, *Dictyoglomi*, *Epsilonproteobacteria*, *Nitrospirae* and *Thermotogae*, which are made up mostly of thermophiles, were more prevalent in VWM than in WG3 (Fig. 5B). This is indicative of a substantial thermodynamic barrier to microbial colonization at ~60°C. The 19 groups, which include *Alphaproteobacteria*, *Betaproteobacteria* and *Gammaproteobacteria*, *Bacteroidetes*, *Chlorobi*, *Chloroflexi*, *Cyanobacteria*, and *Verrucomicrobia*, and for which prevalence was lower at 66°C than at 56°C, are made up mostly of mesophilic or thermotolerant members incapable of laboratory growth at >60°C. The presence of these taxa at *insitu* temperatures of >60°C, suggests that (a) hitherto unidentified environmental factor(s) is(are) acting to mitigate the cellular stresses induced by high temperature. Furthermore, the relative abundances of most of the major phyla/classes (20 out of 26) were lower at 56°C, in WG3, than at 46°C, in WG4 (Fig. 5B; Supplementary Fig. 5). This suggests that temperatures between 56°C and 46°C impose an additional thermodynamic barrier to habitability for many of the microbial taxa. In microbiomes for which habitability of some taxa is constrained by other parameters, a comparable drop in diversity is observed for xerophiles and halophiles at 0.720 water activity⁵⁵. Furthermore, at the distal end of the wet thermal gradient, the relative abundances of 16 out of the 26 major groups were lesser at 46°C (WG4) than at 38°C (WG5), implying that there is another colonization barrier at 40-42°C.

Simpson Dominance (*D*), Shannon–Wiener Diversity (*H*), and Shannon–Wiener Evenness (*E_H*) Indices were calculated based on the metagenomic data for each mat community (Supplementary Tables 13-20); these values were then compared along each gradient. Trends of variation of these indices provided further evidence for temperature barriers to habitability. For VWM (66°C), *D* value was greater than for any other mat community, whereas *H* and *E_H* were low

relative to those in WG3 and DG3(56 and 52°C, respectively) (Fig. 6). This indicates that, for both the wet, and the drying, thermal gradients, there is a colonization-barrier for many taxa at ~60°C. However, along the wet thermal gradient, from 56 to 46°C (WG3 to WG4), and along the drying thermal gradient, from 52°C to 41°C (DG3 to DG4), increases in H and E_H , were much lower than what were recorded in the respective gradients, across the 60°C barrier (Fig. 6). This indicated that colonization-barriers at lower temperatures (~50°C for the wet thermal gradient and 46-50°C for the drying thermal gradient) are weaker than that at ~60°C. Trends of the above indices further pointed out that below 46°C, along the wet thermal gradient, diversity did not correlate with temperature, so other biotic and/or abiotic parameters could be acting as determinants of community composition in this territory.

For each mat community, the most-abundant genera that collectively accounted for $\geq 50\%$ of all classifiable reads were identified from the results of the metagenome-searches against nr protein database. The number and identities of such genera were then compared along the thermal gradients to interpret the temperature-constrained community dynamics. One genus, *Thermus*, accounted for a mean 50.6% of VWM metagenomes, and the genera *Sulfurihydrogenibium*, *Meiothermus* and *Aquifex* constituted 21.6%, 2.2% and 2.1%, respectively. For the DG3 and DG4 communities, 50% of their metagenomic reads were made up of 12 and 50 genera, respectively (Supplementary Table 21), and for WG3, WG4, WG5, WG6 and WG7, 50% of reads represented one, 11, 17, 35, 68 and 81 genera, respectively (Supplementary Table 22). In order to confirm the identifications of genera present in the individual mat communities, genus-level analysis of their duplicate metagenomes was carried out by searching against the 16S rRNA gene sequence database of RDP. By this approach (which is distinct from the amplified 16S rRNA gene sequence-based metataxonomic approach, used only for the vent-water community) diverse bacterial, but no archaeal, genera were identified in all the eight mat communities (Supplementary Tables 23-30). The numbers of genera detected in this way varied along the two thermal gradients, and were consistent with the variations in microbial diversity indices (Fig. 6). For the drying thermal gradient, genus-count was considerably less at 66°C than at 52°C or 41°C (Fig. 6D). For the wet thermal gradient, genus-count was far less at 66°C than at 56°C or 46°C; unexpectedly, however, genus-count was higher at 46°C than at 38°C, even though it was much lower at 38°C than at 36°C or 33°C (Fig. 6H). The trends in microbial diversity that were revealed from the direct classifications of the metagenomic reads were consistent with the results of diversity analyses based on assembly of contigs and binning of population genomes from the mat metagenomes (Supplementary Note 2).

Key metabolic attributes of the *Shivlinga* mat communities

Analysis of the metagenomic data of individual mat communities for comparative richness of genes [or Clusters of Orthologous Groups (COGs) of Proteins] under various metabolic/ functional categories, followed by hierarchical clustering of the mat communities in terms of their enrichment of various COG categories, revealed a dichotomous bifurcation between DG3, DG4 and WG5 on one side, and VWM, WG3, WG4, WG6 and WG7 on the other (Fig. 7A). DG4 and WG5 clustered on the basis of their similarities with respect to high/low presence of COGs affiliated to the categories Cell motility; Replication, recombination and repair; Signal transduction mechanisms; and Translation, ribosomal structure and biogenesis. DG3 joined this cluster based on significantly high and low presence of COGs affiliated to Signal transduction mechanisms and Cell motility respectively (Fig. 7B). In the other major cluster, the closeness of VWM and WG3 (Fig. 7A) is explained by their similarities in having high and low presence of COGs affiliated to the categories Replication, recombination and repair; and Signal transduction mechanisms respectively (Fig. 7B). WG6 joined the VWM-WG3 cluster on the basis of significantly high presence of COGs affiliated to Replication, recombination and repair (Fig. 7B). WG4 and WG7, in turn, associated on the basis low presence of COGs for Replication, recombination and repair. VWM, WG3, WG4 and WG6 were further unified by the significantly low presence of COGs affiliated to Signal transduction mechanisms. Despite the significantly low presence of COGs affiliated to Signal transduction mechanisms in a number of mat communities, number species-level matches as well as relative abundance for genes encoding bacterial two component kinases such as histidine kinase, serine threonine protein kinase, diguanylate cyclase, PAS sensor protein, etc. were considerably high for all the communities. This implied that the geothermal adaptations of complex microbial mat communities involve efficient response regulations to a wide range of environmental signals.

The merged metagenomic readsets of individual mat communities were searched for genes putatively encoding reverse gyrase enzymes, which are typical of hyperthermophilic bacteria and archaea, but never found in mesophilic microorganisms⁵⁶. As expected, metagenomic reads matching reverse gyrases from 30 different bacterial species were identified in VWM, but in no other community of the drying thermal gradient. Along the wet thermal gradient, such reads were found exclusively in communities living at $\geq 46^{\circ}\text{C}$.

Metagenomic reads matching genes that encode key enzymes of the autotrophic Calvin–Benson–Bassham and Wood–Ljungdahl pathways, namely ribulose 1,5-bisphosphate carboxylase large chain (*rbcL*) and acetyl-coenzyme A synthetase (*acsA*), were identified in all the mat communities. Even as autotrophy is ubiquitous throughout the ecosystem, Wood–Ljungdahl pathway

is apparently utilized by majority of the community members across *Shivlinga*'s thermal gradients. The numbers of species-level matches identified for *acsA*-related reads were an order of magnitude greater than those for *rbcL*; across the communities, species-level matches for *acsA* ranged between 112 (in WG5) and 477 (in WG7) while those for *rbcL* ranged from 18 (in DG4 and WG5) to 54 (in WG7). Furthermore, metagenomic reads corresponding to genes encoding the large subunit of ATP citrate lyase (AclA), a key enzyme of the reverse tricarboxylic acid (rTCA) or Arnon–Buchanan cycle - which is more energy-efficient, oxygen-sensitive, and phylogenetically ancient than the Calvin cycle or the Wood–Ljungdahl pathway^{57,58} - were detected only in the communities of the higher-temperature sites having typically low *in situ* oxygen, i.e. VWM and DG3 along the drying thermal gradient, and VWM, WG3 and WG4 along the wet thermal gradient.

Metagenomic reads matching genes for the gluconeogenic enzyme phosphoenolpyruvate carboxykinase (PEPCK) were detected in all the mat communities. Number of species-level matches for the PEPCK-related reads increased steadily from 32 in VWM to 102 in DG4, along the drying thermal gradient; and from 32 in VWM to 175 in WG7, along the wet thermal gradient. PEPCK governs the interconversion of carbon-metabolites at the phosphoenolpyruvate–pyruvate–oxaloacetate junction of major chemoorganoheterotrophic pathways, there by controlling carbon flux among various catabolic, anabolic, and energy-supplying processes⁵⁹. Variations in the number of species-level matches for PEPCK-related reads, therefore, were considered to be reflective of a steady rise in organoheterotrophic inputs in community productivity along both the hydrothermal gradients.

In view of the considerable abundance of dissolved sulfide, elemental sulfur, thiosulfate and sulfate in *Shivlinga*'s vent-water, occurrence and phylogenetic diversity of two key sulfur-chemolithotrophic genes, namely, the thiol esterase-encoding *soxB* of bacteria and the thiosulfate:quinone oxidoreductase-encoding *tqoAB* of archaea⁶⁰, were investigated in the metagenomes of all the mat communities. While *tqoAB* was not present in any metagenome, *soxB* was detected in all of them. Number of species-level matches for *soxB*-related reads increased steadily from 4 in VWM to 16 in DG4, along the drying thermal gradient; and from 4 in VWM to 39 in WG7, along the wet thermal gradient. Sox-based sulfur-chemolithotrophs being predominantly aerobic⁶⁰, these trends were consistent with the increase in oxygen tension along the vent-to-apron trajectories of the hydrothermal gradients.

Metagenomic reads matching genes encoding cytochrome *c* oxidase subunit 1 (*coxI*), the key enzyme of aerobic respiration⁶¹, are widespread in the *Shivlinga* ecosystem. Number of species-level matches for *coxI*-affiliated reads increased progressively from 32 in VWM to 193 in DG4, along the drying thermal gradient; and from 32 in VWM to 267 in WG7, along the wet thermal gradient.

Metagenomic reads matching genes encoding dissimilatory sulfite reductase alpha and beta subunits (*dsrAB*), which is central to the energy-conserving reduction of sulfite to sulfide in anaerobic sulfite/sulfate-reducing prokaryotes⁶², were detected only in some of the mat communities. Number of species-level matches for *dsrAB* reads were 6, 0 and 3 in VWM, DG3 and DG4, respectively; and 6, 9, 17, 0, 2 and 16 in VWM, WG3, WG4, WG5, WG6 and WG7, respectively. No gene for N-oxide (NO/N₂O) or nitrate (NO₃) reduction was found in any mat community. All these data suggest that *Shivlinga*'s mat communities are adept in utilizing whatever low oxygen is there in their watery to semi-watery habitat. This hypothesis is further supported by the considerable occurrence and diversity (across the thermal gradients) of genes involved in the biogenesis of *cbb3* cytochrome oxidase, which is known to be instrumental in respiration under very low oxygen tension⁶³. For instance, the number of species-level matches for metagenomic reads ascribable to genes encoding the *cbb3* cytochrome oxidase biogenesis protein CcoG⁶⁴ increased progressively from 0 in VWM to 44 in DG4, along the drying thermal gradient; and from 0 in VWM to 87 in WG7, along the wet thermal gradient.

Discussion

An extreme yet highly habitable ecosystem

Diverse lines of evidence indicated that many of *Shivlinga*'s native microorganisms can bypass thermodynamic hurdles to habitation. Phylogenetic relatives of a wide variety of mesophilic bacteria colonizing the high-temperature locations, presence of psychrophilic bacteria at 33-52°C sites, localized but dense populations of diatoms within the mat communities of 52°C site, and occurrence of established populations of mosses, fungi, green and red algae, and slime mold at sites of > 50°C, collectively indicate that this ecosystem is highly habitable, biodiverse and complex. The taxonomically diversified and biomass-dense microbiome of this otherwise extreme site (thermal stress, high UV, low pressure) is further complemented by the abundance of taxa at temperatures below their recognized minima for growth, and the abundance of taxa that are ubiquitous throughout the ecosystem irrespective of temperature. For instance, the genera *Chloroflexus*, *Roseiflexus*, *Sulfurihydrogenibium*, *Synechococcus* and *Thermus* remained prevalent over wide ranges of temperature along both the gradients; these genera are known to be physiologically interdependent. *Sulfurihydrogenibium* scavenges dissolved oxygen from hot-spring waters, thereby generating anoxic condition for organisms such as *Chloroflexus* and *Roseiflexus* that under anaerobic light conditions harvest energy via photoheterotrophy and switch back to chemoheterotrophy when it is dark⁶⁵. At the same time, *Synechococcus*, by virtue of producing glycolate and fermenting glycogen, has been shown to promote photoheterotrophic growth of

Roseiflexus in laboratory mixed cultures⁶⁶. *Roseiflexus*, in turn, is capable of synthesizing glycosides and wax esters that can be utilized for gluconeogenesis by other members of the community⁶⁷.

Studies of microbial ecology in diverse extreme habitats have characterized many interactions between bacteria and eukaryotic microbes which boost the metabolism and enhance the stress biology of one or more partners^{54,68}. For instance, fungal (and bacterial) saprotrophs can make nutrients available to other microbes, many microbes may co-metabolize complex substrates, and photosynthetic bacteria and algae may release compatible solutes to be used by other microorganisms of the community. So, despite the relatively small numbers of eukaryotes in the *Shivlinga* habitat, we believe that the ecological success of bacteria (as reflected by their > 97% relative abundance in all mat communities) is reliant, in part at least, on the former. Presence of the moss *Physcomitrella* in the *Shivlinga* microbiome, with highest relative abundance at the 66°C site, is also noteworthy. Worldwide, mosses are known to colonize geothermal sites which are characterized by various temperature and moisture regimes. Substratum temperatures up to 75°C have been recorded at 2.5-5 cm beneath mosses, and temperatures up to 60°C have been recorded on moss-covered surfaces^{69,70}. Like fungi, mosses also exhibit preference for vegetative propagation (over sexual reproduction) to conserve adaptations to environmental challenges such as high temperature^{71,72}. We could not find any evidence for either the sexual stage (the diploid sporophyte) or the intermediate stage (the haploid gametophyte) of *Physcomitrella* at the *Shivlinga* site. We suspect, therefore, that *Physcomitrella* exists within the *Shivlinga* mats only in its plesiomorphic (ancestral) form, which is characterized by algae-like, thalloid structures that do not have diverse tissue types and are known as juvenile gametophytes⁴⁹. This plesiomorphic form is made up of microscopic filaments known as protonema that are formed by chains of haploid cells⁴⁹. A number of studies have shown that *Physcomitrella* efficiently renders homologous-recombination-based error-free DNA damage repair, an attribute that is likely to confer adaptive advantage in high-temperature habitats that are generally associated with higher rates of DNA damage⁷³. Together with a plausible vegetative/asexual lifestyle, error-free DNA damage repair capabilities can act to reduce genetic variability in *Physcomitrella* and, ultimately, slow down evolution via conservation of genomes^{74,75}. These attributes, therefore, may help this bryophyte to colonize *Shivlinga* via retention of the plesiomorphic form (a phenomenon termed stasigenesis).

Phylogenetic relatives of mesophilic genera in *Shivlinga*'s high-temperature sites

When all the genus-level annotation data obtained via searching the metagenomes against the nr protein sequence and RDP 16S rRNA gene sequence databases were collated, at least 26 genera were confirmed as present in every mat community that was sampled (Supplementary Tables 31 and 32);

at least 18 additional genera were ubiquitous along the wet, but not the drying, thermal gradient (Supplementary Table 32). It is remarkable that these bacteria have colonized the entire *Shivlinga* system despite the various thermodynamic constraints on microbial diversity. Furthermore, these genera are not all known to be thermophilic; and many of them, for example *Clostridium*, *Lactobacillus*, *Pseudomonas* and *Salinibacter*, are archetypal ‘weeds’ that have a robust potential to withstand stress and maintain dominant positions within microbial communities⁷⁶. The *Shivlinga* site may, therefore, provide a useful model system for future studies of microbial weed ecology under hydrothermal conditions.

In the genus-level analyses of the metagenomic sequence data, a considerable number of the genera were also found to be present at temperatures outside their windows for growth *in vitro*. For instance, entities affiliated to at least 11 genera of typical thermophiles were detected at temperatures below the minima recognized for laboratory growth of the cultured strains of those genera (Supplementary Table 33). These were *Dictyoglomus*, *Hydrogenobaculum*, *Meiothermus*, *Persephonella*, *Petrogona*, *Sulfurihydrogenibium*, *Thermodesulfatator*, *Thermodesulfobacterium*, *Thermotoga*, *Thermus* and *Thermosipho*. Conversely, phylogenetic relatives of at least 40 such bacterial genera were present in > 50°C mat communities, no cultured members of which have any report of laboratory growth at >45°C (see Table 2 and its references given in Supplementary references). The composition of the vent-water community was also consistent with this finding; for instance, no strain of four out of the 12 genera identified in the 70°C VW community (*Achromobacter*, *Alcaligenes*, *Paenibacillus* and *Propionibacterium*) grow at > 45°C, according to *in vitro* studies. Moreover, strains of some of the reportedly-mesophilic genera detected at the high-temperature ends of *Shivlinga*’s hydrothermal gradients - for example, *Dolichospermum*, *Flavobacterium*, *Magnetospirillum*, *Planktothrix*, *Prochlorothrix*, *Thiohalocapsa*, *Treponema* and *Xylella* - are not even known to grow in the laboratory at temperatures > 30°C. Interestingly, psychrophilic microbes such as *Chryseobacterium* and *Nitrosomonas*⁷⁷ were also present in all the mat communities except VWM and WG3, and their frequencies increased with decrease in temperature. Diverse lines of evidence thus indicated that the *Shivlinga* hot-spring system is not dominated by thermophiles, but hosts an ecophysiologicaly diversified microbiome that includes several phylogenetic relatives of mesophilic taxa.

Insights into the biophysics of the *Shivlinga* ecosystem

Extremes of temperature constrain microbial function at the level of macromolecules, the cell system, ecosystems, and the biosphere. The ecology of *Shivlinga*’s microbiome is undoubtedly influenced by the high temperature. Interestingly, however, and although microbial diversity

decreases at around 50 and 60°C, several phyla/genera inhabit locations having temperatures above their *invitro* growth limits. This is analogous to the habitability of otherwise hostile chaotropic brines (> 2.50 M MgCl₂) that is facilitated by kosmotropic (compensatory) effects of sodium and sulfate^{5,7}. Although *Shivlinga* is a high-temperature and low-pressure habitat for microbes its spring-water and sinters contain high concentrations of borates, sodium, bicarbonate, thiosulfate and sulfate. In addition, the system has lower, but significant, concentrations of sulfite, sulfide and lithium. Borates, sodium, bicarbonate, thiosulfate, sulfate, sulfite, and sulfide are kosmotropic¹¹, and it is possible that their cumulative kosmotropic activity enables colonization of high-temperature sites by thermophilic taxa, a phenomenon which parallels the way in which kosmotropes facilitate colonization of chaotropic environments^{5,7,10,19}. We believe that the kosmotropic ions within the *Shivlinga*'s system might also enhance biotic activity of the thermotolerant and thermophilic microbes present.

Methods

Site Description

Within the Puga geothermal area, which is a part of the greater Ladakh-Tibet borax-spring zone⁴⁴, surface expressions of geothermal activity, including the *Shivlinga* microbialite spring (GPS coordinates: 33° 13' 46.2" N and 78° 21' 18.7" E), are largely confined to the eastern part of the 15 km-long and 1 km-wide east-west orientated valley. More information on the geography, geology, and geothermal activity of Puga can be found in Supplementary Note 1. Of the number of distinct axes of *Shivlinga*'s spring-water transit/dissipation, two trajectories representing a progressively-drying, and a wet, thermal gradient were investigated for their geomicrobiological characteristics. Collation of the microbiological and geochemical data revealed three distinct geomicrobiological zones within the *Shivlinga* system. The first geomicrobial zone of the *Shivlinga* microbiome, ***the vent and the microbialite body*** together form a unit that is elevated above the ground level. The chimney-shaped microbialite is made up of hardened hydrothermal mineral deposits (sinters); the water vented from within the microbialite, at the time of sampling (23 July 2013), was characterized by 70°C temperature, pH 7.0, and 25 mL s⁻¹ flow-rate. The vent water community (VW) was sampled from the vent opening located at the microbialite summit (Fig. 1C, I). A microbial mat is anchored to the inner surface of the vent's rim for the entirety of its circumference, and has grown inwards across the surface of the water. Most of the filamentous structures that form this vent-water mat (VWM) are white, but are interspersed with minute green-hued elements (Fig. 1C, I). VW and VWM represented the initial sample-points for both the wet, and the drying, thermal gradients, for which all subsequently-sampled mat communities were named

using the prefixes WG and DG, respectively. Starting from where VWM attached to the sintered rim of the vent, a 1-cm-thick, green mat containing occasional red patches (community DG3) spread radially over the flat mineral surface that circumvents the opening at the top of *Shivlinga*'s body (Fig. 1C, I). The next community surrounding the vent (sampled as DG4) forms another cm-thick mat which is pigmented purple with a greenish shimmer; it forms an unbroken ring extending from the DG3 community to the edge of *Shivlinga*'s summit (Fig. 1C, I). In contrast to VWM, DG3 and DG4 are not in contact with a flowing body of water; instead they are located on the moist sinters of the flat summit which surrounds the vent and progressively desiccates towards its outer edge (scraping off sections of the mats revealed no flowing water beneath). VW, VWM, DG3 and DG4 together form a continuum of microbial communities along this drying thermal gradient (Fig. 1C, I). Across a ~10-cm arc of *Shivlinga*'s circular top, the vent-water spills down the south-west-facing side of the microbialite body. The filamentous structures of VWM extend across the rim, along the spring-water flow, down the side of *Shivlinga* where they were designated as the community WG3 and sampled at a point 22 cm beneath the summit (Fig. 1C, I). WG3, like VWM, is white, but interspersed with apparently greater proportion of green filaments.

The microbialite's base (including the sloping bedrock), the second geomicrobiological zone of the *Shivlinga* site, has a lower temperature (38-46°C), lesser flow-rates, pH of ~8, and two morphologically distinct microbial mats. This bedrock, on which the microbialite is situated, is a conical section of sedimentary limestone which protrudes from the regolith. The original surface of this bedrock has been eroded by the spring-water, and coated with new mineral deposits and/or microbial mats. The WG3 streamer, which follows the spring-water down one side of the microbialite body, does not extend beyond the base of *Shivlinga*. Instead, it gives way to a green mat containing occasional yellow patches (community WG4), which in turn is restricted to the first 10's cms of the slope along the trajectory of the spring-water transit (Fig. 1C, D, I, J). Further along the water flow, a stretch of rust-colored mat (community WG5) covers the rest of the limestone outcrop (Fig. 1D, J).

The apron is the outer (and last) geomicrobiological zone of the *Shivlinga* microbiome; it starts where the slope of the bedrock ends and extends across a circular area of the regolith that is ~1.5 m in radius around the bedrock. Its surface is composed of a loose, heterogeneous mixture of fluvioglacial sediments, aeolian sand, clay and scree which overlay the bedrock. The terrain of the apron is only gently inclined, so the spring-waters (pH ~8.5) flow very slowly (Table 1) along channels in the regolith (these are 1- to 2-cm-deep and 5- to 50-cm-wide) before dissipating into the dry loose valley-fill material. Across the inner half of the apron, the floors of the outflow channels

are covered with intensely red nodules (Fig. 1B, E, H, K) formed by the nucleation of hydrothermal minerals onto microbial cells and extracellular organic substances (community WG6). In the outer half of the apron, 3 to 10 mm-thick tufts of dark grey streamers (community WG7) grow along the outflow (Fig. 1B, F, H, L). VW, VWM, WG3, WG4, WG5, WG6 and WG7 together form a continuum of microbial communities along this wet thermal gradient.

Sampling and collection of *in situ* data

At the discrete sample-sites within the *Shivlinga* system, temperatures were measured with a mercury-column glass thermometer while pH values were measured using Neutralit indicator strips (Merck, Germany). The discharge rate of *Shivlinga*'s vent-water was determined (in mL s⁻¹) using the soluble-tracer dilution technique described previously⁷⁸. Flow rates of spring-water over the sampled mat communities were determined (in cm s⁻¹) using a modified insoluble-dye tracer technique⁷⁹.

Shivlinga's vent-water was collected at the same time in separate bottles for chemical and microbiological analyses using separate, 25 mL sterile pipettes on each occasion. For analyses of water chemistry, VW samples were passed through a 0.22 μm syringe filter. Every 100 mL batch of VW sample meant for the quantification of metallic elements was acidified (to pH ≤2) by adding 69% (w/v) HNO₃ (400 μl). To stop all biotic activity for bicarbonate estimation, 100 μl saturated HgCl₂ solution was added to every 2 mL batch of VW sample. For microbiology, 1000 mL vent-water was passed through a sterile 0.22 μm cellulose acetate filters (Sartorius Stedim Biotech, Germany), following which the filter was put into an 8-mL cryovial containing 50 mM Tris:EDTA (5 mL, pH 7.8) and immediately placed in dry ice.

Every mat community was sampled once for microscopic studies and twice for metagenome analysis: the duplicate sets of metagenomic data generated were used to evaluate the statistical significance of the differences in relative abundance of taxa between communities. For each mat community, in each of the three sampling rounds (one for microscopy and two for metagenomics), fresh and intact material (2.5 cm² and located 5 mm from the other two mat portions sampled) was scraped off using a sterile scalpel, without disturbing the mat's internal structure or the substratum. The stable structure of the mats and consistent physicochemical conditions of the environment recorded over the years, together with the fresh and intact appearance of the mat samples used for all analyses were consistent with a relative absence of necromass.

Mat samples were put in sterile Petri plates containing 3 mL 70% (v/v) ethanol:acetic acid:formaldehyde (9:1:1 v/v/v) or a 15 mL cryovial containing 5 mL Tris:EDTA (50 mM; pH 7.8),

depending on whether they were required for microscopic or metagenomic analysis, respectively. The flakes of precipitating mineral salts were not removed from the mat samples meant for microscopic analysis. Petri plates were sealed with Parafilm (Bemis Company Inc., USA) and packed in polyethylene bags, and the cryovials were sealed using Parafilm and then placed in dry ice. Dry ice in the sample-transportation boxes was replenished *en route* to the laboratory at Bose Institute (Kolkata). Samples destined for metagenomic analysis were stored in the laboratory at -20°C , while those for microscopic, chemical or mineralogical studies were kept at 4°C .

Analyses of vent-water chemistry

Concentrations of boron, calcium, lithium, magnesium, and potassium were determined on a Thermo iCAP QICPMS (Thermo Fisher Scientific, USA); standard curves were prepared using ICPMS standards supplied by Sigma Aldrich (USA) and VHG Labs Inc. (USA). Based on replicate analyses of the standards, deviations from actual concentrations were less than 2%, 1%, 2.1%, 1% and 2.5% for boron, calcium, lithium, magnesium and potassium, respectively. Concentrations of sodium were determined using an Agilent 240AA atomic absorption spectrometer (Agilent Technologies, USA); standard curves were prepared from Sigma Aldrich AAS standards. Based on multiple analyses of the standard, deviations from actual sodium concentrations were $<3\%$. Silicon concentration was determined using a UV-visible spectrophotometer (CARY 100, Varian Deutschland GmbH, Germany), as described previously⁸⁰. Chloride was quantified by precipitation titration with silver nitrate (0.1 N) using a Titrino 799GPT auto titrator (Metrohm AG, Switzerland). Bicarbonate concentrations were calculated from the dissolved inorganic carbon (DIC) content and total alkalinity of the water samples according to⁸¹. Total alkalinity was determined using Gran titration method (and the Titrino 799GPT auto titrator), while dissolved inorganic carbon was determined by CM 5130 carbon coulometer (UIC Inc., USA). Thiosulfate and sulfate concentrations in the vent-water were determined by iodometric titration, and gravimetric precipitation using barium chloride, respectively^{82,83}. Sulfite was analyzed spectrophotometrically with pararosaniline hydrochloride (Sigma Aldrich) as the indicator⁸⁴. Dissolved sulfides (ΣHS^- , which includes H_2S , HS^- and/or S_x^{2-}) were precipitated as CdS from the vent-water *in situ* with cadmium nitrate [$\text{Cd}(\text{NO}_3)_2$] in crimp-sealed butyl septum bottles leaving no head space; colorimetric measurement was then carried out based on the principle that N, N-dimethyl-p-phenylene diamine dihydrochloride and H_2S react stoichiometrically in the presence of FeCl_3 and HCl to form a blue-colored complex⁸⁵. Sulfate, sulfite and thiosulfate were also quantified in the CdS-precipitated, ΣHS^- -free VW sample using a Metrohm ion chromatograph (Basic IC plus 883) equipped with a suppressed conductivity detector (Metrohm, IC detector 1.850.9010) and a Metrosep ASupp 5 (150/4.0) anion exchange column (Metrohm AG).

Microscopy of mats and mineralogy of sinters

For phase contrast microscopy or laser scanning confocal microscopy, 1-mm² portions of the mat samples were put on grease-free glass slides, teased apart gently with sterile needles after adding 50 mM phosphate buffer (pH 7.0) or a few drops of DPX Mountant (SigmaAldrich), and examined using an BX-50 phase contrast microscope (Olympus Corporation, Japan) or a LSM 510 Meta confocal microscope (Carl Zeiss AG, Germany). Electronic images of the auto fluorescence of microbial cells were recorded using confocal microscopy at various excitation and emission-detection wavelengths. To analyze the mineral salts precipitated on the mat samples the latter were also subjected to EDS following SEM on an FEI Quanta 200 microscope (Field Electron and Ion Company, USA). To give contrast to the biological components of the microbe-mineral assemblages, samples were prefixed with vapors of 1% (w/v) osmium tetroxide in deionized water.

Elemental composition of *Shivlinga*'s sinters was determined standard inorganic tests, and then EDS, EPMA, and XRD. EDS was carried out using an EDAX system attached to the FEI Quanta 200. Quantitative analyses and atomic density ratios were derived using the GENESIS software controlling the EDAX. XRD was carried out using an XPert Pro X-ray Diffractometer (PANalytical, the Netherlands) equipped with a copper target, operating at 40 kV and 30 mA, and scanned from 4 to 70° 2 θ . For EPMA, grain-mount slides of the sinter materials were prepared and elemental composition analyzed using an SX100EPMA machine (CAMECA, France); electron beam size of 1 μ m, accelerating voltage of 15 kV and current of 12 nA were used. The sinter sample slides were also imaged under the EPMA machine via electron backscattering to identify any encrusted microorganisms.

Isolation of total environmental DNA from *Shivlinga*'s vent-water

The filter through which 1000 mL of *Shivlinga*'s vent-water was passed during sampling was cut into pieces with sterile scissors, within the 50-mM-Tris:EDTA(pH 7.8)-containing 8-mL-cryovialin which it had come from the samplesite. The cryovial was vortexed for 30 min, following which the filter fragments were discarded and the remaining Tris:EDTA was distributed equally to five 1.5mL microfuge tubes. These were centrifuged (10,800 g for 30 min at 4°C), and then 900 μ l Tris:EDTA was removed by pipette from the top of each tube and discarded. The remaining Tris:EDTA (100 μ l) in each tube was vortexed for 15 min and the contents of all five tubes pooled by placing into a single microfuge tube. The pooled Tris:EDTA (500 μ l) was again centrifuged (10,800 g for 30 min at 4°C), following which 400 μ l was removed from the top and discarded. The remaining 100 μ l contained all of the microbial cells that were present in the original 1000mLVW sample. DNA was

isolated from this 100 µl cell suspension by the QIAamp DNA Mini Kit (Qiagen, Germany), following manufacturer's protocol.

Assessment of metataxonomic diversity in the *Shivlinga* vent-water community

V3 regions of all 16S rRNA genes present in the total environmental DNA extracted from the VW sample were PCR-amplified using Bacteria-/Archaea-specific universal oligonucleotide primers and sequenced by Ion Torrent Personal Genome Machine (Ion PGM) (Thermo Fisher Scientific), following the fusion primer protocol described previously^{25,26}. For bacterial 16S rRNA genes, amplification was carried out using the universal forward primer 341f (5' - CCTACGGGAGGCAGCAG - 3') prefixed with an Ion Torrent adapter and a unique sample-specific barcode or multiplex identifier; the reverse primer had a trP1 adapter followed by the universal reverse primer 515r (5' - TATTACCGCGGCTGCTGG - 3'). To amplify archaeal 16S rRNA genes, we used the universal forward primer 344f (5' - AATTGGANTCAACGCCGG - 3') prefixed with an Ion Torrent adapter and a unique sample-specific barcode or multiplex identifier; the reverse primer had a trP1 adapter followed by the universal reverse primer 522r (5' - TCGRCGGCCATGCACCWC - 3'). Prior to sequencing, size distribution and DNA concentration within the V3 amplicon pool was checked using a Bioanalyzer 2100 (Agilent Technologies) and adjusted to 26 pM. Amplicons were then attached to the surface of Ion Sphere Particles (ISPs) using an Ion Onetouch 200 Template kit (Thermo Fisher Scientific). Manually enriched, templated-ISPs were then sequenced by PGM on an Ion 316 Chip for 500 flows.

Before retrieval from the sequencing machine, all reads were filtered by the inbuilt PGM software to remove low-quality- and polyclonal-sequences; sequences matching the PGM 3' adaptor were also trimmed. The sequence file was deposited to the NCBI Sequence Read Archive (SRA) with the run accession number SRR2904995 under the BioProject accession number PRJNA296849. Reads were filtered a second time for high quality value (QV 20) and length threshold of 100 bp; OTUs were created at 97% identity level using the various modules of UPARSE⁸⁶, and singletons were discarded. A Perl programming-script, available within UPARSE, was used to determine the Abundance-based Coverage Estimator, and Shannon and Simpson Indices. Rarefaction analysis was carried out using the Vegan Package in R⁸⁷. The consensus sequence of every OTU was taxonomically classified by the RDP Classifier tool located at <http://rdp.cme.msu.edu/classifier/classifier.jsp>.

Extraction, sequencing and analysis of metagenomes from the mat communities

Total community DNA (metagenome) was extracted separately from each of the duplicate samples available for all the mat communities using PowerMax Soil DNA Isolation Kit (MoBio, Carlsbad, CA, USA). Deep-shotgun sequencing of the 16 metagenomes obtained was carried out as described previously²⁵. The Ion PGM or the Ion Proton platforms (Thermo Fisher Scientific) were employed for this purpose, using 400-bp read chemistry on the Ion 318 chip or 200-bp read chemistry on the PI V2 chip, respectively. All metagenomic readsets (mean read-length 138-231 nucleotides) were deposited to the NCBI SRA under the BioProject PRJNA296849 with the run accession numbers provided in Supplementary Tables 4 and 5.

The two metagenomic readsets sequenced from the sample replicates of each mat community were annotated separately by searching against the nr protein sequence database of NCBI, using the Organism Abundance tool of MG-RAST⁸⁸. In the process, two independent values were obtained for the relative abundance of every taxon within a community. Subsequently, mean relative abundance of each taxon was calculated using the duplicate values, and then used for comparisons between communities along the hydrothermal gradients. To determine the significance of population fluctuation for a taxon between community 'x' and community 'y', its mean relative abundance values in 'x' and 'y' were compared in combination with the actual ranges of the data (i.e. the independent relative abundance values). From 'x' to 'y', relative abundance of a taxon was considered to have increased significantly when the lower range of its relative abundance in 'y' was greater than the upper range of the corresponding value in 'x'. Similarly, a taxon was considered to have declined significantly from 'x' to 'y' when the upper range of its relative abundance in 'y' was smaller than the lower range of the corresponding value in 'x'. In this way it could be ascertained whether the inferred relative abundance fluctuations were significant.

Within the MG-RAST pipeline, sequences were trimmed so as to contain no more than five bases below the Phred quality score of 15; taxonomic classification of reads was carried out using the Organism Abundance tool following the Best Hit Classification algorithm. For classification down to the phylum-, class- or genus-level, read sets were searched by BlastX against the nr protein sequence database with a minimum alignment length of 45 bp (15 amino acids) and a minimum identity cut-off point of 60%. Percentage allocation of metagenomic reads to individual taxa (whether at the phylum-, class- or genus-level) was considered as a direct measure of the relative abundance of those taxa within the community in question^{25,89}. Furthermore, to corroborate the genus-level identifications, each read set was searched for 16S rRNA genes against the RDP database using BlastN with minimum alignment length of 50 bp and 70% minimum identity cut-off. A read was assigned to a

genus only when it shared >94% 16S rRNA sequence identity with a known species of that genus. Maximum e-value cut-off used in all the above analyses was $1e^{-5}$. Matching of DG3-sample-derived metagenomic reads with the 16S rRNA gene sequences (FN556455 through FN556457) of some mesophilic *Paracoccus* strains isolated previously from DG3-equivalent (52°C) *Shivlinga* mat samples validated that the above method was efficient in not only detecting microorganisms that are potentially present in small quantities but also adept to classifying metagenomic reads up to the genus level. Furthermore, it corroborated that *Shivlinga*'s microbial communities, including the mesophilic components, were structurally stable over time.

Statistical analysis of associations between variables

Pair-wise Pearson correlation coefficients (r) were determined to quantify the level of association existing between variations in the mean relative abundances of individual phyla along the wet thermal gradient and the *insitu* parameters such as temperature, pH, distance from the vent and flow-rate. In these single-inference statistical procedures a confidence level corresponding to P-value <0.05 was considered as indicative of significant correlation between a pair of variables – this implied that there was a probability of 0.05 for the null hypothesis to be rejected mistakenly and the inference to be actually insignificant. However, these confidence levels (P-values) were applicable to the individual statistical tests and could not be considered simultaneously in multiple-comparison procedures involving individual families of tests (such as those for individual phyla versus temperature), which were desirable in the present scenario. Towards the latter end, P values were subjected to correction for multiple testing using Benjamini-Hochberg method for controlling false discovery rate⁹⁰; this was carried out separately for mean relative abundances of individual phyla along the wet thermal gradient versus temperature, pH, distance from vent center, or flow rate. Benjamini-Hochberg critical value was determined as $(i \div m) * Q$ where i = rank of the individual p-value, m = total number of tests, and Q = the false discovery rate (presently taken as 20%).

Quantification of microbial diversity in the mat communities using metagenomic data

Microbial diversity within each mat community was estimated, as described previously²⁵, by using the mean relative abundance value for each bacterial phylum/proteobacterial class present to calculate Simpson Dominance and, Shannon–Wiener Diversity and Evenness Indices⁹¹. First, to quantify the extent to which the different bacterial phyla/proteobacterial classes dominated a given community, Simpson Dominance Index was determined using Equation 1 (below). Here, the n_i/n ratio, denoted as p_i , gave the proportion of representation of the i^{th} bacterial phylum/proteobacterial class in the community, while S denoted the total number of such taxa present. The mean percentage

of all metagenomic reads ascribable to a bacterial phylum/proteobacterial class (Supplementary Tables 34 and 35) was taken as its n_i/n value (Supplementary Tables 13-20). Shannon Diversity Index (H) was calculated using Equation 2 (below): first the p_i [or the (n_i / n)] value of each phylum was taken as above; then each p_i value was multiplied by its natural logarithm ($\ln p_i$); in the end, the $(p_i \times \ln p_i)$ products obtained for all the bacterial phyla and proteobacterial classes were summed-up and multiplied by -1. In order to determine whether there is evenness within a community in terms of the prevalence (relative abundance) of bacterial phyla/proteobacterial classes, Shannon Equitability Index (E_H) was calculated using Equation 3 (below). E_H was determined by dividing the H value of the community by H_{\max} , which is known to be equal to $\ln S$ (S denoted the total number of phyla and proteobacterial class present).

$$D = \sum_{i=1}^S \left(\frac{n_i}{n}\right)^2 = \sum p_i^2 \quad \text{Equation 1}$$

$$H = - \sum_{i=1}^S p_i \ln p_i \quad \text{Equation 2}$$

$$E_H = \frac{H}{H_{\max}} = \frac{H}{\ln S} \quad \text{Equation 3}$$

Functional analysis of the mat metagenomes

For each mat community, a complete gene catalogue was prepared by searching, and functionally annotating, its merged metagenomic readset against the EggNOG (evolutionary genealogy of genes: Non-supervised Orthologous Groups) database⁹². Genes ascribable to Clusters of Orthologous Groups (COGs) of Proteins⁹³ were shortlisted from the catalogue, and the COG-counts under individual functional categories were determined for the community. Whether individual COG-counts under different functional categories across the eight communities were significantly high or low was determined by Chi Square test. The contingency table for this test (Supplementary Table 36) was constructed with the help of an *inhouse* script (P value < 0.001 was used as the cut-off for estimating whether attendance of COGs within a functional category was high or low for a community). Here, pair-wise differential COG-count for two functional categories was placed in two rows (with a degree of freedom =1) in the 2x2 contingency table and the Chi Square significance test performed for the two individual communities. Furthermore, hierarchical clustering⁹⁴ was carried out to quantitatively decipher the relatedness between the mat communities in terms of their enrichment of various COG categories. Heat map depicting the results of hierarchical cluster analysis was drawn with an *in house* R script (Supplementary Note 3) using complete linkage method (Johnson's maximum method)⁹⁵.

In addition to the above analyses, diversities of ecophysiological important functional genes within individual mat communities were separately determined by searching their total metagenomic reads against the Protein Subsystems database using the Functional Abundance tool and Hierarchical Classification algorithm of MG-RAST⁸⁸ [with minimum alignment length of 45 bp (15 amino acids) and minimum identity cutoff of 60%]; total number of species-level matches for each of the relevant functional genes was also identified. In this way, diversities of true thermophiles (organisms that grow in the laboratory exclusively at $\geq 80^{\circ}\text{C}$), autotrophs, heterotrophs, sulfur-chemolithotrophs, aerobes, and anaerobes were estimated within each community, and then compared across the hydrothermal gradients.

Data availability

All sequence data sets generated under this study are available in the NCBI SRA repository under the BioProject accession number PRJNA296849 (<https://www.ncbi.nlm.nih.gov/sra>).

References

1. Wächtershäuser, G. From volcanic origins of chemoautotrophic life to Bacteria, Archaea and Eukarya. *Phil. Trans. R. Soc. B* **361**, 1787-1806 (2006).
2. Martin, W., Baross, J., Kelley, D., & Russell, MJ. Hydrothermal vents and the origin of life. *Nat. Rev. Microbiol.* **6**,805-814 (2008).
3. Stevenson, A. et al. Multiplication of microbes below 0.690 water activity: implications for terrestrial and extraterrestrial life. *Environ. Microbiol.* **17**,257-277 (2015).
4. Fields P. A. Protein function at thermal extremes: balancing stability and flexibility. *Comp. Biochem. Physiol. A Mol. Integr. Physiol.* **129**,417-431 (2001).
5. Hallsworth, J. E. et al. Limits of life in MgCl_2 -containing environments: chaotropicity defines the window. *Environ. Microbiol.* **9**,801-813 (2007).
6. Chin, J. P. et al. Solutes determine the temperature windows for microbial survival and growth. *Proc. Natl. Acad. Sci.* **107**,7835-7840 (2010).
7. Yakimov, M. M. et al. Microbial community of the deep-sea brine Lake Kryos seawater-brine interface is active below the chaotropicity limit of life as revealed by recovery of mRNA. *Environ. Microbiol.* **17**,364-382 (2015).
8. Ball, P. & Hallsworth, J. E. Water structure and chaotropicity: their uses, abuses and biological implications. *Phys. Chem. Chem. Phys.* **17**,8297-8305 (2015).
9. Bhaganna, P., Bielecka, A., Molinari, G., & Hallsworth, J. E. Protective role of glycerol against benzene stress: insights from the *Pseudomonasputida* proteome. *Curr. Genet.* **62**,419-429 (2016).

10. Cono, V. L. et al. The discovery of Lake Hephæstus, the youngest magnesium-saturated athalassohaline formation on Earth. *Sci. Rep.* **9**, 1679; 10.1038/s41598-018-38444-z (2019).
11. Cray, J. A., Russell, J. T., Timson, D. J., Singhal, R. S., & Hallsworth, J. E. A universal measure of chaotropicity and kosmotropicity. *Environ. Microbiol.* **15**, 287-296 (2013).
12. Bhaganna, P. et al. Hydrophobic substances induce water stress in microbial cells. *Microbiol. Biotechnol.* **3**, 701-716 (2010).
13. Brown, A. D. *Microbial water stress physiology* (John Wiley and Sons, 1990).
14. Koynova, R., Brankov, J., & Tenchov, B. Modulation of lipid phase behavior by kosmotropic and chaotropic solutes: Experiment and thermodynamic theory. *Eur. Biophys. J.* **25**, 261-274 (1997).
15. Wiggins, P. M. High and low density water and resting, active and transformed cells. *Cell. Biol. Int.* **20**, 429-435 (1996).
16. Hribar, B. et al. How ions affect the structure of water. *J. Am. Chem. Soc.* **124**, 12302-12311 (2002).
17. Hallsworth, J. E., Prior, B. A., Nomura, Y., Iwahara, M., & Timmis, K. N. Compatible solutes protect against chaotrope (ethanol)-induced, nonosmotic water stress. *Appl. Environ. Microbiol.* **69**, 7032-7034 (2003).
18. de Lima Alves, F. et al. Concomitant osmotic and chaotropicity-induced stresses in *Aspergillus wentii*: compatible solutes determine the biotic window. *Curr. Genet.* **61**, 457-477 (2015).
19. Cray, J. A. et al. Chaotropicity: a key factor in product tolerance of biofuel-producing microorganisms. *Curr. Opin. Biotechnol.* **33**, 228-259 (2015).
20. Reysenbach, A.L., Ehringer, M., & Hershberger, K. Microbial diversity at 83 degrees C in Calcite Springs, Yellowstone National Park: another environment where the Aquificales and "Korarchaeota" coexist. *Extremophiles* **4**, 61-67 (2000).
21. Blank, C.E., Cady, S.L., & Pace, N.R. Microbial composition of near-boiling silica-depositing thermal springs throughout Yellowstone National Park. *Appl. Environ. Microbiol.* **68**, 5123-5135 (2002).
22. Lacap, D. C., Barraquio, W., & Pointing, S. B. Thermophilic microbial mats in a tropical geothermal location display pronounced seasonal changes but appear resilient to stochastic disturbance. *Environ. Microbiol.* **9**, 3065-3076 (2007).
23. Reigstad, L. J., Jorgensen, S. L., & Schleper, C. Diversity and abundance of Korarchaeota in terrestrial hot springs of Iceland and Kamchatka. *ISME J.* **4**, 346-356 (2010).
24. Chan, C.S., Chan, K.G., Tay, Y.L., Chua, Y.H., & Goh, K.M. Diversity of thermophiles in a Malaysian hot spring determined using 16S rRNA and shotgun metagenome sequencing. *Front. Microbiol.* **6**, 177; 10.3389/fmicb.2015.00177 (2015).

25. Ghosh, W. et al. Resilience and receptivity worked in tandem to sustain a geothermal mat community amidst erratic environmental conditions. *Sci. Rep.* **5**, 12179; 10.1038/srep12179 (2015).
26. Roy, C. et al. Global Association between Thermophilicity and Vancomycin Susceptibility in Bacteria. *Front. Microbiol.* **7**, 412; 10.3389/fmicb.2016.00412(2016).
27. Miller, S.R., Strong, A.L., Jones, K.L., &Ungerer, M.C. Bar-coded pyrosequencing reveals shared bacterial community properties along the temperature gradients of two alkaline hot springs in Yellowstone National Park. *Appl. Environ. Microbiol.* **75**, 4565-4572 (2009).
28. Cole, J.K. et al. Sediment microbial communities in Great Boiling Spring are controlled by temperature and distinct from water communities. *ISME J.* **7**, 718-729 (2013).
29. Johnson, D. B., Okibe, N., & Roberto, F. F. Novel thermo-acidophilic bacteria isolated from geothermal sites in Yellowstone National Park: physiological and phylogenetic characteristics. *Arch. Microbiol.* **180**, 60-68 (2003).
30. Roeselers, G. et al. Diversity of phototrophic bacteria in microbial mats from Arctic hot springs (Greenland). *Environ. Microbiol.* **9**, 26-38 (2007).
31. Owen, R. B., Renaut, R. W., & Jones, B. Geothermal diatoms: a comparative study of floras in hot spring systems of Iceland, New Zealand, and Kenya. *Hydrobiologia* **610**, 175-192 (2008).
32. Hall, J.R. et al. Molecular characterization of the diversity and distribution of a thermal spring microbial community by using rRNA and metabolic genes. *Appl. Environ. Microbiol.* **74**, 4910-4922 (2008).
33. Meyer-Dombard, D. R. et al. Hydrothermal ecotones and streamer biofilm communities in the Lower Geyser Basin, Yellowstone National Park. *Environ. Microbiol.* **13**, 2216-2231 (2011).
34. Everroad, R.C., Otaki, H., Matsuura, K., &Haruta, S. Diversification of bacterial community composition along a temperature gradient at a thermal spring. *Microbes Environ.* **27**, 374-381 (2012).
35. Swingley, W.D. et al. Coordinating environmental genomics and geochemistry reveals metabolic transitions in a hot spring ecosystem. *PLoS One* **7**, e38108; 10.1371/journal.pone.0038108 (2012).
36. Huang, Q. et al. Archaeal and bacterial diversity in acidic to circumneutral hot springs in the Philippines. *FEMS Microbiol. Ecol.* **85**, 452-464 (2013).
37. Wang, S. et al. Control of temperature on microbial community structure in hot springs of the Tibetan Plateau. *PLoS One* **8**, e62901; 10.1371/journal.pone.0062901 (2013).
38. Sharp, C.E. et al. Humboldt's spa: microbial diversity is controlled by temperature in geothermal environments. *ISME J.* **8**, 1166-1174 (2014).

39. Skirnisdottir, S. et al. Influence of sulfide and temperature on species composition and community structure of hot spring microbial mats. *Appl. Environ. Microbiol.* **66**, 2835-2841 (2000).
40. Garrett, D. E. *Borates: handbook of deposits, processing, properties, and use*(Academic Press, 1998).
41. Rai, A. P. Compilation of data on chemical analysis of water and gas samples from North West Himalaya and adjoining areas, Bulletin Series-C, No. 5, Geological Survey of India, Kolkata.(2001).
42. Ghosh, W. et al. Molecular and Cellular Fossils of a Mat-Like Microbial Community in Geothermal Boratic Sinters. *Geomicrobiol. J.* **29**,879-885 (2012).
43. Riding, R. Microbial carbonates: the geological record of calcified bacterial–algal mats and biofilms. *Sedimentology***47**, 179-214 (2000).
44. Harinarayana, T. et al. Exploration of geothermal structure in Puga geothermal field, Ladakh Himalayas, India by magnetotelluric studies. *J. Appl. Geophys.***58**,280-295 (2006).
45. Hunt, T.M. Geothermal resources in New Zealand: An overview. *GHC Bulletin***19**, 5-9 (1998).
46. Hetzer, A., Morgan, H.W., McDonald, I.R. & Daughney, C.J. Microbial life in Champagne Pool, a geothermal spring in Waiotapu, New Zealand. *Extremophiles***11**, 605-614 (2007).
47. Marchesi, J. R. & Ravel, J. The vocabulary of microbiome research: a proposal. *Microbiome.* **3**, 31; 10.1186/s40168-015-0094-5(2015).
48. Schoenfeld, T. et al. Assembly of Viral Metagenomes from Yellowstone Hot Springs. *Appl. Environ. Microbiol.***74**,4164-4174 (2008).
49. Schaefer, D. G. & Zryd, J. The Moss *Physcomitrella patens*, Now and Then. *Plant Physiol.***127**,1430-1438 (2001).
50. Matsuzaki, M. et al. Genome sequence of the ultrasmall unicellular red alga *Cyanidioschyzon merolae* 10D. *Nature***428**, 653-657 (2004).
51. Eichinger, L. & Noegel, A. A. Crawling in to a new era – the *Dictyostelium* genome project. *EMBO J.* **22**, 1941-1946 (2003).
52. Nicholson, W. L. et al. Exploring the low-pressure growth limit: Evolution of *Bacillus subtilis* in the laboratory to enhanced growth at 5 Kilopascals. *Appl. Environ. Microbiol.***76**,7559-7565 (2010).
53. Hallsworth, J. E., Heim, S., & Timmis, K. N. Chaotropic solutes cause water stress in *Pseudomonas putida*. *Environ. Microbiol.***5**,1270-1280 (2003).
54. Cray, J. A. et al. Biocontrol agents promote growth of potato pathogens, depending on environmental conditions. *Microb. Biotechnol.* **9**, 330-354 (2016).

55. Stevenson, A. et al. Is there a common water-activity limit for the three domains of life? *ISME J.* **9**,1333-1351 (2015).
56. Forterre, P., Bergerat, A., & Lopez-Garcia, P. The unique DNA topology and DNA topoisomerases of hyperthermophilic archaea. *FEMS Microbiol. Rev.* **18**, 237-248 (1996).
57. Hugler, M., Wirsén, C. O., Fuchs, G., Taylor, C. D., & Sievert, S. M. Evidence for autotrophic CO₂ fixation via the reductive tricarboxylic acid cycle by members of the epsilon subdivision of proteobacteria. *J. Bacteriol.* **187**,3020-3027 (2005).
58. Berg, I. A. et al. Autotrophic carbon fixation in archaea. *Nat. Rev. Microbiol.* **8**,447-460 (2010).
59. Sauer, U. & Eikmanns, B. J. The PEP-pyruvate-oxaloacetate node as the switch point for carbon flux distribution in bacteria. *FEMS Microbiol. Rev.* **29**,765-794 (2005).
60. Ghosh, W. & Dam, B. Biochemistry and molecular biology of lithotrophic sulfur-oxidation by taxonomically and ecologically diverse bacteria and archaea. *FEMS Microbiol. Rev.* **33**,999-1043 (2009).
61. Iwata, S. Structure and function of bacterial cytochrome c oxidase. *J. Biochem.* **123**,369-375 (1998).
62. Loy, A., Duller, S., & Wagner, M. *Evolution and Ecology of Microbes Dissimilating Sulfur Compounds: Insights from Siroheme Sulfite Reductases*(ed. Dahl, C.& Friedrich, C.G.) 46-59 (Springer, 2008).
63. de Gier, J. W. et al. Structural and functional analysis of aa3-type and cbb3-type cytochrome c oxidases of *Paracoccus denitrificans* reveals significant differences in proton-pump design. *Mol. Microbiol.* **20**,1247-1260 (1996).
64. Ekici, S., Pawlik, G., Lohmeyer, E., Koch, H. G., & Daldal, F. Biogenesis of cbb3-type cytochrome c oxidase in *Rhodobacter capsulatus*. *Acta .Biophys .Biochim* **1817**,898-910 (2012).
65. Kubo, K., Knittel, K., Amann, R., Fukui, M., & Matsuura, K. Sulfur-metabolizing bacterial populations in microbial mats of the Nakabusa hot spring, Japan. *Syst. Appl. Microbiol.* **34**, 293-302 (2011).
66. van der Meer, M. T. et al. Diel variations in carbon metabolism by green nonsulfur-like bacteria in alkaline siliceous hot spring microbial mats from Yellowstone National Park. *Appl. Environ. Microbiol.* **71**, 3978-3986 (2005).
67. van der Meer, M. T. et al. Alkane-1, 2-diol-based glycosides and fatty glycosides and wax esters in *Roseiflexus castenholzii* and hot spring microbial mats. *Arch. Microbiol.* **178**, 229-237 (2002).
68. Ramanan, R., Kim, B. H., Cho, D. H., Oh, H. M., & Kim, H. S. Algae-bacteria interactions: Evolution, ecology and emerging applications. *Biotechnol. Adv.* **34**, 14-29 (2016).
69. Burns, B. Vegetation change along a geothermal stress gradient at the Te Kopia streamfield. *J. Roy. Soc. New Zeal.* **27**, 279-294 (1997).

70. Convey, P. & Lewis Smith, R. I. Geothermal bryophyte habitats in the South Sandwich Islands, maritime Antarctic. *J. Veg. Sci.* **17**, 529-538 (2006).
71. Kis-Papo, T., Kirzhner, V., Wasser, S. P., & Nevo, E. Evolution of genomic diversity and sex at extreme environments: fungal life under hypersaline Dead Sea stress. *Proc. Natl. Acad. Sci.* **100**, 14970-14975 (2003).
72. Eppley, S. M., Rosenstiel, T. N., Graves, C. B., & Garcia, E. L. Limits to sexual reproduction in geothermal bryophytes. *Int. J. Plant Sci.* **172**, 870-878 (2011).
73. Kantidze, O. L., Velichko, A. K., Luzhin, A. V., & Razin, S. V. Heat Stress-Induced DNA Damage. *Acta Naturae* **8**, 75-78 (2016).
74. Reski, R. Development, genetics and molecular biology of mosses. *Bot. Acta* **111**, 1-15 (1998).
75. Markmann-Mulisch, U. et al. Differential Requirements for RAD51 in *Physcomitrella patens* and *Arabidopsis thaliana* Development and DNA Damage Repair. *Plant Cell* **19**, 3080-3089 (2007).
76. Cray, J. A. et al. The biology of habitat dominance; can microbes behave as weeds? *Microb. Biotechnol.* **6**, 453-492 (2013).
77. Rummel, J. D. et al. A new analysis of Mars "Special Regions": findings of the second MEPAG Special Regions Science Analysis Group (SR-SAG2). *Astrobiology* **14**, 887-968 (2014).
78. Rantz, S. E. *Measurement of discharge by tracer dilution. In: Measurement and computation of streamflow: volume 1. Measurement of stage and discharge* 211-259 (United States Geological Survey and U.S. Government Printing Office, 1982).
79. Mathon, B. R., Schoonen, M. A., Riccardi, A. L., & Borda, M. J. Measuring flow rates and characterizing flow regimes in hot springs. *Appl. Geochem.* **62**, 234-246 (2015).
80. Grasshoff, K., Kremling, K., & Ehrhardt, M. *Methods of seawater analysis* 206-207 (John Wiley & Sons, 1999).
81. Lewis, E. & Wallace, D. W. R. CO2SYS_calc_DOS_Original, program developed for CO₂ system calculations ORNL/CDIAC-105. Carbon Dioxide Information Analysis Center Oak Ridge National Laboratory, US Department of Energy, Oak Ridge, Tennessee. (1998).
82. Kelly, D. P. & Wood, A. P. Synthesis and determination of thiosulfate and polythionates. *Methods Enzymol.* **243**, 475-501 (1994).
83. Alam, M., Pyne, P., Mazumdar, A., Peketi, A., & Ghosh, W. Kinetic enrichment of ³⁴S during proteobacterial thiosulfate oxidation and the conserved role of SoxB in S-S bond breaking. *Appl. Environ. Microbiol.* **79**, 4455-4464 (2013).
84. West, P. W. & Gaeke, G. C. Fixation of sulfur dioxide as disulfitomercurate (II) and subsequent colorimetric estimation. *Anal. Chem.* **28**, 1816-1819 (1956).
85. Cline, J. D. Spectrophotometric determination of hydrogen sulfide in natural water. *Anal. Chem.* **41**, 454-458 (1969).

86. Edgar, R. C. UPARSE: highly accurate OTU sequences from microbial amplicon reads. *Nat. Methods***10**,996-998 (2013).
87. R Core, Team. R: A Language and Environment for Statistical Computing. Vienna: R Core Team. <http://www.R-project.org/>. (2014).
88. Meyer, F. et al. The metagenomics RAST server - a public resource for the automatic phylogenetic and functional analysis of metagenomes. *BMC Bioinformatics***9**,386; 10.1186/1471-2105-9-386 (2008).
89. Tringe, S. G. et al. Comparative metagenomics of microbial communities. *Science***308**, 554-557 (2005).
90. Benjamini, Y. & Hochberg, Y. Controlling the false discovery rate: a practical and powerful approach to multiple testing. *J. R. Stat. Soc. B Stat. Methodol.* **1**,289-300 (1995).
91. Magurran, A. E. *Measuring biological diversity*(Blackwell Publishing Limited, 2003).
92. Huerta-Cepas, J. et al. eggNOG 4.5: a hierarchical orthology framework with improved functional annotations for eukaryotic, prokaryotic and viral sequences. *Nucleic Acids Res.***44**,286-293 (2016).
93. Tatusov, R. L. et al. The COG database: an updated version includes eukaryotes. *BMC. Bioinformatics***4**, 41; 10.1186/1471-2105-4-41(2003).
94. Köhn, H. F. & Hubert, L. J. Hierarchical cluster analysis. Wiley StatsRef: Statistics Reference Online. **14**,1-3 (2014).
95. Johnson, S. C. Hierarchical clustering schemes. *Psychometrika***32**,241-54 (1967).

Acknowledgements

This research was financed by Bose Institute as well as Science and Engineering Research Board (SERB), Government of India (GoI) (SERB grant numbers were SR/FT/LS-204/2009 and EMR/2016/002703). Sri Pankaj Kumar Ghosh (Chinsurah, West Bengal, India) provided additional travel grants philanthropically. We are indebted to our friends Asgar Ali, Baishali Ghosh, Bikash Jana, Lotus Sonam, Amrit Pal Singh, Rimjhim Bhattacharjee and Srabana Bhattacharjee for on-field support during the explorations of the *Shivlinga* site. CR and MJR received fellowships from University Grants Commission, GoI. PP and RR received fellowships from the Council of Scientific & Industrial Research, GoI. SB received fellowship from Bose Institute. SM received fellowship from Department of Science and Technology, GoI. NM received fellowship from SERB, GoI.

Author contributions

WG initiated and developed the work, designed the experiments, interpreted the results and wrote the paper along with JEH and RC. JEH and RC also helped interpret the results alongside SKM and AM.

CR anchored the metagenomic work, and performed the laboratory experiments and bioinformatic analyses. WG, CR, MJR, PKH and PP carried out the fieldworks. MJR, PKH, NM, UB, PP, SB, RR and SM participated in metagenomic experiments and bioinformatic analyses. AP, SF and AM carried out the geochemical analyses. TM performed the statistical analyses. WG, PKH, PP and CR performed the microscopic studies. WKO worked towards improving the text and documents. All authors read and vetted the manuscript.

Competing interests

The authors declare no competing interests.

Additional Information

Supplementary information is available in the online version of the paper.

Figure legends

Figure 1. The environmental context of the *Shivlinga* microbialite hot-spring system at the time of sampling on 23 July 2013: (A) the three geomicrobiological zones, scale bar represents 1 m; (B) view of *Shivlinga*'s microbial communities showing the spring-water transit that represented the wet thermal gradient, scale bar represents 1 m; (C) microbialite body showing the vent and position of the two thermal gradients that were sampled, scale bar represents 10 cm; (D) bedrock slope around *Shivlinga*'s base, showing the microflora, scale bar represents 10 cm; (E and F) WG6 and WG7, respectively, scale bars represent 5 cm for E and 10 cm for F. For (G), the light blue circle indicates the microbialite body, the yellow oval demarcation indicates the bedrock slope around the base, the purple oval demarcation shows *Shivlinga*'s apron, and the cyan arrow shows the direction of water flow through the apron, away from the microbialite hot spring. For (H), the cyan curved-line with an arrow-head shows the meandering path of the spring-water along the apron, away from the microbialite body (this also represents part of the wet thermal gradient), the pink triangles indicate the sample sites for WG6 and WG7, the orange triangle indicates the location of the Sinter-Sample 4 (SS4). For (I), the green curved-line with an arrow-head indicates the trajectory of the drying thermal gradient, while the cyan curved-line with an arrow-head indicates part of the wet thermal gradient which starts at the vent and leads to the first mat of the bedrock slope (the latter also represents the direction of water flow); the red triangles indicate the position of the sampled communities VW and VWM; the green triangles indicate the sampling-positions for communities DG3 and DG4; the pink triangles indicate the sample sites for WG3 and WG4; and the orange triangles indicate the locations of the Sinter-Samples 1, 2 and 5 (SS1, SS2 and SS5, respectively). For (J), the cyan curved-line with an arrow-head indicates part of the wet thermal gradient that runs along the bedrock slope surrounding *Shivlinga*'s base; the pink triangles indicate the sample sites for WG4 and WG5; and the orange triangle indicates the location of the Sinter-Sample 3 (SS3). For (K) and (L), the pink triangles indicate the sampling-positions for communities WG6 and WG7, while the cyan curved-lines with an arrow-head each show the direction of water flow.

Figure 2. Macro-/micro-scale microbe-mineral structures at the *Shivlinga* site: (A) green microbial mat (pink arrows), and white spherules (red arrow) that collectively form shrub-like mineral bodies (orange circle), on the upper surfaces of the vent's rim (blue scale bar = 10 mm); (B) sinter particles from 5-cm-deep inside the wall of the microbialite, associated with bacterial filaments (red arrow); these microbe-mineral assemblages had formed within *Shivlinga*'s vent-water (image was taken using SEM, blue scale bar = 150 μ m); and (C) a diatom cell (golden arrow) associated with the particles shown in (B) (using SEM, blue scale bar = 20 μ m).

Figure 3. Microbial structures from the *Shivlinga* site: (A and B) microbial cell filaments from streamers of VWM and WG3, respectively; (C) microbial biomass of DG3; (D) diatoms from the

surface of the microbial mass which makes up WG4 and DG4 (**D1** and **D2** respectively); (**E** and **F**) cells from the core of the microbial mass which makes up DG4 and WG5, respectively; (**G**) Chroococcales-like cyanobacteria in the core of the microbial mass which makes up DG3; (**H**) fungal hyphae and diatoms near the edge of the microbial mass which makes up DG4. All images were recorded using phase contrast microscopy except for (**C**) that was recorded using laser-scanning confocal microscopy. For (**C1**) excitation was carried out at 488 nm and detection at 630-650 nm; (**C2**) is a differential interference contrast image with blue arrows indicating diatom cells; and for (**C3**), excitation was carried out at 543 nm and detection at 650 nm.

Figure 4. Organization of microbial cells in the various layers of the WG7 sample: (row **A**) top-most layer of the microbial mat; (row **B**) sub-surface layer 1 (from a depth of 1-2mm); (row **C**) sub-surface layer 2 (from a depth of 3-4mm); and (row **D**) diatom cells and borax crystals in sub-surface layer 3 (from a depth of 5-8 mm); (Column **I**) images were taken using phase contrast microscopy; (column **II**, except row **D**) images were taken using laser-scanning confocal microscopy, at 488 nm excitation and 630-650 nm detection; (column **III**, except row **D**) used differential interference contrast to modify the image from column II; and (column **IV**, except row **D**) used laser-scanning confocal microscopy (543 nm excitation and long pass 650 nm detection) to further modify the image from column II. Photographs of (row **D**) were taken using phase contrast microscopy.

Figure 5. Mean percentage of reads ascribed to bacterial phyla, and classes within the *Proteobacteria*, in the duplicate metagenomes obtained from each mat community of (**A**) the drying thermal gradient and (**B**) the wet thermal gradient. The 21 phyla and five proteobacterial classes represented account for >0.1% reads in at least one of the 16 metagenomes analyzed. The category 'others' encompass the phyla that accounted for <0.1% reads in every metagenome analyzed. Statistical significance of the fluctuations in the relative abundance of the taxa along the hydrothermal gradients can be seen in Supplementary Figs. 4 and 5 where their mean relative abundance within each mat community has been plotted alongside the two original relative abundance values obtained from the duplicate metagenomes (shown as vertical range bar in Supplementary Figs. 4 and 5).

Figure 6. Variation of Simpson Dominance (**A** and **E**), Shannon Diversity (**B** and **F**) and Shannon Equitability (**C** and **G**) Indices, and that of the total genera count (**D** and **H**), along the drying (**A-D**), and wet (**E-H**), thermal gradients.

Figure 7. Functional analysis of the metagenomes isolated from the eight microbial mat communities of *Shivlinga*: (**A**) heat map comparing the richness of the metabolic/functional categories across the communities, determined in terms of the number of Clusters of Orthologous Groups (COGs) of Proteins that are ascribed to the categories in individual communities; a two-dimensional clustering is also shown, involving the eight mat communities on one hand and the 18 functional categories of COGs on the other; color gradient of the heat map varied from high (red) to low (green), through moderate (yellow), richness of the categories across the communities; (**B**) Statistically significant high (green circles) or low (red circles) richness of the functional categories across the communities, as determined by Chi Square test with $p < 0.001$.

Table 1. Microbial communities sampled at the *Shivlinga* ecosystem on 23 July 2013, and the temperature, pH, and flow-rate, of the vent-water, as well as those of the spring-water flowing over the mat samples, at the time of their collection.

* Measured by a measuring tape running along the flow of water.

Measuring moisture content was applicable only to the samples DG3 and DG4 of the progressively-drying

Name of the sample	Description of the sample	Distance, in cm, from the vent center*	Temperature, in °C, at the time of sampling	Moisture content, in % w/w, of the <i>Shivlinga</i> sinter on which the mat grew [#]	Flow rate of spring-water, in cm s ⁻¹ , at the sampling point [§]	pH
VW	Water discharged from <i>Shivlinga</i> 's vent	0	70	NA	25	7.0
VWM	White streamers made up of filamentous structures	8	66	NA	25	7.1
DG3	Green mat containing occasional red patches	11	52	41.7	NA	7.3
DG4	Purple mat with a greenish shimmer	14	41	28.9	NA	7.5
WG3	White streamer interspersed with green filaments	22	56	NA	22	7.5
WG4	Green mat containing occasional yellow patches	65	46	NA	15	8.0
WG5	Rust-colored mat	120	38	NA	11	8.2
WG6	Intensely red microbe-mineral nodules	190	36	NA	7	8.3
WG7	Dark grey streamers	290	33	NA	5	8.5

thermal gradient as these mats grew on moist sinter surfaces off the outflow channel. Flow rates were measured for all the other communities as they grew directly on the hot water outflow.

[§] Flow rate of water only at the vent (i.e. at sample sites of VW and VWM) was measured as ml s⁻¹.

Table 2. Microbial genera¹ that are comprised primarily of mesophilic strains (no laboratory growth reported at >45°C) and phylogenetic relatives of which were detected in *Shivlinga*'s mat communities growing at >50°C.

Phyla	Genera	Highest temperature at which culture-based growth has been reported	Reference ² pertaining to the highest temperature at which culture-based growth was reported	VW M (66°C)	DG3 (52°C)	DG4 (41°C)	WG 3 (56°C)	WG 4 (46°C)	W G5 (38°C)	W G6 (36°C)	W G7 (33°C)
<i>Bacteroidetes</i>	<i>Alistipes</i>	45°C	(Rautio <i>et al.</i> , 2003)	+	+	+	+	+	-	+	+
	<i>Cytophaga</i>	35°C	(Christensen, 1980)	+	+	+	-	+	+	+	+
	<i>Hymenobacter</i>	40°C	(Subhash <i>et al.</i> , 2014)	-	+	+	+	+	+	+	+
	<i>Flexithrix</i>	40°C	(Hosoya and Yokota, 2007)	-	+	+	+	+	+	+	+
	<i>Bacteroides</i>	45°C	(Hatamoto <i>et al.</i> , 2014)	-	-	+	+	+	-	+	+
	<i>Porphyromonas</i>	37°C	(Shah and Collins, 1988)	-	-	+	+	+	-	+	+
	<i>Flavobacterium</i>	30°C	(Bernardet and Bowman, 2015)	-	+	-	+	+	+	+	+
<i>Actinobacteria</i>	<i>Streptomyces</i>	42°C	(Han <i>et al.</i> , 2015)	-	+	+	+	+	+	+	+
	<i>Propionibacterium</i> ³	45°C	(Koussimon <i>et al.</i> , 2001)	-	+	-	+	+	-	-	+
	<i>Actinoplanes</i>	37°C	(Sun <i>et al.</i> , 2009)	+	+	-	+	+	-	-	-
	<i>Enterorhabdus</i>	40°C	(Clavel <i>et al.</i> , 2010)	-	-	-	+	+	-	-	-
	<i>Kitasatospora</i>	42°C	(Zhang <i>et al.</i> , 1997)	-	+	-	+	+	-	-	+

Proteobacteria	<i>Pseudomonas</i>	41°C	(Wang <i>et al.</i> , 2016)	+	+	+	+	+	+	+	+
	<i>Acinetobacter</i>	44°C	(Rooney <i>et al.</i> , 2016)	-	+	-	-	+	+	+	-
	<i>Thiobacillus</i>	42°C	(Brinkhoff <i>et al.</i> , 1999)	+	-	-	+	-	-	-	-
	<i>Acidithiobacillus</i>	45°C	(Kelly and Wood, 2000)	+	+	-	-	+	-	-	-
	<i>Campylobacter</i>	42°C	(Koziel <i>et al.</i> , 2014)	+	+	-	+	+	-	-	+
	<i>Thiohalocapsa</i>	30°C	(Anil Kumar <i>et al.</i> , 2009)	+	-	-	-	-	-	-	-
	<i>Xanthomonas</i>	45°C	(Rautio <i>et al.</i> , 2003)	-	-	+	+	+	-	+	+
	<i>Helicobacter</i>	35°C	(Christensen, 1980)	-	+	+	+	+	+	+	+
	<i>Magnetospirillum</i>	30°C	(Schleifer <i>et al.</i> , 1991)	-	-	-	+	+	-	-	+
	<i>Comamonas</i>	44°C	(Chang <i>et al.</i> , 2002)	-	-	-	+	-	-	-	-
	<i>Neisseria</i>	42°C	(Wolfgang <i>et al.</i> 2011)	-	-	-	+	-	-	-	-
	<i>Halochromatium</i>	35°C	(Imhoff <i>et al.</i> , 1998)	-	-	-	+	-	-	-	-
	<i>Halorhodospira</i>	35°C	(Hirschler-Rea <i>et al.</i> , 2003)	-	-	-	+	+	-	-	-
	<i>Thiohalospira</i>	35°C	(Sorokin <i>et al.</i> , 2008)	-	-	-	+	-	-	-	-
	<i>Xylella</i>	28°C	(Wells <i>et al.</i> , 1987)	-	-	+	+	+	-	+	+
	<i>Marichromatium</i>	35°C	(Sucharita <i>et al.</i> , 2010)	-	-	-	+	+	-	-	-
	<i>Paracoccus</i>	40°C	(Kim <i>et al.</i> , 2010)	-	+	+	-	-	-	+	+
<i>Methylobacterium</i>	37°C	(Wood <i>et al.</i> , 1998)	-	+	-	-	-	+	+	+	
Cyanobacteria	<i>Gloeobacter</i>	37°C	(Castenholz,	-	-	-	+	+	-	-	-

			2001)								
	<i>Cylindrospermopsis</i>	35°C	(Briand <i>et al.</i> , 2004)	-	-	-	+	-	-	-	-
	<i>Nostoc</i>	25°C	(Castenholz, 2001)	-	-	+	+	+	+	-	+
	<i>Prochlorothrix</i>	30°C	(Castenholz, 2001)	-	+	-	+	+	+	+	+
	<i>Dolichospermum</i>	30°C	(Castenholz, 2001)	-	+	-	+	+	-	+	+
	<i>Planktothrix</i>	30°C	(Castenholz, 2001)	-	+	-	+	+	-	+	+
<i>Spirochaetes</i>	<i>Treponema</i>	30°C	(Evans <i>et al.</i> , 2009)	+	+	+	-	+	+	+	+
	<i>Leptospira</i>	37°C	(Smythe <i>et al.</i> , 2013)	-	+	+	+	+	+	+	+
<i>Tenericutes</i>	<i>Acholeplasma</i>	37°C	(Tully <i>et al.</i> , 1994)	+	-	+	-	-	-	+	+
<i>Firmicutes</i>	<i>Streptococcus</i>	45°C	(Sherman <i>et al.</i> , 1931)	+	-	+	-	+	-	-	+
	<i>Paenibacillus</i> ³	37°C	(Shida <i>et al.</i> , 1997)	+	-	-	+	+	+	+	+

¹ Identified in RDP searches of the metagenomes.

² References used in this table have been given in Supplementary References.

³ These genera were also identified in the V3 sequence-based OTU analysis of the VW community.

Supplementary Information for the paper

Microbiome and ecology of a hot spring-microbialite system on the Trans-Himalayan Plateau

Chayan Roy¹, Moidu Jameela Rameez¹, Prabir Kumar Haldar¹, Aditya Peketi², Nibendu Mondal¹, Utpal Bakshi³, Tarunendu Mapder⁴, Prosenjit Pyne¹, Svetlana Fernandes², Sabyasachi Bhattacharya¹, Rimi Roy^{1,\$}, Subhrangshu Mandal¹, William Kenneth O'Neill⁵, Aninda Mazumdar², Subhra Kanti Mukhopadhyay⁶, Ambarish Mukherjee⁷, Ranadhir Chakraborty⁸, John Edward Hallsworth⁵ and Wriddhiman Ghosh^{1*}

Addresses:

- ¹ Department of Microbiology, Bose Institute, P-1/12 CIT Scheme VIIM, Kolkata 700054, India.
- ² Gas Hydrate Research Group, Geological Oceanography, CSIR-National Institute of Oceanography, Dona Paula, Goa - 403004, India.
- ³ Microbiome Program, Center for Individualized Medicine, Mayo Clinic, Rochester, MN-55905, USA.
- ⁴ ARC CoE for Mathematical and Statistical Frontiers, School of Mathematical Sciences, Queensland University of Technology, Brisbane, QLD 4000, Australia.
- ⁵ Institute for Global Food Security, School of Biological Sciences, Queen's University Belfast, 19 Chlorine Gardens, Belfast, BT9 5DL, Northern Ireland.
- ⁶ Department of Microbiology, University of Burdwan, Burdwan, West Bengal 713104, India.
- ⁷ Department of Botany, University of Burdwan, Burdwan, West Bengal 713104, India.
- ⁸ Department of Biotechnology, University of North Bengal, Siliguri, West Bengal 734013, India.

Present Addresses:

- ^{\$} Department of Botany, Jagannath Kishore College, Purulia - 723101, West Bengal, India.

* **Correspondence:** Email: wriman@jcbose.ac.in; Wriman@rediffmail.com

Phone: +91-33-25693246

Fax: +91-33-23553886

Contents

Supplementary Notes

Supplementary Note 1. Geography, geology and geothermal activity of the study-site.

Supplementary Note 2. Phylogenomic diversity analysis for the individual *Shivlinga* mats.

Supplementary Note 3. The R script used to draw the heat map depicting the results of hierarchical cluster analysis.

Supplementary Figures

Supplementary Fig. 1. Location of Puga Valley in eastern Ladakh. (A) map showing the location of Leh, the capital of the union territory of Ladakh (red shape numbered as 1), and Puga Valley (red shape numbered as 2); (B) satellite image showing the position of *Shivlinga* (red shape numbered as 1) at the eastern extremity of Puga Valley, in context with the nearest village Sumdo (red shape numbered as 2) and the road that leads to Puga Valley from Leh (indicated by green arrows), running all along the Indus river and veering

south across the river just before the village of Mahe (red shape numbered as 3); (C) zoomed-in satellite view of the eastern-extremity of Puga Valley showing the *Shivlinga* site and the Sumdo village. A, B and C, were sourced from the publicly available databases <http://maps.google.com/> and <http://earth.google.com/>, respectively.

Supplementary Fig. 2. Photographic monitoring of the mineralization process over a mat portion situated at the margin of the spring-water flow, on the upper surface of the vent's rim: (A) picture taken on Day 1, thin layers of white mineral covering the green mat; (B) picture taken on Day 7, soft white spherules and shrub-like bodies of accreted minerals cover the mat (minute green bodies can be seen protruding out of the spherules); (C), picture taken on Day 14, further growth of the green mat over the white mineral deposits; (D), picture taken on Day 21, the green mat grows completely out of the mineral covering. The green scale bar (= 10 mm) shown in panel C applies to all four panels.

Supplementary Fig. 3. Rarefaction curve showing the proportionality between OTU-level metataxonomic diversity revealed and the number of amplified 16S rRNA gene sequence (V3 region) reads analyzed for the sample VW. Number of reads used in OTU building are plotted along the X-axis, while number of OTUs (including singletons) created at the 97% sequence identity level are plotted along the Y-axis.

Supplementary Fig. 4. Fluctuations in the relative abundance of bacterial phyla/proteobacterial classes along the drying thermal gradient. For each phylum/class within a community, its mean relative abundance has been plotted alongside the two original relative abundance values obtained from the duplicate metagenomes (shown as vertical range bar). To compare the widely unequal relative abundance values comprehensively, their log to the base 10 are plotted along the Y-axis. Only those taxa which had > 1% read share in at least one of the six metagenomic readsets analyzed are shown.

Supplementary Fig. 5. Fluctuations in the relative abundance of bacterial phyla/proteobacterial classes along the wet thermal gradient. For each phylum/class within a community, its mean relative abundance has been plotted alongside the two original relative abundance values obtained from the duplicate metagenomes (shown as vertical range bar). In order to compare the widely unequal relative abundance values comprehensively, their log to the base 10 are plotted along the Y-axis. Only those taxa which had > 1% read share in at least one of the twelve metagenomic readsets analyzed are shown.

Supplementary Tables

Supplementary Table 1. Maximum and minimum temperature, pH, and flow-rate recorded at the *Shivlinga* sample-sites during explorations prior to July 2013.

Supplementary Table 2. Elemental composition of sinters deposited on the top, sides, interior, base, and apron, of *Shivlinga*.

Supplementary Table 3. Summary statistics of metataxonomic analysis of the *Shivlinga* vent water community (VW).

Supplementary Tables 4 and 5. Summary of metagenomic investigation of the mat communities of the drying, and the wet, thermal gradients, respectively.

Supplementary Table 6-12. Pair-wise Pearson correlation coefficients (CC) calculated between the fluctuations in the relative abundances of individual phyla/classes along the wet thermal gradient and, variations in temperature, pH, distance from the vent, or flow-rate of the spring-water, along the same

trajectory. CC values (r) which were significant according to Benjamini-Hochberg-corrected probability (P) values are shown in Table S5. Calculations for all the CC, and corresponding Benjamini-Hochberg-corrected P , values are shown in Tables S6-S11.

Supplementary Tables 13-20. Calculation of ecological indices for VWM, DG3, DG4, WG3, WG4, WG5, WG6 and WG7, respectively, using phylum-/class-level distribution of shotgun metagenomic reads.

Supplementary Table 21. Genera collectively accounting for average 50% of all classifiable read (after searching against the nr protein sequence database) in the metagenomes of the mat communities VWM, DG3 and DG4.

Supplementary Table 22. Genera collectively accounting for average 50% of all classifiable read (after searching against the nr protein sequence database) in the metagenomes of WG3, WG4, WG5, WG6 and WG7.

Supplementary Tables 23-30. Total number of genera identified in VWM, DG3, DG4, WG3, WG4, WG5, WG6 and WG7, respectively, after searching their duplicate metagenomic readsets against the RDP database.

Supplementary Tables 31 and 32. Microbial genera that were detected in all the mat communities of the progressively-drying, and the wet, thermal gradients, respectively.

Supplementary Table 33. Microbial genera comprised primarily of thermophilic species but present even at low-temperature (33-46°C) sites.

Supplementary Tables 34 and 35. Phylum- or class-level percentage distribution of the total bacterial metagenomic reads identified in the mat samples of the drying, and the wet, thermal gradients respectively.

Supplementary Table 36. The contingency table that was used to determine by Chi-square test whether individual COG-counts under different functional categories¹ across the eight communities were significantly high or low.

Supplementary References

Supplementary references used in Table 2 of the main text and the Supplementary Table 33.

Supplementary Notes

Supplementary Note 1

Geography, geology, and geothermal activity of the study-site

The Puga geothermal area, which is a part of the greater Ladakh-Tibet borax-spring zone (Harinarayana *et al.*, 2006), is located in the Eastern part of the Ladakh district of Jammu and Kashmir, the northern-most state of India. It is connected to the district headquarter Leh by a 180 km metalled road, which runs along the river Indus for the first ~150 km from Leh before veering south across the Indus to reach the valley of Puga (average altitude ~4500 m from the sea level). Puga is situated just south of the tectonically-active collision junction between the Indian and Asian continental crusts involved in Himalayan orogeny (Gansser, 1964). All the surface expressions of geothermal activity, including *Shivlinga*, are restricted to the eastern part of the 15 km-long and 1 km-wide east-west orientated valley. While several lines of geochemical evidence suggest a direct association of the Puga hot springs with underlying magmatic sources (Chowdhury *et al.*, 1974; Chowdhury *et al.*, 1984; Saxena and D'Amore, 1984; Shanker *et al.*, 1999), geophysical studies show the subsurface to be underlain by two geothermal reservoirs at two sequential depths (Harinarayana *et al.*, 2006, Azeez and Harinarayana, 2007). A shallow heat-reservoir (having temperature ~160°C) is present at a depth of ~450 m, in the fractured basement rocks (breccia) saturated with hot water. The main geothermal reservoir (having temperature up to 260°C) commences at a depth of ~2 km and extends vertically across the upper Himalayan crust up to a depth of ~8 km. Beneath these levels, i.e. in the mid-to-lower Himalayan crust, lie the magma chambers or partial melts, which resulted from the high pressures and temperatures generated from the collision and subduction of the Indian continental plate with the Asian plate during Himalayan orogeny (Shanker *et al.*, 1976; Shanker, 1988; Harinarayana *et al.*, 2006). These molten rocks are the ultimate source of the high heat-flow (540 mW m⁻²) and geothermal activity (manifested as gentle to vigorous hot springs having surface temperatures 45 to 85°C, sulfur condensates, borax deposits, mud pools and fumaroles) in the region (Shanker *et al.*, 1976; Harinarayana *et al.*, 2006).

References used in Supplementary Note 1

- Azeez KKA, and Harinarayana T. Magnetotelluric evidence of potential geothermal resource in Puga, Ladakh, NW Himalaya. *Curr Sci.* 2007;93:323-329.
- Chowdhury AN, Bose BB, Pal J, Yudhisthir, Sengupta NR. Studies of some minor and rare elements in hot spring deposit from Puga, Ladakh. *Geol Surv India Spec Publ.* 1984;12:585–591.
- Chowdhury AN, Handa BK, Das AK. High lithium, rubidium and cesium contents of thermal spring water, spring sediments and borax deposits in Puga valley, Kashmir, India. *Geochem J.* 1974;8:61-65.
- Gansser A. *Geology of the Himalayas.* Interscience: London. 1964.

Harinarayana T, Azeez KKA, Murthy DN, Veeraswamy K, Rao SPE, Manoj C, et al. Exploration of geothermal structure in Puga geothermal field, Ladakh Himalayas, India by magnetotelluric studies. *J Appl Geophys.* 2006;58:280–295.

Saxena VK, and D'Amore F. Aquifer chemistry of the Puga and Chumathang high temperature geothermal systems in India. *J Volcanol Geotherm.* 1984;21:333–346.

Shanker R. Heat flow map of India and discussions on its geological and economic significance. *Indian Miner.* 1988;42:89-110.

Shanker R, Padhi RN, Arora CL, Prakash G, Thussu JL, Dua KJS. Geothermal exploration of the Puga and Chhumathang geothermal fields, Ladakh, India. In: *Proceedings of the 2nd United Nations symposium on the development and use of geothermal resources; May 20–29, 1975; San Francisco, CA. Washington, DC: U.S. Energy Research and Development Administration.* 1976.

Shanker R, Absar A, Srivastava GC, Pandey SN. Source and significance of anomalously high cesium in geothermal fluid at Puga, Ladakh, India. In *Proceedings of the 21st New Zealand Geothermal Workshop.* 1999;21:79-82.

Supplementary Note 2

Phylogenomic diversity analysis for the individual *Shivlinga* mats corroborated the trends of community dynamics along the hydrothermal gradients

The duplicate metagenomic readsets of each community were co-assembled using GS *De Novo* Assembler (<http://www.454.com>) with all default parameters excepting that the minimum contig size was 1000 nucleotide. These contigs were classified down to phylum level using the software package Phyla-Amphora (Wang *et al.*, 2013): all the protein coding sequences present in the contigs were identified, and then the conserved marker gene sequences were taxonomically annotated by searching against the custom database obtained from <http://wolbachia.biology.virginia.edu/WuLab/Software.html>. The numbers of contigs affiliated to phyla present in the mat communities were compared along the two thermal gradients.

Furthermore, the contigs obtained for each mat community was clustered into population genomes by differential coverage binning. For this purpose, the duplicate readsets were separately mapped onto the contigs using the BWA Software 0.7.10 (Dubrin, 2009); the resulting BAM files were sorted and indexed using Samtools 1.2 (Handsaker *et al.*, 2009); eventually, the BAM files and the corresponding contigs were parsed into GroopM 0.3.0 (Imelfort *et al.*, 2014) to generate an interactive groopm database. This led to the creation of core bins, which were then refined to eliminate putative chimeric bins from the groopm database. No further recruitment of unbinned contigs was made at this stage. Finally, the binned contigs were extracted, and evaluated using CheckM 0.7.0 (Parks *et al.*, 2015) to determine the completeness, contamination percentage and heterogeneity for each bin. The numbers of population genome bins obtained from each mat community were compared along the two thermal gradients.

Diversity analyses based on contig assembly from the mat metagenomes were consistent with the trends revealed from direct classifications of the metagenomic reads (statistics of the contig assembly procedure are given in Table A). For VWM (66°C), the total number of taxonomically-classified contigs was far lower than in DG3 or WG3 (located at 52°C and 56°C, respectively). However, along the drying thermal gradient, the number of taxonomically-classified contigs in DG3 (52°C) was remarkably higher than in DG4 (41°C) (Table B). This loss of diversity may be attributable to colonization constraints imposed by dehydration. Again, the phylum-level break-up of the classifiable contigs obtained from each mat community of this gradient showed that, with the fall in temperature from 66°C to 52°C, contig count increased for almost all the phyla present. The sole exceptions were *Aquificae*, *Deinoccus-Thermus* and *Thermotogae* that continued to decrease until the end of the gradient (41°C) (Table B). Notably, contig counts were higher in DG3 (52°C) than in DG4 (41°C) for all phyla, except *Proteobacteria*. Along the wet thermal gradient, the total number of classified contigs in WG3 (56°C) was lower than that in WG4 (46°C) (Table B); below 46°C however, classified-contig count first decreased in WG5 (38°C), but subsequently increased in WG6 (36°C) and then increased further in WG7 (33°C). Phylum-level break-up of the classifiable contigs obtained from each mat community of this gradient showed that, with the drop in temperature from 66°C to 46°C (VWM to WG4), contig count increased progressively for all phyla including *Aquificae* and *Deinoccus-Thermus*. The sole exception was *Thermotogae*, for which contig count decreased between 66°C and 56°C, and then increased sharply again at 46°C. Increase in contig count with decreasing temperature was expected for the mesophile-dominated phyla, but for the thermophile-dominated *Aquificae*, *Deinoccus-Thermus* and *Thermotogae* this trend was unexpected. In this context it is noteworthy that when the contigs ascribed to *Aquificae*, *Deinoccus-Thermus* or *Thermotogae* in each mat community were clustered into population-genome bins (on the basis of differential coverage and GC content), bin count for *Aquificae* increased from three at the 66°C site (VWM) to five in the 46°C site (WG4), while those for *Thermotogae* increased from one in VWM to three in WG4. Below 46°C, however, *Aquificae* bin count went down to one each for WG5, WG6 and WG7; whereas for *Thermotogae*, bin count was zero, one and one for WG5, WG6 and WG7, respectively. For any mat community, the contigs ascribed to *Deinoccus-Thermus* did not cluster into population-genome bins having acceptable quality parameters (see Methods). These data indicate that only moderately thermophilic species of *Aquificae* and *Thermotogae* colonize the 46°C site of the wet thermal gradient. Furthermore, as temperature dropped below 46°C, along the wet thermal gradient, contig counts for the phyla present, generally decreased in WG5 (38°C), and then increased sharply in WG6 and WG7 (36°C and 33°C, respectively). The sole exception was *Verrucomicrobia* for which contig count increased throughout the gradient (Table B). It appears, therefore, that parameters other than temperature act as key determinants of community composition at sample sites below 46°C.

The number of population-genome bins, a direct function of the total phylogenomic diversity present, for the 66°C sites was only 13 as compared to 120 and 85 for the 52°C (DG3) and 56°C sites (WG3), respectively (Table A). This underscored the presence of a thermodynamic hurdle for bacterial colonization at ~60°C. Along the wet thermal gradient there was again a small increase in bin count (from 85 to 92) commensurate with the fall in temperature from 56°C to 46°C. For the drying thermal gradient, however, bin count decreased (from 120 to 94) with the fall in temperature from 52°C to 41°C (Table B). This again illustrates that dehydration can constrain colonization along the drying thermal gradient. Along the wet thermal gradient, bin count dropped at 38°C, rose sharply at 36°C, and then dropped slightly at 33°C; so bin count did not correlate with temperature below 46°C.

References used in Supplementary Note 2

Imelfort M, Parks D, Woodcroft BJ, Dennis P, Hugenholtz P, Tyson GW. GroopM: an automated tool for the recovery of population genomes from related metagenomes. *PeerJ*. 2014;2:e603.

Li H, Durbin R. Fast and accurate short read alignment with Burrows-Wheeler transform. *Bioinformatics*. 2009;25:1754-1760.

Li H, Handsaker B, Wysoker A, Fennell T, Ruan J, Homer N, et al. Genome Project Data Processing S: The Sequence Alignment/Map format and SAMtools. *Bioinformatics*. 2009;25:2078-2079.

Parks DH, Imelfort M, Skennerton CT, Hugenholtz P, Tyson GW. CheckM: assessing the quality of microbial genomes recovered from isolates, single cells, and metagenomes. *Genome Res*. 2015;25:1043-1055.

Wang Z, Wu M. A phylum-level bacterial phylogenetic marker database. *Mol Biol Evol*. 2013;30:1258-1262.

Table A. Results of co-assembly of the duplicate metagenomic readsets of every mat community, and differential-coverage-based binning of the obtained contigs.

Sample	No. of reads used in assembly¹	No. of bases used in assembly¹	No. of reads participating in assembly	Size of the assembled sequence	No. of >1000-base pair (bp) contigs	No. of >100 Kb contigs	Size of largest contig (in bp)	Mean contig size (in bp)	No. of contigs taking part in bin formation	No. of bins formed
VWM	11,254,012	1,908,849,578	5,266,783	71,063,234	62,227	0	65,333	1,142	41,793	13
DG3	9,648,653	1,694,499,349	5,396,127	75,243,783	34,334	4	129,117	2,192	32,704	120
DG4	8,715,943	1,556,519,247	5,116,823	60,252,725	28,641	7	198,928	2,104	26,057	94
WG3	2,521,391	492,364,192	1,309,310	39,642,539	16,979	0	54,144	2,335	14,142	85
WG4	24,014,870	3,633,127,285	22,182,958	125,303,784	47,133	9	143,403	2,659	41,981	92
WG5	2,975,340	592,395,606	1,658,938	35,814,819	17,369	0	46,712	2,062	15,225	81
WG6	17,193,650	2,619,830,340	16,024,268	82,086,031	30,263	2	164,113	2,713	28,629	169
WG7	17,811,683	2,932,487,022	10,208,241	215,172,945	119,905	19	278,584	1,795	117,027	158

¹ After removing <30 bp reads.

Table B. Phylum-level classification¹ of the >1000-bp contigs obtained from co-assembly of the duplicate metagenomic readsets of every mat community.

	VW M	DG 3	DG 4	VW M	WG 3	WG 4	WG 5	WG 6	WG 7
Classification of the >1000-bp contigs									
Number of >1000-bp contigs obtained from co-assembly	62,22 7	34,3 34	28,6 41	62,22 7	16,9 79	47,1 33	17,3 69	30,2 63	119, 905
Total number of classified contigs	2371	680 2	480 5	2371	5105	1213 3	3558	5208	1682 6
<i>Bacteroidetes</i> contigs	66	728	534	66	234	1072	134	1122	3505
<i>Proteobacteria</i> contigs	109	249	558	109	382	1070	62	948	2889
<i>Cyanobacteria</i> contigs	38	166 1	726	38	652	1179	668	565	2494
<i>Chlorobi</i> contigs	194	164 7	141 0	194	1068	1490	1393	1024	2233
<i>Chloroflexi</i> contigs	46	152 4	132 3	46	916	1773	915	971	1908
<i>Acidobacteria</i> contigs	9	30	19	9	22	78	12	23	1073
<i>Planctomycetes</i> contigs	7	73	29	7	18	110	30	129	828
<i>Spirochaetes</i> contigs	3	257	71	3	5	358	186	17	609
<i>Firmicutes</i> contigs	65	118	45	65	88	706	33	113	519
<i>Verrucomicrobia</i> contigs	0	99	7	0	9	23	41	123	214
<i>Deinococcus-Thermus</i> contigs	372	281	41	372	728	700	30	67	167
<i>Aquificae</i> contigs	705	44	9	705	921	1981	11	29	97
<i>Chlamydiae</i> contigs	3	25	3	3	7	43	11	25	75
<i>Thermotogae</i> contigs	746	18	10	746	30	1399	10	14	75
<i>Actinobacteria</i> contigs	3	39	14	3	13	49	18	24	61
<i>Fibrobacteres</i> contigs	4	4	0	4	3	32	2	7	44
<i>Fusobacteria</i> contigs	1	5	5	1	9	59	2	6	32
<i>Tenericutes</i> contigs	0	0	1	0	0	11	0	1	3

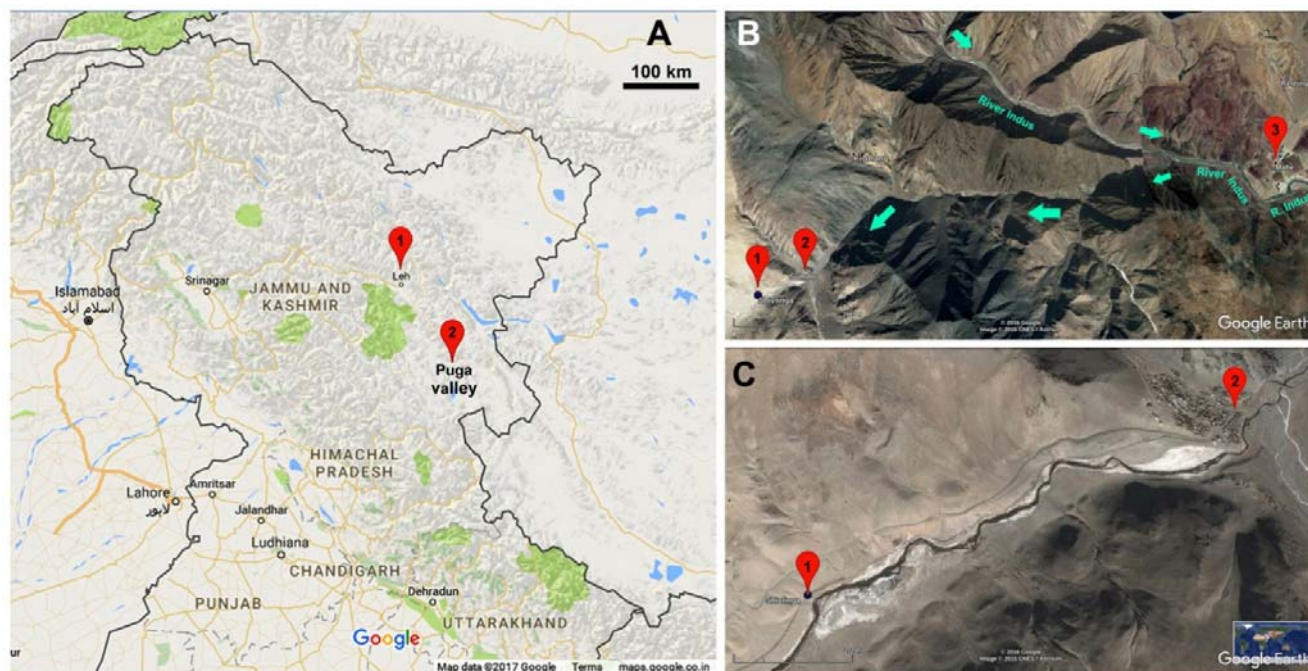
¹ Contigs were classified on the basis of the annotation of the conserved protein-coding marker genes present within them.

Supplementary Note 3

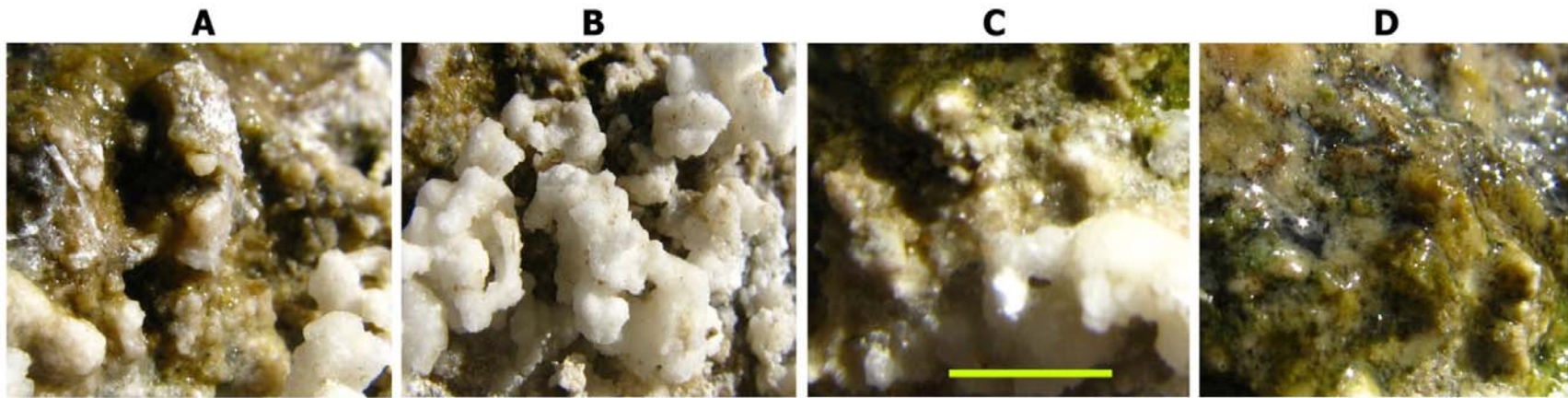
The R script used to draw the heat map depicting the results of hierarchical cluster analysis

```
library(gplots)
library("RColorBrewer")
aa<- read.csv("input.csv", sep=",")
row.names(aa) <- aa$Name
aa<- aa[,2:21]
aa_matrix <- data.matrix(aa)
hc.rows <- hclust(dist(aa_matrix))
plot(hc.rows)
hc.cols <- hclust(dist(t(aa_matrix)))
heatmap.2(as.matrix(aa_matrix), scale="none",key=TRUE, col=brewer.pal(9,"YlGn"), symkey=FALSE,
density.info="none", trace="none", cexRow=0.5, lhei = c(2, 8))
```

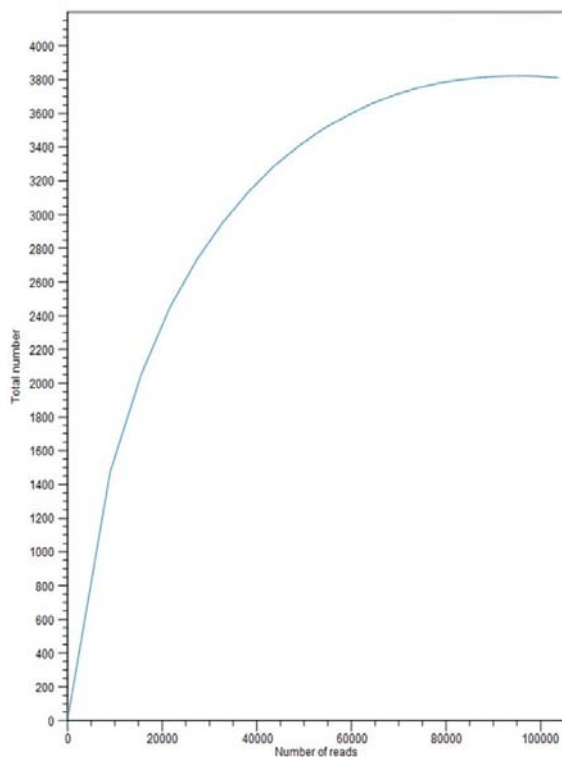
Supplementary Figures



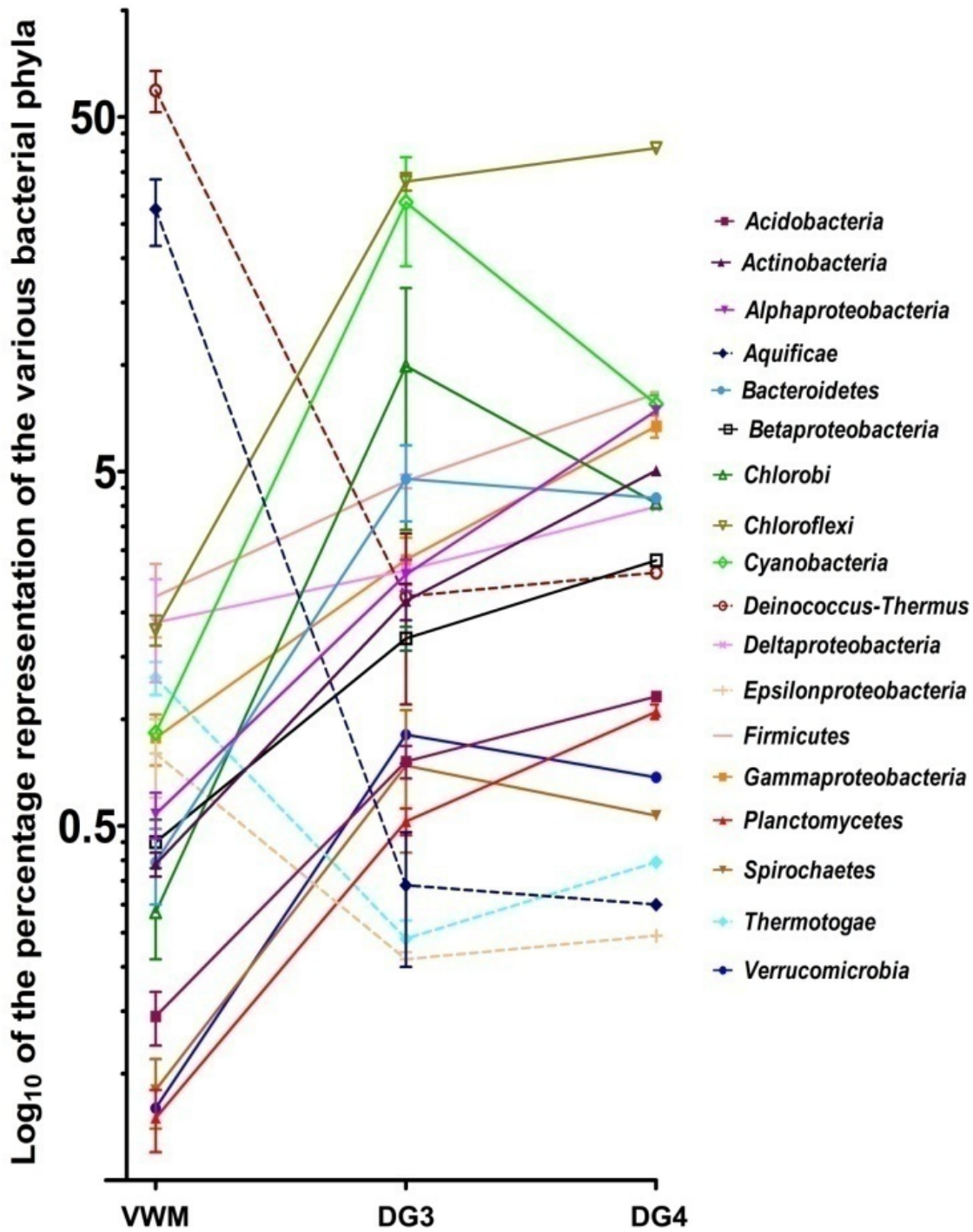
Supplementary Fig. 1. Location of Puga Valley in eastern Ladakh. (A) map showing the location of Leh, the capital of the union territory of Ladakh (red shape numbered as 1), and Puga Valley (red shape numbered as 2); (B) satellite image showing the position of *Shivlinga* (red shape numbered as 1) at the eastern extremity of Puga Valley, in context with the nearest village Sumdo (red shape numbered as 2) and the road that leads to Puga Valley from Leh (indicated by green arrows), running all along the Indus river and veering south across the river just before the village of Mahe (red shape numbered as 3); (C) zoomed-in satellite view of the eastern-extremity of Puga Valley showing the *Shivlinga* site and the Sumdo village. A, B and C, were sourced from the publicly available databases <http://maps.google.com/> and <http://earth.google.com/>, respectively.



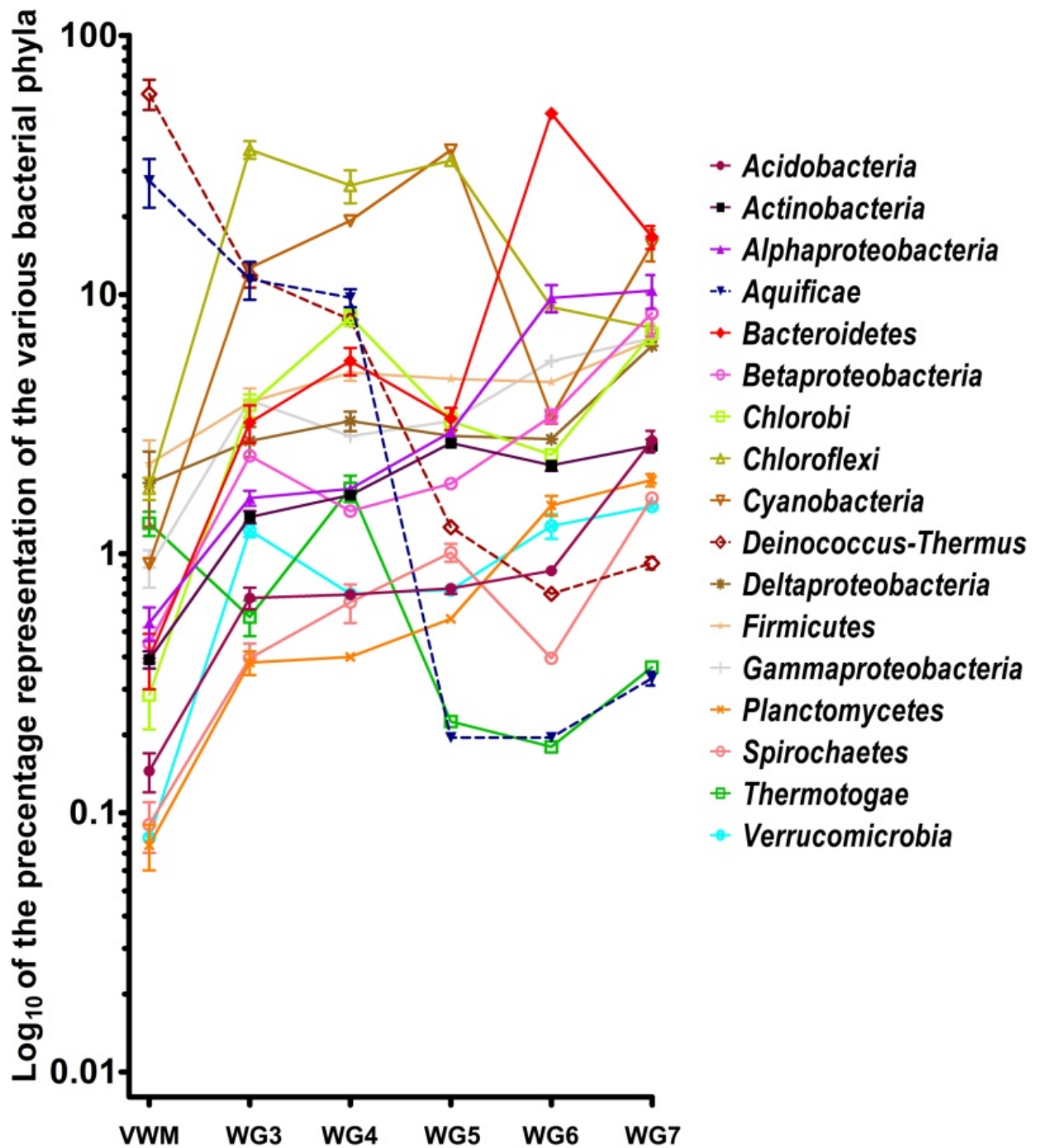
Supplementary Fig. 2. Photographic monitoring of the mineralization process over a mat portion situated at the margin of the spring-water flow, on the upper surface of the vent's rim: (A) picture taken on Day 1, thin layers of white mineral covering the green mat; (B) picture taken on Day 7, soft white spherules and shrub-like bodies of accreted minerals cover the mat (minute green bodies can be seen protruding out of the spherules); (C), picture taken on Day 14, further growth of the green mat over the white mineral deposits; (D), picture taken on Day 21, the green mat grows completely out of the mineral covering. The green scale bar (= 10 mm) shown in panel C applies to all four panels.



Supplementary Fig. 3. Rarefaction curve showing the proportionality between OTU-level metataxonomic diversity revealed and the number of amplified 16S rRNA gene sequence (V3 region) reads analyzed for the sample VW. Number of reads used in OTU building are plotted along the X-axis, while number of OTUs (including singletons) created at the 97% sequence identity level are plotted along the Y-axis.



Supplementary Fig. 4. Fluctuations in the relative abundance of bacterial phyla/proteobacterial classes along the drying thermal gradient. For each phylum/class within a community, its mean relative abundance has been plotted alongside the two original relative abundance values obtained from the duplicate metagenomes (shown as vertical range bar). To compare the widely unequal relative abundance values comprehensively, their log to the base 10 are plotted along the Y-axis. Only those taxa which had > 1% read share in at least one of the six metagenomic readsets analyzed are shown.



Supplementary Fig. 5. Fluctuations in the relative abundance of bacterial phyla/proteobacterial classes along the wet thermal gradient. For each phylum/class within a community, its mean relative abundance has been plotted alongside the two original relative abundance values obtained from the duplicate metagenomes (shown as vertical range bar). In order to compare the widely unequal relative abundance values comprehensively, their log to the base 10 are plotted along the Y-axis. Only those taxa which had > 1% read share in at least one of the twelve metagenomic readsets analyzed are shown.

Supplementary Tables

Supplementary Table 1. Maximum and minimum temperature, pH, and flow-rate recorded at the *Shivlinga* sample-sites during explorations prior to 23 July 2013 (previous dates of measurement are given in parenthesis after each value).

Name of the Sample	Maximum and minimum temperatures (in °C)	Maximum and minimum moisture (in % w/w) [*]	Maximum and minimum flow rate (in cm s ⁻¹) [#]	Maximum and minimum pH of the spring-water
VW	73 (23.08.2008) and 68 (12.08.2010)	NA	26.5 (12.08.2010) and 24.0 (23.08.2008)	7.2 (12.08.2010) and 6.8 (23.08.2008)
VWM	69 (23.08.2008) and 64 (12.08.2010)	NA	26.5 (12.08.2010) and 24.0 (23.08.2008)	7.2 (12.08.2010) and 6.8 (23.08.2008)
DG3	54 (23.08.2008) and 50 (12.08.2010)	42.5 (12.08.2010) and 40.0 (23.08.2008)	NA	7.4 (12.08.2010) and 7.1 (23.08.2008)
DG4	44 (23.08.2008) and 39 (12.08.2010)	30.0 (12.08.2010) and 27.2 (23.08.2008)	NA	7.6 (12.08.2010) and 7.2 (23.08.2008)
WG3	58 (23.08.2008) and 53 (12.08.2010)	NA	23.0 (12.08.2010) and 20.0 (23.08.2008)	7.6 (12.08.2010) and 7.3 (23.08.2008)
WG4	48(23.08.2008) and 45 (12.08.2010)	NA	16.0 (12.08.2010) and 13.0 (23.08.2008)	8.0 (12.08.2010) and 7.8 (23.08.2008)
WG5	40 (23.08.2008) and 37 (12.08.2010)	NA	12.0 (12.08.2010) and 9.5 (23.08.2008)	8.3 (12.08.2010) and 8.0 (23.08.2008)
WG6	37 (23.08.2008) and 34 (12.08.2010)	NA	8.0 (12.08.2010) and 6.0 (23.08.2008)	8.4 (12.08.2010) and 8.0 (23.08.2008)
WG7	34 (23.08.2008) and 31 (12.08.2010)	NA	5.0 (12.08.2010) and 4.5 (23.08.2008)	8.5 (12.08.2010) and 8.2 (23.08.2008)

* Measuring moisture content was applicable only to the samples DG3 and DG4 of the progressively-drying thermal gradient as these mats grew on moist sinter surfaces off the outflow channel. Flow rates were measured for all the other communities as they grew directly on the hot water outflow.

[#]Flow rate of water only at the vent (i.e. at sample sites of VW and VWM) was measured in ml s⁻¹.

SupplementaryTable 2. Elemental composition (amount measured as percent of total on a w/w basis*) of sinters deposited on the top, sides, interior, base, and apron, of *Shivlinga*.

Chemical element	Sinter sample 1 from one top-edge of <i>Shivlinga</i>'s body¹	Sinter sample 2 from one side-surface of <i>Shivlinga</i>'s body¹	Sinter sample 3 from the bedrock slope around <i>Shivlinga</i>'s base¹	Sinter sample 4 from <i>Shivlinga</i>'s apron¹	Sinter sample 5 from 5cm-deep within <i>Shivlinga</i>'s side²
B	26.23	25.22	22.85	21.08	20.04
O	29.76	30	31.89	32.75	28.33
C	13.62	10.2	5.47	12	8.8
Na	10.1	12.7	11.82	9.69	9.37
Si	1.26	1.37	0.73	1.52	3.2
K	3.04	2.56	0.9	0.31	2.39
Ca	4.07	3.98	3.6	3.22	3.28
Cl	0.58	0.63	0.46	0.29	0.43
Al	5.59	6.88	12.07	2.24	14.53
Au	5.1	5.74	5.08	0.82	6.6
S	0.07	0.18	1.7	0.15	3.18
Fe	0.08	0.07	0.7	3.56	0.09
Mn	0.13	0.25	0.53	1.53	0.16
Zn	0.09	0.15	0.46	1.74	0.2
Mo	0.79	0.61	0.84	1.29	0.36
Pb	0.62	0.57	0.77	1.68	0.44
Ag	0.43	0.33	0.66	3.27	0.25
Ni	0.31	0.24	0.23	1.75	0.1
Co	0.29	0.27	0.42	1.9	0.13

* Given values are means of five replicate analyses each by EDS and EPMA; hence totals may not add up to exactly 100%; standard deviations were <10% of the means.

¹ All these four samples were recently-formed sinters occurring as mm- to cm-sized white amorphous spherules and shrubs.

² Only this sample involved relatively older and harder sinters.

SupplementaryTable 3.Summary statistics of metataxonomic analysis¹ of the Shivlinga vent-water community (VW).

BioSample Accession Number	SAMN04241741
Run Accession Number	SRR2904995
Total reads	243,609
Reads after Quality & Length filtering	199,783
Reads after Dereplication	20,987
Total OTUs (minus singletons)	64
Singletons Only	6,890
ACE estimation (minus singletons)	64
Shannon index (minus singletons)	1.47278
Simpson index (minus singletons)	0.886

¹ V3 regions of all bacterial 16S rRNA genes present in the total environmental DNA isolated from the VW sample was amplified and sequenced using Ion PGM. OTUs were clustered at the 97% sequence similarity level.

SupplementaryTable 4. Summary of metagenomic investigation of the mat communities of the progressively-drying thermal gradient.

	VWM		DG3		DG4	
Sampling	1 st sample	2 nd sample	1 st sample	2 nd sample	1 st sample	2 nd sample
Run accession no.	SRR2625861	SRR2626156	SRR2625863	SRR2626157	SRR2625864	SRR2626159
Data volume (no. of mega bases)	362	1,240	400	1,294	475	1,082
Read throughput	1,875,410	7,784,680	1,902,386	7,746,267	2,233,295	6,482,648
Mean read-length (no. of bases)	193	159	210	167	213	167
No. of reads finally annotated after quality filtering ¹	955,353	6,644,298	808,927	4,903,766	1,060,639	3,647,816
No. of reads ascribed to <i>Archaea</i> ¹	4,340 (0.45 %)	50,772 (0.76 %)	4,470 (0.55 %)	27,519 (0.56 %)	10,078 (0.95 %)	34,532 (0.95 %)
No. of reads ascribed to <i>Bacteria</i> ¹	874,680 (91.56 %)	5,847,280 (88 %)	594859 (73.54 %)	3642131 (74.27 %)	795944 (75.04 %)	2724833 (74.7 %)
No. of reads ascribed to <i>Eukarya</i> ¹	2,263 (0.24 %)	14,628 (0.22 %)	4927 (0.61 %)	48950 (1 %)	9095 (0.86 %)	31302 (0.86 %)
No. of reads ascribed to Viruses ¹	2,823 (0.3 %)	11,593 (0.17 %)	64 (0.01 %)	1072 (0.02 %)	116 (0.01 %)	471 (0.01 %)
No. of unannotable reads ¹	71,247 (7.46 %)	720,025 (10.84 %)	204607 (25.29 %)	1184094 (24.15 %)	245406 (23.14 %)	856678 (23.48 %)

¹ As determined using the Organism Abundance tool of MG-RAST. Reads were searched by BlastX against the *nr* protein database following the Best Hit Classification approach with minimum alignment length of 15 amino acids and minimum identity cutoff of 60%. Values in parenthesis express read counts as percentages of the total number of annotable reads.

Supplementary Table 5. Summary of metagenomic investigation of the mat communities¹ of the wet thermal gradient.

	WG3		WG4		WG5		WG6		WG7	
Sampling	1 st sample	2 nd sample	1 st sample	2 nd sample	1 st sample	2 nd sample	1 st sample	2 nd sample	1 st sample	2 nd sample
Run accession no.	SRR26258 66	SRR26264 28	SRR26258 65	SRR26261 60	SRR26258 67	SRR26261 64	SRR26260 12	SRR26261 85	SRR26261 52	SRR26263 09
Data volume (no. of mega bases)	253	240	1,721	1,912	318	274	1,486	1,134	1,700	1,232
Read throughput	1,484,481	1,036,910	10,202,786	13,812,084	1,785,852	1,189,488	9,055,702	8,137,948	10,301,770	7,509,913
Mean read-length(no. of bases)	170	231	169	138	178	231	164	139	165	164
No. of reads finally annotated after quality filtering ²	967,344	1,028,280	5,465,737	9,061,326	867,988	984,610	3,151,051	4,043,750	3,876,194	4,062,948
No. of reads ascribed to <i>Archaea</i> ²	5380 (0.56 %)	8051 (0.78 %)	39779 (0.73 %)	81826 (0.9 %)	5144 (0.59 %)	5991 (0.61 %)	14455 (0.46 %)	19263 (0.48 %)	30515 (0.79 %)	33729 (0.83 %)
No. of reads ascribed	700263 (72.39 %)	767239 (74.61 %)	4147079 (75.87 %)	7076793 (78.1 %)	644915 (74.3 %)	738345 (74.99 %)	2432437 (77.19 %)	3113661 (77 %)	3139039 (80.98 %)	3296247 (81.13 %)

to <i>Bacteria</i>²										
No. of reads ascribed to <i>Eukarya</i>²	3798 (0.39 %)	4583 (0.45 %)	30495 (0.56 %)	56683 (0.63 %)	8825 (1.02 %)	9152 (0.93 %)	29725 (0.94 %)	38760 (0.96 %)	42558 (1.1 %)	47061 (1.16 %)
No. of reads ascribed to <i>Viruses</i>²	304 (0.03 %)	337 (0.03 %)	874 (0.02 %)	1691 (0.02 %)	153 (0.02 %)	259 (0.03 %)	779 (0.02 %)	1430 (0.04 %)	651 (0.02 %)	978 (0.02 %)
No. of unannota ble reads²	257599 (26.63 %)	248070 (24.12 %)	1247510 (22.82 %)	1844333 (20.35 %)	208951 (24.07 %)	230863 (23.45 %)	673655 (21.38 %)	870636 (21.53 %)	663431 (17.12 %)	684933 (16.86 %)

¹ VWM has been excluded from this table to avoid repetition of data already given in Table S1. Notably, however, VWM was also a part of the community continuum along the wet thermal gradient.

²As determined using the Organism Abundance tool of MG-RAST. Reads were searched by BlastX against the *nr* protein database following the Best Hit Classification approach with minimum alignment length of 15 amino acids and minimum identity cutoff of 60%. Values in parenthesis express read counts as percentages of the total number of annotable reads.

SupplementaryTable 6. Significant pair-wise Pearson correlation coefficients (CC) [and their corresponding Benjamini-Hochberg-corrected probability (*P*) values]* determined between phylum-/class-level population-fluctuations along the wet thermal gradient and variations in temperature, pH, distance from the vent, and flow-rate of the spring-water along the same trajectory.

* Positive and negative CC values are shaded light green and pink respectively; CC values not found to be significant according to Benjamini-Hochberg-corrected *P* values are not shown (gray cells).

	Temperature		pH		Distance		Flow rate	
	CC	<i>P</i>	CC	<i>P</i>	CC	<i>P</i>	CC	<i>P</i>
<i>Deinococcus-Thermus</i>	0.875	0.022	-0.872	0.024	-0.621	0.188	0.787	0.063
<i>Aquificae</i>	0.961	0.002	-0.944	0.005	-0.767	0.075	0.904	0.013
<i>Firmicutes</i>	-0.883	0.020	0.914	0.011	0.844	0.035	-0.863	0.027
<i>Deltaproteobacteria</i>	-0.646	0.166	0.687	0.132	0.828	0.042	-0.680	0.137
<i>Chloroflexi</i>	-0.034	0.949	0.021	0.968	-0.357	0.488	0.150	0.777
<i>Thermotogae</i>	0.571	0.237	-0.506	0.306	-0.581	0.227	0.557	0.251
<i>Cyanobacteria</i>	-0.447	0.374	0.437	0.386	0.123	0.816	-0.306	0.556
<i>Gammaproteobacteria</i>	-0.812	0.050	0.814	0.049	0.886	0.019	-0.830	0.041
<i>Epsilonproteobacteria</i>	0.816	0.047	-0.783	0.066	-0.533	0.276	0.709	0.114
<i>Alphaproteobacteria</i>	-0.795	0.059	0.791	0.061	0.944	0.005	-0.874	0.023
<i>Betaproteobacteria</i>	-0.669	0.146	0.690	0.129	0.898	0.015	-0.723	0.104
<i>Bacteroidetes</i>	-0.566	0.242	0.544	0.265	0.585	0.222	-0.640	0.171
<i>Actinobacteria</i>	-0.963	0.002	0.950	0.004	0.790	0.061	-0.908	0.012
<i>Nitrospirae</i>	0.354	0.492	-0.274	0.599	-0.378	0.460	0.351	0.495
<i>Chlorobi</i>	-0.496	0.317	0.564	0.243	0.389	0.446	-0.445	0.376
<i>Acidobacteria</i>	-0.681	0.137	0.710	0.114	0.881	0.020	-0.722	0.105
<i>Deferribacteres</i>	0.071	0.894	0.012	0.982	-0.158	0.765	0.087	0.870
<i>Dictyoglomi</i>	0.199	0.706	-0.123	0.816	-0.334	0.517	0.227	0.665
<i>Spirochaetes</i>	-0.751	0.085	0.773	0.071	0.795	0.059	-0.735	0.096
Unclassified Bacteria	-0.970	0.001	0.970	0.001	0.866	0.026	-0.942	0.005
<i>Verrucomicrobia</i>	-0.695	0.125	0.696	0.125	0.713	0.112	-0.677	0.140
<i>Planctomycetes</i>	-0.813	0.049	0.817	0.047	0.967	0.002	-0.884	0.019
<i>Synergistetes</i>	-0.615	0.194	0.671	0.144	0.703	0.119	-0.617	0.192
<i>Fusobacteria</i>	-0.764	0.077	0.802	0.055	0.846	0.034	-0.811	0.050
Others	-0.822	0.044	0.851	0.032	0.921	0.009	-0.854	0.030
Unclassified <i>Proteobacteria</i>	-0.817	0.047	0.819	0.046	0.902	0.014	-0.824	0.044
<i>Tenericutes</i>	-0.685	0.133	0.722	0.105	0.652	0.161	-0.721	0.106
<i>Chlamydiae</i>	-0.897	0.015	0.909	0.012	0.956	0.003	-0.929	0.007
<i>Gemmatimonadetes</i>	-0.795	0.059	0.825	0.043	0.878	0.021	-0.804	0.054

SupplementaryTable 7. Raw data used for determining the pair-wise Pearson correlation coefficients between phylum-/class-level population-fluctuations along the wet thermal gradient and variations in temperature, pH, distance from the vent, and flow-rate of the spring-water along the same trajectory.

	VWM	WG3	WG4	WG5	WG6	WG7
Temperature	66	56	46	38	36	33
pH	7.1	7.5	8	8.2	8.3	8.5
Distance	8	22	65	120	190	290
Flow rate	25	22	15	11	7	5
<i>Deinococcus-Thermus</i>	59.465	11.825	7.995	1.265	0.7	0.92
<i>Aquificae</i>	27.48	11.445	9.715	0.195	0.195	0.33
<i>Firmicutes</i>	2.22	3.84	4.99	4.73	4.59	6.665
<i>Deltaproteobacteria</i>	1.875	2.72	3.25	2.845	2.765	6.335
<i>Chloroflexi</i>	1.785	36.22	26.345	32.895	8.95	7.425
<i>Thermotogae</i>	1.31	0.57	1.79	0.225	0.18	0.365
<i>Cyanobacteria</i>	0.915	12.66	19.275	36.055	3.375	15.565
<i>Gammaproteobacteria</i>	0.885	3.905	2.84	3.25	5.53	6.78
<i>Epsilonproteobacteria</i>	0.74	0.465	0.495	0.2	0.4	0.385
<i>Alphaproteobacteria</i>	0.54	1.64	1.78	2.95	9.71	10.345
<i>Betaproteobacteria</i>	0.45	2.385	1.46	1.865	3.395	8.475
<i>Bacteroidetes</i>	0.395	3.205	5.545	3.325	49.98	16.68
<i>Actinobacteria</i>	0.39	1.385	1.685	2.67	2.195	2.61
<i>Nitrospirae</i>	0.29	0.205	0.475	0.13	0.12	0.22
<i>Chlorobi</i>	0.285	3.74	8.195	3.245	2.41	7.07
<i>Acidobacteria</i>	0.145	0.675	0.695	0.735	0.86	2.735
<i>Deferribacteres</i>	0.13	0.14	0.35	0.07	0.1	0.165
<i>Dictyoglomi</i>	0.11	0.085	0.285	0.06	0.045	0.085
<i>Spirochaetes</i>	0.09	0.395	0.65	1.01	0.395	1.64
<i>Unclassified Bacteria</i>	0.09	0.305	0.35	0.415	0.47	0.53
<i>Verrucomicrobia</i>	0.08	1.23	0.7	0.725	1.28	1.52
<i>Planctomycetes</i>	0.075	0.38	0.4	0.56	1.535	1.925
<i>Synergistetes</i>	0.06	0.11	0.155	0.105	0.095	0.225
<i>Fusobacteria</i>	0.06	0.1	0.14	0.085	0.16	0.195
Others	0.05	0.155	0.195	0.155	0.245	0.385
<i>Unclassified Proteobacteria</i>	0.04	0.055	0.055	0.09	0.07	0.125
<i>Tenericutes</i>	0.03	0.04	0.055	0.035	0.06	0.055
<i>Chlamydiae</i>	0.025	0.07	0.085	0.085	0.135	0.17
<i>Gemmatimonadetes</i>	0.01	0.07	0.08	0.07	0.085	0.17

SupplementaryTable 8. Pearson correlation co-efficient (CC) values (r) and corresponding probability (P) values between phylum-/class-level population fluctuations in the mats of the wet thermal gradient and the variations in environmental parameters along the same trajectory.

	Pearson CC values (r)				P values obtained for individual r values			
	Temperature	pH	Distance	Flow rate	Temperature	pH	Distance	Flow rate
<i>Deinococcus-Thermus</i>	0.875	-0.872	-0.621	0.787	0.022	0.024	0.188	0.063
<i>Aquificae</i>	0.961	-0.944	-0.767	0.904	0.002	0.005	0.075	0.013
<i>Firmicutes</i>	-0.883	0.914	0.844	-0.863	0.020	0.011	0.035	0.027
<i>Deltaproteobacteria</i>	-0.646	0.687	0.828	-0.680	0.166	0.132	0.042	0.137
<i>Chloroflexi</i>	-0.034	0.021	-0.357	0.150	0.949	0.968	0.488	0.777
<i>Thermotogae</i>	0.571	-0.506	-0.581	0.557	0.237	0.306	0.227	0.251
<i>Cyanobacteria</i>	-0.447	0.437	0.123	-0.306	0.374	0.386	0.816	0.556
<i>Gammaproteobacteria</i>	-0.812	0.814	0.886	-0.830	0.050	0.049	0.019	0.041
<i>Epsilonproteobacteria</i>	0.816	-0.783	-0.533	0.709	0.047	0.066	0.276	0.114
<i>Alphaproteobacteria</i>	-0.795	0.791	0.944	-0.874	0.059	0.061	0.005	0.023
<i>Betaproteobacteria</i>	-0.669	0.690	0.898	-0.723	0.146	0.129	0.015	0.104
<i>Bacteroidetes</i>	-0.566	0.544	0.585	-0.640	0.242	0.265	0.222	0.171
<i>Actinobacteria</i>	-0.963	0.950	0.790	-0.908	0.002	0.004	0.061	0.012
<i>Nitrospirae</i>	0.354	-0.274	-0.378	0.351	0.492	0.599	0.460	0.495
<i>Chlorobi</i>	-0.496	0.564	0.389	-0.445	0.317	0.243	0.446	0.376
<i>Acidobacteria</i>	-0.681	0.710	0.881	-0.722	0.137	0.114	0.020	0.105
<i>Deferribacteres</i>	0.071	0.012	-0.158	0.087	0.894	0.982	0.765	0.870
<i>Dictyoglomi</i>	0.199	-0.12	-0.334	0.227	0.706	0.816	0.517	0.665

		3						
<i>Spirochaetes</i>	-0.751	0.77 3	0.795	-0.735	0.085	0.07 1	0.059	0.096
<i>Unclassified Bacteria</i>	-0.970	0.97 0	0.866	-0.942	0.001	0.00 1	0.026	0.005
<i>Verrucomicrobia</i>	-0.695	0.69 6	0.713	-0.677	0.125	0.12 5	0.112	0.140
<i>Planctomycetes</i>	-0.813	0.81 7	0.967	-0.884	0.049	0.04 7	0.002	0.019
<i>Synergistetes</i>	-0.615	0.67 1	0.703	-0.617	0.194	0.14 4	0.119	0.192
<i>Fusobacteria</i>	-0.764	0.80 2	0.846	-0.811	0.077	0.05 5	0.034	0.050
Others	-0.822	0.85 1	0.921	-0.854	0.044	0.03 2	0.009	0.030
<i>Unclassified Proteobacteria</i>	-0.817	0.81 9	0.902	-0.824	0.047	0.04 6	0.014	0.044
<i>Tenericutes</i>	-0.685	0.72 2	0.652	-0.721	0.133	0.10 5	0.161	0.106
<i>Chlamydiae</i>	-0.897	0.90 9	0.956	-0.929	0.015	0.01 2	0.003	0.007
<i>Gemmatimonadetes</i>	-0.795	0.82 5	0.878	-0.804	0.059	0.04 3	0.021	0.054

SupplementaryTable 9.Benjamini-Hochberg correction¹ of the *P* values obtained for individual Pearson correlation co-efficient (CC) values (*r*) between the phylum-/class-level population fluctuations along the wet thermal gradient and the variations in temperature along the same trajectory.

	CC value (<i>r</i>)	<i>P</i> value	Rank	Benjamini-Hochberg critical value
<i>Unclassified Bacteria</i>	-0.970	0.001	1	0.006896552
<i>Actinobacteria</i>	-0.963	0.002	2	0.013793103
<i>Aquificae</i>	0.961	0.002	3	0.020689655
<i>Chlamydiae</i>	-0.897	0.015	4	0.027586207
<i>Firmicutes</i>	-0.883	0.020	5	0.034482759
<i>Deinococcus-Thermus</i>	0.875	0.022	6	0.04137931
<i>Others</i>	-0.822	0.044	7	0.048275862
<i>Unclassified Proteobacteria</i>	-0.817	0.047	8	0.055172414
<i>Epsilonproteobacteria</i>	0.816	0.047	9	0.062068966
<i>Planctomycetes</i>	-0.813	0.049	10	0.068965517
<i>Gammaproteobacteria</i>	-0.812	0.050	11	0.075862069
<i>Gemmatimonadetes</i>	-0.795	0.059	12	0.082758621
<i>Alphaproteobacteria</i>	-0.795	0.059	13	0.089655172
<i>Fusobacteria</i>	-0.764	0.077	14	0.096551724
<i>Spirochaetes</i>	-0.751	0.085	15	0.103448276
<i>Verrucomicrobia</i>	-0.695	0.125	16	0.110344828
<i>Tenericutes</i>	-0.685	0.133	17	0.117241379
<i>Acidobacteria</i>	-0.681	0.137	18	0.124137931
<i>Betaproteobacteria</i>	-0.669	0.146	19	0.131034483
<i>Deltaproteobacteria</i>	-0.646	0.166	20	0.137931034
<i>Synergistetes</i>	-0.615	0.194	21	0.144827586
<i>Thermotogae</i>	0.571	0.237	22	0.151724138
<i>Bacteroidetes</i>	-0.566	0.242	23	0.15862069
<i>Chlorobi</i>	-0.496	0.317	24	0.165517241
<i>Cyanobacteria</i>	-0.447	0.374	25	0.172413793
<i>Nitrospirae</i>	0.354	0.492	26	0.179310345
<i>Dictyoglomi</i>	0.199	0.706	27	0.186206897
<i>Deferribacteres</i>	0.071	0.894	28	0.193103448
<i>Chloroflexi</i>	-0.034	0.949	29	0.2

¹ Phyla/classes were arranged in the ascending order of their *P* values (the one with the lowest *P* was ascribed rank 1); Benjamini-Hochberg critical values were determined as described in the Methods section; correlations were considered significant up to that phylum/class rank (see the phylum/class names that are in red font) where Benjamini-Hochberg critical value was still greater than the *P* value.

SupplementaryTable 10.Benjamini-Hochberg correction¹ of the *P* values obtained for individual Pearson correlation co-efficient (CC) values (*r*) between the phylum-/class-level population fluctuations along the wet thermal gradient and the variations in pH along the same trajectory.

	CC value (<i>r</i>)	<i>P</i> value	Rank	Benjamini-Hochberg critical value
<i>Unclassified Bacteria</i>	0.970	0.001	1	0.006896552
<i>Actinobacteria</i>	0.950	0.004	2	0.013793103
<i>Aquificae</i>	-0.944	0.005	3	0.020689655
<i>Firmicutes</i>	0.914	0.011	4	0.027586207
<i>Chlamydiae</i>	0.909	0.012	5	0.034482759
<i>Deinococcus-Thermus</i>	-0.872	0.024	6	0.04137931
<i>Others</i>	0.851	0.032	7	0.048275862
<i>Gemmatimonadetes</i>	0.825	0.043	8	0.055172414
<i>unclassified Proteobacteria</i>	0.819	0.046	9	0.062068966
<i>Planctomycetes</i>	0.817	0.047	10	0.068965517
<i>Gammaproteobacteria</i>	0.814	0.049	11	0.075862069
<i>Fusobacteria</i>	0.802	0.055	12	0.082758621
<i>Alphaproteobacteria</i>	0.791	0.061	13	0.089655172
<i>Epsilonproteobacteria</i>	-0.783	0.066	14	0.096551724
<i>Spirochaetes</i>	0.773	0.071	15	0.103448276
<i>Tenericutes</i>	0.722	0.105	16	0.110344828
<i>Acidobacteria</i>	0.710	0.114	17	0.117241379
<i>Verrucomicrobia</i>	0.696	0.125	18	0.124137931
<i>Betaproteobacteria</i>	0.690	0.129	19	0.131034483
<i>Deltaproteobacteria</i>	0.687	0.132	20	0.137931034
<i>Synergistetes</i>	0.671	0.144	21	0.144827586
<i>Chlorobi</i>	0.564	0.243	22	0.151724138
<i>Bacteroidetes</i>	0.544	0.265	23	0.15862069
<i>Thermotogae</i>	-0.506	0.306	24	0.165517241
<i>Cyanobacteria</i>	0.437	0.386	25	0.172413793
<i>Nitrospirae</i>	-0.274	0.599	26	0.179310345
<i>Dictyoglomi</i>	-0.123	0.816	27	0.186206897
<i>Chloroflexi</i>	0.021	0.968	28	0.193103448
<i>Deferribacteres</i>	0.012	0.982	29	0.2

¹ Phyla/classes were arranged in the ascending order of their *P* values (the one with the lowest *P* was ascribed rank 1); Benjamini-Hochberg critical values were determined as described in the Methods section; correlations were considered significant up to that phylum/class rank (see the phylum/class names that are in red font) where Benjamini-Hochberg critical value was still greater than the *P* value.

SupplementaryTable 11. Benjamini-Hochberg correction¹ of the *P* values obtained for individual Pearson correlation co-efficient (CC) values (*r*) between the phylum-/class-level population fluctuations along the wet thermal gradient and the variations in the distance of the sample-sites from the vent center.

	CC value (<i>r</i>)	<i>P</i> value	Rank	Benjamini-Hochberg critical value
<i>Planctomycetes</i>	0.967	0.002	1	0.006896552
<i>Chlamydiae</i>	0.956	0.003	2	0.013793103
<i>Alphaproteobacteria</i>	0.944	0.005	3	0.020689655
Others	0.921	0.009	4	0.027586207
Unclassified <i>Proteobacteria</i>	0.902	0.014	5	0.034482759
<i>Betaproteobacteria</i>	0.898	0.015	6	0.04137931
<i>Gammaproteobacteria</i>	0.886	0.019	7	0.048275862
<i>Acidobacteria</i>	0.881	0.020	8	0.055172414
<i>Gemmatimonadetes</i>	0.878	0.021	9	0.062068966
Unclassified <i>Bacteria</i>	0.866	0.026	10	0.068965517
<i>Fusobacteria</i>	0.846	0.034	11	0.075862069
<i>Firmicutes</i>	0.844	0.035	12	0.082758621
<i>Deltaproteobacteria</i>	0.828	0.042	13	0.089655172
<i>Spirochaetes</i>	0.795	0.059	14	0.096551724
<i>Actinobacteria</i>	0.790	0.061	15	0.103448276
<i>Aquificae</i>	-0.767	0.075	16	0.110344828
<i>Verrucomicrobia</i>	0.713	0.112	17	0.117241379
<i>Synergistetes</i>	0.703	0.119	18	0.124137931
<i>Tenericutes</i>	0.652	0.161	19	0.131034483
<i>Deinococcus-Thermus</i>	-0.621	0.188	20	0.137931034
<i>Bacteroidetes</i>	0.585	0.222	21	0.144827586
<i>Thermotogae</i>	-0.581	0.227	22	0.151724138
<i>Epsilonproteobacteria</i>	-0.533	0.276	23	0.15862069
<i>Chlorobi</i>	0.389	0.446	24	0.165517241
<i>Nitrospirae</i>	-0.378	0.460	25	0.172413793
<i>Chloroflexi</i>	-0.357	0.488	26	0.179310345
<i>Dictyoglomi</i>	-0.334	0.517	27	0.186206897
<i>Deferribacteres</i>	-0.158	0.765	28	0.193103448
<i>Cyanobacteria</i>	0.123	0.816	29	0.2

¹Phyla/classes were arranged in the ascending order of their *P* values (the one with the lowest *P* was ascribed rank 1); Benjamini-Hochberg critical values were determined as described in the Methods section; correlations were considered significant up to that phylum/class rank (see the phylum/class names that are in red font) where Benjamini-Hochberg critical value was still greater than the *P* value.

SupplementaryTable 12.Benjamini-Hochberg correction¹ of the *P* values obtained for individual Pearson correlation co-efficient (CC) values (*r*) between the phylum-/class-level population fluctuations along the wet thermal gradient and the variations in the flow-rate of hot water along the same trajectory.

	CC value (<i>r</i>)	<i>P</i> value	Rank	Benjamini-Hochberg critical value
<i>Unclassified Bacteria</i>	-0.942	0.005	1	0.006896552
<i>Chlamydiae</i>	-0.929	0.007	2	0.013793103
<i>Actinobacteria</i>	-0.908	0.012	3	0.020689655
<i>Aquificae</i>	0.904	0.013	4	0.027586207
<i>Planctomycetes</i>	-0.884	0.019	5	0.034482759
<i>Alphaproteobacteria</i>	-0.874	0.023	6	0.04137931
<i>Firmicutes</i>	-0.863	0.027	7	0.048275862
<i>Others</i>	-0.854	0.030	8	0.055172414
<i>Gammaproteobacteria</i>	-0.830	0.041	9	0.062068966
<i>Unclassified Proteobacteria</i>	-0.824	0.044	10	0.068965517
<i>Fusobacteria</i>	-0.811	0.050	11	0.075862069
<i>Gemmatimonadetes</i>	-0.804	0.054	12	0.082758621
<i>Deinococcus-Thermus</i>	0.787	0.063	13	0.089655172
<i>Spirochaetes</i>	-0.735	0.096	14	0.096551724
<i>Betaproteobacteria</i>	-0.723	0.104	15	0.103448276
<i>Acidobacteria</i>	-0.722	0.105	16	0.110344828
<i>Tenericutes</i>	-0.721	0.106	17	0.117241379
<i>Epsilonproteobacteria</i>	0.709	0.114	18	0.124137931
<i>Deltaproteobacteria</i>	-0.680	0.137	19	0.131034483
<i>Verrucomicrobia</i>	-0.677	0.140	20	0.137931034
<i>Bacteroidetes</i>	-0.640	0.171	21	0.144827586
<i>Synergistetes</i>	-0.617	0.192	22	0.151724138
<i>Thermotogae</i>	0.557	0.251	23	0.15862069
<i>Chlorobi</i>	-0.445	0.376	24	0.165517241
<i>Nitrospirae</i>	0.351	0.495	25	0.172413793
<i>Cyanobacteria</i>	-0.306	0.556	26	0.179310345
<i>Dictyoglomi</i>	0.227	0.665	27	0.186206897
<i>Chloroflexi</i>	0.150	0.777	28	0.193103448
<i>Deferribacteres</i>	0.087	0.870	29	0.2

¹ Phyla/classes were arranged in the ascending order of their *P* values (the one with the lowest *P* was ascribed rank 1); Benjamini-Hochberg critical values were determined as described in the Methods section; correlations were considered significant up to that phylum/class rank (see the phylum/class names that are in red font) where Benjamini-Hochberg critical value was still greater than the *P* value.

SupplementaryTable 13. Calculation of ecological indices for VWM using phylum-/class-level distribution of shotgun metagenomic reads.

	Dominance (D)*		Shannon diversity index (H)#	
	$p_i = n_i / n$	p_i^2	$\ln p_i$	$p_i (\ln p_i)$
<i>Acidobacteria</i>	0.001	0.203	-6.536	-0.009
<i>Actinobacteria</i>	0.004	0.000	-5.547	-0.022
<i>Alphaproteobacteria</i>	0.005	0.000	-5.221	-0.028
<i>Aquificae</i>	0.275	0.076	-1.292	-0.355
<i>Bacteroidetes</i>	0.004	0.603	-5.534	-0.022
<i>Betaproteobacteria</i>	0.005	0.000	-5.404	-0.024
<i>Chlamydiae</i>	0.000	0.003	-8.294	-0.002
<i>Chlorobi</i>	0.003	0.123	-5.860	-0.017
<i>Chloroflexi</i>	0.018	0.003	-4.026	-0.072
<i>Cyanobacteria</i>	0.009	0.723	-4.694	-0.043
<i>Deferribacteres</i>	0.001	0.000	-6.645	-0.009
<i>Deinococcus-Thermus</i>	0.595	0.354	-0.520	-0.309
<i>Deltaproteobacteria</i>	0.019	0.000	-3.977	-0.075
<i>Dictyoglomi</i>	0.001	0.000	-6.812	-0.007
<i>Epsilonproteobacteria</i>	0.007	0.000	-4.906	-0.036
<i>Firmicutes</i>	0.022	0.000	-3.808	-0.085
<i>Fusobacteria</i>	0.001	0.000	-7.419	-0.004
<i>Gammaproteobacteria</i>	0.009	0.323	-4.727	-0.042
<i>Gemmatimonadetes</i>	0.000	0.000	-9.210	-0.001
<i>Nitrospirae</i>	0.003	0.000	-5.843	-0.017
Others	0.001	0.000	-7.601	-0.004
<i>Planctomycetes</i>	0.001	0.063	-7.195	-0.005
<i>Spirochaetes</i>	0.001	0.000	-7.013	-0.006
<i>Synergistetes</i>	0.001	0.000	-7.419	-0.004
<i>Tenericutes</i>	0.000	0.000	-8.112	-0.002
<i>Thermotogae</i>	0.013	0.000	-4.335	-0.057
unclassified <i>Bacteria</i>	0.001	0.000	-7.013	-0.006
unclassified <i>Proteobacteria</i>	0.000	0.000	-7.824	-0.003
<i>Verrucomicrobia</i>	0.001	0.000	-7.131	-0.006
$D = \sum p_i^2$		0.431		
$\sum p_i (\ln p_i)$				-1.273
$H = -\sum p_i (\ln p_i)$				1.273
$E_H = H / H_{max}$				0.378

* Mean percentage representations (relative abundance) of phyla/classes were directly used as their (n_i / n) values.

Shannon's equitability (E_H) was obtained by dividing H by H_{max} . H_{max} is known to be $\ln S$, where $S =$ total number of phyla/classes in the community. Thus, here $H_{max} = \ln 29 = 3.367$.

SupplementaryTable 14. Calculation of ecological indices for DG3 using phylum-/class-level distribution of shotgun metagenomic reads.

	Dominance (D) *		Shannon diversity index (H) #	
	$p_i = n_i / n$	p_i^2	$\text{Ln } p_i$	$p_i (\text{Ln } p_i)$
<i>Acidobacteria</i>	0.008	0.000	-4.880	-0.037
<i>Actinobacteria</i>	0.022	0.000	-3.837	-0.083
<i>Alphaproteobacteria</i>	0.026	0.001	-3.665	-0.094
<i>Aquificae</i>	0.003	0.000	-5.684	-0.019
<i>Bacteroidetes</i>	0.048	0.002	-3.044	-0.145
<i>Betaproteobacteria</i>	0.017	0.000	-4.080	-0.069
<i>Chlamydiae</i>	0.001	0.063	-7.195	-0.005
<i>Chlorobi</i>	0.099	0.010	-2.310	-0.229
<i>Chloroflexi</i>	0.328	0.108	-1.113	-0.366
<i>Cyanobacteria</i>	0.287	0.083	-1.247	-0.358
<i>Deferribacteres</i>	0.001	0.003	-7.070	-0.006
<i>Deinococcus-Thermus</i>	0.022	0.000	-3.808	-0.085
<i>Deltaproteobacteria</i>	0.026	0.001	-3.638	-0.096
<i>Dictyoglomi</i>	0.001	0.000	-7.419	-0.004
<i>Epsilonproteobacteria</i>	0.002	0.000	-6.166	-0.013
<i>Firmicutes</i>	0.047	0.002	-3.060	-0.144
<i>Fusobacteria</i>	0.001	0.093	-6.959	-0.007
<i>Gammaproteobacteria</i>	0.028	0.001	-3.568	-0.101
<i>Gemmatimonadetes</i>	0.001	0.000	-7.013	-0.006
<i>Nitrospirae</i>	0.001	0.000	-6.571	-0.009
Others	0.002	0.403	-6.470	-0.010
<i>Planctomycetes</i>	0.005	0.003	-5.269	-0.027
<i>Spirochaetes</i>	0.007	0.000	-4.906	-0.036
<i>Synergistetes</i>	0.001	0.023	-6.768	-0.008
<i>Tenericutes</i>	0.000	0.123	-7.958	-0.003
<i>Thermotogae</i>	0.002	0.000	-6.032	-0.014
unclassified <i>Bacteria</i>	0.004	0.000	-5.599	-0.021
unclassified <i>Proteobacteria</i>	0.001	0.003	-7.339	-0.005
<i>Verrucomicrobia</i>	0.009	0.103	-4.705	-0.043
$D = \sum p_i^2$		0.208		
$\sum p_i (\text{Ln } p_i)$				-2.042
$H = -\sum p_i (\text{Ln } p_i)$				2.042
$E_H = H / H_{max}$				0.606

* Mean percentage representations (relative abundance) of phyla/classes were directly used as their (n_i / n) values.

Shannon's equitability (E_H) was obtained by dividing H by H_{max} . H_{max} is known to be $\text{Ln } S$, where S = total number of phyla/classes in the community. Thus, here $H_{max} = \text{Ln } 29 = 3.367$.

SupplementaryTable 15. Calculation of ecological indices for DG4 using phylum-/class-level distribution of shotgun metagenomic reads.

	Dominance (<i>D</i>) *		Shannon diversity index (<i>H</i>) #	
	$p_i = n_i / n$	p_i^2	$\ln p_i$	$p_i (\ln p_i)$
<i>Acidobacteria</i>	0.012	0.000	-4.457	-0.052
<i>Actinobacteria</i>	0.050	0.003	-2.991	-0.150
<i>Alphaproteobacteria</i>	0.074	0.006	-2.601	-0.193
<i>Aquificae</i>	0.003	0.000	-5.809	-0.017
<i>Bacteroidetes</i>	0.042	0.002	-3.168	-0.133
<i>Betaproteobacteria</i>	0.028	0.001	-3.574	-0.100
<i>Chlamydiae</i>	0.001	0.156	-6.685	-0.008
<i>Chlorobi</i>	0.041	0.002	-3.202	-0.130
<i>Chloroflexi</i>	0.409	0.167	-0.895	-0.366
<i>Cyanobacteria</i>	0.077	0.006	-2.559	-0.198
<i>Deferribacteres</i>	0.001	0.103	-6.859	-0.007
<i>Deinococcus-Thermus</i>	0.026	0.001	-3.654	-0.095
<i>Deltaproteobacteria</i>	0.040	0.002	-3.224	-0.128
<i>Dictyoglomi</i>	0.001	0.103	-6.859	-0.007
<i>Epsilonproteobacteria</i>	0.002	0.003	-6.012	-0.015
<i>Firmicutes</i>	0.083	0.007	-2.489	-0.207
<i>Fusobacteria</i>	0.001	0.103	-6.536	-0.009
<i>Gammaproteobacteria</i>	0.067	0.004	-2.702	-0.181
<i>Gemmatimonadetes</i>	0.001	0.001	-6.768	-0.008
<i>Nitrospirae</i>	0.002	0.063	-6.348	-0.011
Others	0.002	0.203	-6.190	-0.013
<i>Planctomycetes</i>	0.009	0.000	-4.699	-0.043
<i>Spirochaetes</i>	0.005	0.003	-5.231	-0.028
<i>Synergistetes</i>	0.002	0.000	-6.320	-0.011
<i>Tenericutes</i>	0.001	0.023	-7.339	-0.005
<i>Thermotogae</i>	0.004	0.000	-5.534	-0.022
unclassified <i>Bacteria</i>	0.008	0.000	-4.816	-0.039
unclassified <i>Proteobacteria</i>	0.001	0.000	-6.908	-0.007
<i>Verrucomicrobia</i>	0.007	0.692	-4.984	-0.034
$D = \sum p_i^2$		0.199		
$\sum p_i (\ln p_i)$				-2.218
$H = -\sum p_i (\ln p_i)$				2.218
$E_H = H / H_{max}$				0.659

* Mean percentage representations (relative abundance) of phyla/classes were directly used as their (n_i / n) values.

Shannon's equitability (E_H) was obtained by dividing H by H_{max} . H_{max} is known to be $\ln S$, where S = total number of phyla/classes in the community. Thus, here $H_{max} = \ln 29 = 3.367$.

SupplementaryTable 16. Calculation of ecological indices for WG3 using phylum-/class-level distribution of shotgun metagenomic reads.

	Dominance (D) *		Shannon diversity index (H) #	
	$p_i = n_i / n$	p_i^2	$\text{Ln } p_i$	$p_i (\text{Ln } p_i)$
<i>Acidobacteria</i>	0.007	0.001	-4.998	-0.034
<i>Actinobacteria</i>	0.014	0.000	-4.279	-0.059
<i>Alphaproteobacteria</i>	0.016	0.000	-4.110	-0.067
<i>Aquificae</i>	0.114	0.013	-2.168	-0.248
<i>Bacteroidetes</i>	0.032	0.001	-3.440	-0.110
<i>Betaproteobacteria</i>	0.024	0.001	-3.736	-0.089
<i>Chlamydiae</i>	0.001	0.000	-7.264	-0.005
<i>Chlorobi</i>	0.037	0.001	-3.286	-0.123
<i>Chloroflexi</i>	0.362	0.131	-1.016	-0.368
<i>Cyanobacteria</i>	0.127	0.016	-2.067	-0.262
<i>Deferribacteres</i>	0.001	0.000	-6.571	-0.009
<i>Deinococcus-Thermus</i>	0.118	0.014	-2.135	-0.252
<i>Deltaproteobacteria</i>	0.027	0.001	-3.605	-0.098
<i>Dictyoglomi</i>	0.001	0.003	-7.070	-0.006
<i>Epsilonproteobacteria</i>	0.005	0.003	-5.371	-0.025
<i>Firmicutes</i>	0.038	0.001	-3.260	-0.125
<i>Fusobacteria</i>	0.001	0.000	-6.908	-0.007
<i>Gammaproteobacteria</i>	0.039	0.002	-3.243	-0.127
<i>Gemmatimonadetes</i>	0.001	0.000	-7.264	-0.005
<i>Nitrospirae</i>	0.002	0.003	-6.190	-0.013
Others	0.002	0.001	-6.470	-0.010
<i>Planctomycetes</i>	0.004	0.000	-5.573	-0.021
<i>Spirochaetes</i>	0.004	0.003	-5.534	-0.022
<i>Synergistetes</i>	0.001	0.000	-6.812	-0.007
<i>Tenericutes</i>	0.000	0.000	-7.824	-0.003
<i>Thermotogae</i>	0.006	0.000	-5.167	-0.029
unclassified <i>Bacteria</i>	0.003	0.000	-5.793	-0.018
unclassified <i>Proteobacteria</i>	0.001	0.003	-7.506	-0.004
<i>Verrucomicrobia</i>	0.012	0.000	-4.398	-0.054
$D = \sum p_i^2$		0.182		
$\sum p_i (\text{Ln } p_i)$				-2.202
$H = -\sum p_i (\text{Ln } p_i)$				2.202
$E_H = H / H_{max}$				0.654

* Mean percentage representations (relative abundance) of phyla/classes were directly used as their (n_i / n) values.

Shannon's equitability (E_H) was obtained by dividing H by H_{max} . H_{max} is known to be $\text{Ln } S$, where S = total number of phyla/classes in the community. Thus, here $H_{max} = \text{Ln } 29 = 3.367$.

SupplementaryTable 17. Calculation of ecological indices for WG4 using phylum-/class-level distribution of shotgun metagenomic reads.

	Dominance (<i>D</i>) *		Shannon diversity index (<i>H</i>) #	
	$p_i = n_i / n$	p_i^2	$\ln p_i$	$p_i (\ln p_i)$
<i>Acidobacteria</i>	0.007	0.003	-4.969	-0.035
<i>Actinobacteria</i>	0.017	0.000	-4.083	-0.069
<i>Alphaproteobacteria</i>	0.018	0.000	-4.029	-0.072
<i>Aquificae</i>	0.097	0.009	-2.331	-0.227
<i>Bacteroidetes</i>	0.055	0.003	-2.892	-0.160
<i>Betaproteobacteria</i>	0.015	0.000	-4.227	-0.062
<i>Chlamydiae</i>	0.001	0.003	-7.070	-0.006
<i>Chlorobi</i>	0.082	0.007	-2.502	-0.205
<i>Chloroflexi</i>	0.263	0.069	-1.334	-0.351
<i>Cyanobacteria</i>	0.193	0.037	-1.646	-0.317
<i>Deferribacteres</i>	0.004	0.000	-5.655	-0.020
<i>Deinococcus-Thermus</i>	0.080	0.006	-2.526	-0.202
<i>Deltaproteobacteria</i>	0.033	0.001	-3.427	-0.111
<i>Dictyoglomi</i>	0.003	0.003	-5.860	-0.017
<i>Epsilonproteobacteria</i>	0.005	0.003	-5.308	-0.026
<i>Firmicutes</i>	0.050	0.002	-2.998	-0.150
<i>Fusobacteria</i>	0.001	0.000	-6.571	-0.009
<i>Gammaproteobacteria</i>	0.028	0.001	-3.561	-0.101
<i>Gemmatimonadetes</i>	0.001	0.000	-7.131	-0.006
<i>Nitrospirae</i>	0.005	0.000	-5.350	-0.025
Others	0.002	0.003	-6.240	-0.012
<i>Planctomycetes</i>	0.004	0.000	-5.521	-0.022
<i>Spirochaetes</i>	0.007	0.000	-5.036	-0.033
<i>Synergistetes</i>	0.002	0.000	-6.470	-0.010
<i>Tenericutes</i>	0.001	0.003	-7.506	-0.004
<i>Thermotogae</i>	0.018	0.000	-4.023	-0.072
unclassified <i>Bacteria</i>	0.004	0.000	-5.655	-0.020
unclassified <i>Proteobacteria</i>	0.001	0.003	-7.506	-0.004
<i>Verrucomicrobia</i>	0.007	0.000	-4.962	-0.035
$D = \sum p_i^2$		0.138		
$\sum p_i (\ln p_i)$				-2.382
$H = -\sum p_i (\ln p_i)$				2.382
$E_H = H / H_{max}$				0.708

* Mean percentage representations (relative abundance) of phyla/classes were directly used as their (n_i / n) values.

Shannon's equitability (E_H) was obtained by dividing H by H_{max} . H_{max} is known to be $\ln S$, where $S =$ total number of phyla/classes in the community. Thus, here $H_{max} = \ln 29 = 3.367$.

SupplementaryTable 18. Calculation of ecological indices for WG5 using phylum-/class-level distribution of shotgun metagenomic reads.

	Dominance (D) *		Shannon diversity index (H) #	
	$p_i = n_i / n$	p_i^2	$\text{Ln } p_i$	$p_i (\text{Ln } p_i)$
<i>Acidobacteria</i>	0.007	0.002	-4.913	-0.036
<i>Actinobacteria</i>	0.027	0.001	-3.623	-0.097
<i>Alphaproteobacteria</i>	0.030	0.001	-3.523	-0.104
<i>Aquificae</i>	0.002	0.000	-6.240	-0.012
<i>Bacteroidetes</i>	0.033	0.001	-3.404	-0.113
<i>Betaproteobacteria</i>	0.019	0.000	-3.982	-0.074
<i>Chlamydiae</i>	0.001	0.002	-7.070	-0.006
<i>Chlorobi</i>	0.032	0.001	-3.428	-0.111
<i>Chloroflexi</i>	0.329	0.108	-1.112	-0.366
<i>Cyanobacteria</i>	0.361	0.130	-1.020	-0.368
<i>Deferribacteres</i>	0.001	0.000	-7.264	-0.005
<i>Deinococcus-Thermus</i>	0.013	0.000	-4.370	-0.055
<i>Deltaproteobacteria</i>	0.028	0.001	-3.560	-0.101
<i>Dictyoglomi</i>	0.001	0.000	-7.419	-0.004
<i>Epsilonproteobacteria</i>	0.002	0.000	-6.215	-0.012
<i>Firmicutes</i>	0.047	0.002	-3.051	-0.144
<i>Fusobacteria</i>	0.001	0.000	-7.070	-0.006
<i>Gammaproteobacteria</i>	0.033	0.001	-3.427	-0.111
<i>Gemmatimonadetes</i>	0.001	0.000	-7.264	-0.005
<i>Nitrospirae</i>	0.001	0.000	-6.645	-0.009
Others	0.002	0.000	-6.470	-0.010
<i>Planctomycetes</i>	0.006	0.000	-5.185	-0.029
<i>Spirochaetes</i>	0.010	0.000	-4.595	-0.046
<i>Synergistetes</i>	0.001	0.003	-6.859	-0.007
<i>Tenericutes</i>	0.000	0.002	-7.958	-0.003
<i>Thermotogae</i>	0.002	0.063	-6.097	-0.014
unclassified <i>Bacteria</i>	0.004	0.003	-5.485	-0.023
unclassified <i>Proteobacteria</i>	0.001	0.000	-7.013	-0.006
<i>Verrucomicrobia</i>	0.007	0.003	-4.927	-0.036
$D = \sum p_i^2$		0.247		
$\sum p_i (\text{Ln } p_i)$				-1.915
$H = -\sum p_i (\text{Ln } p_i)$				1.915
$E_H = H / H_{max}$				0.569

* Mean percentage representations (relative abundance) of phyla/classes were directly used as their (n_i / n) values.

Shannon's equitability (E_H) was obtained by dividing H by H_{max} . H_{max} is known to be $\text{Ln } S$, where S = total number of phyla/classes in the community. Thus, here $H_{max} = \text{Ln } 29 = 3.367$.

SupplementaryTable 19. Calculation of ecological indices for WG6 using phylum-/class-level distribution of shotgun metagenomic reads.

	Dominance (<i>D</i>) *		Shannon diversity index (<i>H</i>) #	
	$p_i = n_i / n$	p_i^2	$\ln p_i$	$p_i (\ln p_i)$
<i>Acidobacteria</i>	0.009	0.000	-4.756	-0.041
<i>Actinobacteria</i>	0.022	0.000	-3.819	-0.084
<i>Alphaproteobacteria</i>	0.097	0.009	-2.332	-0.226
<i>Aquificae</i>	0.002	0.000	-6.240	-0.012
<i>Bacteroidetes</i>	0.500	0.250	-0.694	-0.347
<i>Betaproteobacteria</i>	0.034	0.001	-3.383	-0.115
<i>Chlamydiae</i>	0.001	0.002	-6.608	-0.009
<i>Chlorobi</i>	0.024	0.001	-3.726	-0.090
<i>Chloroflexi</i>	0.090	0.008	-2.414	-0.216
<i>Cyanobacteria</i>	0.034	0.001	-3.389	-0.114
<i>Deferribacteres</i>	0.001	0.000	-6.908	-0.007
<i>Deinococcus-Thermus</i>	0.007	0.000	-4.962	-0.035
<i>Deltaproteobacteria</i>	0.028	0.001	-3.588	-0.099
<i>Dictyoglomi</i>	0.000	0.000	-7.706	-0.003
<i>Epsilonproteobacteria</i>	0.004	0.000	-5.521	-0.022
<i>Firmicutes</i>	0.046	0.002	-3.081	-0.141
<i>Fusobacteria</i>	0.002	0.000	-6.438	-0.010
<i>Gammaproteobacteria</i>	0.055	0.003	-2.895	-0.160
<i>Gemmatimonadetes</i>	0.001	0.002	-7.070	-0.006
<i>Nitrospirae</i>	0.001	0.000	-6.725	-0.008
Others	0.002	0.003	-6.012	-0.015
<i>Planctomycetes</i>	0.015	0.000	-4.177	-0.064
<i>Spirochaetes</i>	0.004	0.000	-5.534	-0.022
<i>Synergistetes</i>	0.001	0.000	-6.959	-0.007
<i>Tenericutes</i>	0.001	0.000	-7.419	-0.004
<i>Thermotogae</i>	0.002	0.000	-6.320	-0.011
unclassified <i>Bacteria</i>	0.005	0.000	-5.360	-0.025
unclassified <i>Proteobacteria</i>	0.001	0.000	-7.264	-0.005
<i>Verrucomicrobia</i>	0.013	0.000	-4.358	-0.056
$D = \sum p_i^2$		0.277		
$\sum p_i (\ln p_i)$				-1.955
$H = -\sum p_i (\ln p_i)$				1.955
$E_H = H / H_{max}$				0.581

* Mean percentage representations (relative abundance) of phyla/classes were directly used as their (n_i / n) values.

Shannon's equitability (E_H) was obtained by dividing H by H_{max} . H_{max} is known to be $\ln S$, where S = total number of phyla/classes in the community. Thus, here $H_{max} = \ln 29 = 3.367$.

SupplementaryTable 20. Calculation of ecological indices for WG7 using phylum-/class-level distribution of shotgun metagenomic reads.

	Dominance (D) *		Shannon diversity index (H) #	
	$p_i = n_i / n$	p_i^2	$\text{Ln } p_i$	$p_i (\text{Ln } p_i)$
<i>Acidobacteria</i>	0.027	0.001	-3.599	-0.098
<i>Actinobacteria</i>	0.026	0.001	-3.646	-0.095
<i>Alphaproteobacteria</i>	0.103	0.011	-2.269	-0.235
<i>Aquificae</i>	0.003	0.000	-5.714	-0.019
<i>Bacteroidetes</i>	0.167	0.028	-1.791	-0.299
<i>Betaproteobacteria</i>	0.085	0.007	-2.468	-0.209
<i>Chlamydiae</i>	0.002	0.000	-6.377	-0.011
<i>Chlorobi</i>	0.071	0.005	-2.649	-0.187
<i>Chloroflexi</i>	0.074	0.006	-2.600	-0.193
<i>Cyanobacteria</i>	0.156	0.024	-1.860	-0.290
<i>Deferribacteres</i>	0.002	0.002	-6.407	-0.011
<i>Deinococcus-Thermus</i>	0.009	0.000	-4.689	-0.043
<i>Deltaproteobacteria</i>	0.063	0.004	-2.759	-0.175
<i>Dictyoglomi</i>	0.001	0.002	-7.070	-0.006
<i>Epsilonproteobacteria</i>	0.004	0.002	-5.560	-0.021
<i>Firmicutes</i>	0.067	0.004	-2.708	-0.181
<i>Fusobacteria</i>	0.002	0.000	-6.240	-0.012
<i>Gammaproteobacteria</i>	0.068	0.005	-2.691	-0.182
<i>Gemmatimonadetes</i>	0.002	0.000	-6.377	-0.011
<i>Nitrospirae</i>	0.002	0.000	-6.119	-0.013
Others	0.004	0.000	-5.560	-0.021
<i>Planctomycetes</i>	0.019	0.000	-3.950	-0.076
<i>Spirochaetes</i>	0.016	0.000	-4.110	-0.067
<i>Synergistetes</i>	0.002	0.000	-6.097	-0.014
<i>Tenericutes</i>	0.001	0.000	-7.506	-0.004
<i>Thermotogae</i>	0.004	0.000	-5.613	-0.020
unclassified <i>Bacteria</i>	0.005	0.000	-5.240	-0.028
unclassified <i>Proteobacteria</i>	0.001	0.000	-6.685	-0.008
<i>Verrucomicrobia</i>	0.015	0.000	-4.186	-0.064
$D = \sum p_i^2$		0.096		
$\sum p_i (\text{Ln } p_i)$				-2.594
$H = -\sum p_i (\text{Ln } p_i)$				2.594
$E_H = H / H_{max}$				0.770

* Mean percentage representations (relative abundance) of phyla/classes were directly used as their (n_i / n) values.

Shannon's equitability (E_H) was obtained by dividing H by H_{max} . H_{max} is known to be $\text{Ln } S$, where S = total number of phyla/classes in the community. Thus, here $H_{max} = \text{Ln } 29 = 3.367$.

SupplementaryTable 21. Genera collectively accounting for average 50% of all classifiable reads (after searching against the nr protein sequence database) in the metagenomes of the mat communities VWM, DG3 and DG4 (names are in the descending order of their relative abundance within the community).

VWM*	DG3 [§]	DG4 [#]
<i>Thermus</i>	<i>Roseiflexus, Flavobacterium, Thermosynechococcus, Chloroflexus, Chloroherpeton, Cyanothece, Synechococcus, Oscillochloris, Chlorobium, Anabaena, Nostoc, Synechocystis</i>	<i>Roseiflexus, Chloroflexus, Oscillochloris, Herpetosiphon, Anaerolinea, Pseudomonas, Chloroherpeton, Synechococcus, Chlorobium, Bacillus, Cyanothece, Sphaerobacter, Anabaena, Nostoc, Xanthomonas, Paracoccus, Clostridium, Geobacter, Ktedonobacter, Deinococcus, Meiothermus, Thermus, Thermobaculum, Streptomyces, Rubrobacter, Candidatus Solibacter, Truepera, Chlorobaculum, Rhodobacter, Thermomicrobium, Burkholderia, Symbiobacterium, Anaeromyxobacter, Rhodothermus, Geobacillus, Myxococcus, Paenibacillus, Mycobacterium, Desulfovibrio, Thermosynechococcus, Dehalococcoides, Synechocystis, Pelodictyon, Stenotrophomonas, Microcoleus, Gloeobacter, Cytophaga, Bradyrhizobium, Candidatus Koribacter, Spirosoma</i>

* Only one genus accounted for an average 50.64 % of all classifiable reads in VWM.

§ 12 genera accounted for an average 50.12 % of all classifiable reads in DG3.

50 one genus accounted for an average 50.11 % of all classifiable reads in DG4.

Supplementary Table 22. Genera collectively accounting for average 50% of all classifiable reads (after searching against the nr protein sequence database) in the metagenomes of WG3, WG4, WG5, WG6 and WG7 (names are in the descending order of their relative abundance within the community).

WG3 ¹	WG4 ²	WG5 ³	WG6 ⁴	WG7 ⁵
<i>Roseiflexus, Thermus, Sulfurihydrogenibium, Thermosynechococcus, Chloroflexus, Oscillochloris, Cyanothece, Chloroherpeton, Synechococcus, Chlorobium, Aquifex</i>	<i>Roseiflexus, Thermosynechococcus, Sulfurihydrogenibium, Thermus, Chloroflexus, Chloroherpeton, Cyanothece, Oscillochloris, Chlorobium, Anaerolinea, Synechococcus, Thermotoga, Aquifex, Anabaena, Nostoc, Bacteroides, Meiothermus</i>	<i>Roseiflexus, Chloroflexus, Synechococcus, Cyanothece, Oscillochloris, Anabaena, Nostoc, Thermosynechococcus, Herpetosiphon, Synechocystis, Thermus, Sulfurihydrogenibium, Meiothermus, Aquifex, Thermotoga, Deinococcus, Geobacter, Oceanithermus, Chloroherpeton, Chlorobium, Anaerolinea, Pseudomonas, Bacillus, Flavobacterium, Gramella, Chitinophaga, Bacteroides, Pedobacter, Spirosoma, Cytophaga, Maribacter,</i>	<i>Flavobacterium, Roseiflexus, Gramella, Chitinophaga, Bacteroides, Pedobacter, Chloroflexus, Spirosoma, Cytophaga, Maribacter, Dyadobacter, Polaribacter, Robiginitalea, Microscilla, Oscillochloris, Croceibacter, Capnocytophaga, Leeuwenhoekiiella, Marivirga, Zunongwangia, Dokdonia, Chlorobium, Algoriphagus, Cellulophaga, Kordia, Bacillus, Chloroherpeton, Prevotella, Parabacteroides, Leadbetterella, Sphingobacterium, Herpetosiphon, Rhodobacter, Psychroflexus, Synechococcus, Nitrosomonas, Anaerolinea, Mucilaginibacter, Cyanothece, Candidatus Solibacter, Clostridium, Porphyromonas, Rhodothermus, Chryseobacterium, Geobacter, Pseudomonas, Riemerella, Rhodopirellula, Burkholderia, Shewanella, Salinibacter, Sphingomonas, Anabaena,</i>	<i>Roseiflexus, Chloroherpeton, Synechococcus, Cyanothece, Candidatus Solibacter, Chlorobium, Chloroflexus, Anabaena, Hyphomonas, Nostoc, Thermosynechococcus, Bacteroides, Burkholderia, Desulfovibrio, Anaerolinea, Clostridium, Pedobacter, Geobacter, Flavobacterium, Oscillochloris, Cytophaga, Chitinophaga, Spirosoma, Chlorobaculum, Bacillus, Synechocystis, Pseudomonas, Herpetosiphon, Cupriavidus, Dyadobacter, Trichodesmium, Gramella, Ralstonia, Pelodictyon, Rhodobacter, Microscilla, Bordetella, Magnetospirillum, Anaeromyxobacter, Treponema, Planctomyces, Rhodothermus, Rhodospirillum, Acidovorax, Leptospira, Candidatus Koribacter, Prosthecochloris, Rhodopseudomonas, Spirochaeta, Parabacteroides, Marivirga, Prevotella, Rhodopirellula, Syntrophobacter, Microcoleus, Gloeobacter, Chthoniobacter,</i>

		<i>Trichodesmium,</i> <i>Microcystis,</i> <i>Arthrospira,</i> <i>Microcoleus</i>	<i>Nostoc, Planctomyces,</i> <i>Paludibacter, Roseobacter,</i> <i>Alistipes, Ruegeria,</i> <i>Magnetospirillum,</i> <i>Rhodospirillum</i> <i>Desulfovibrio, Chlorobaculum,</i> <i>Xanthomonas, Vibrio,</i> <i>Streptomyces, Chthoniobacter,</i> <i>Sphaerobacter, Pelodictyon</i>	<i>Polaromonas, Microcystis,</i> <i>Bradyrhizobium, Salinibacter,</i> <i>Methylobacterium, Acaryochloris,</i> <i>Shewanella, Pelobacter,</i> <i>Arthrospira, Sphingomonas,</i> <i>Robiginitalea, Myxococcus,</i> <i>Thiobacillus, Streptomyces,</i> <i>Thioalkalivibrio, Nitrosomonas,</i> <i>Methylibium, Oscillatoria,</i> <i>Aromatoleum, Nitrosococcus,</i> <i>Nodularia, Blastopirellula,</i> <i>Sphingobacterium, Leadbetterella</i>
--	--	---	---	---

¹ 11 genera accounted for an average 50.16 % of all classifiable reads in WG3.

² 17 one genus accounted for an average 50.3 % of all classifiable reads in WG4.

³ 35 genera accounted for an average 50.32 % of all classifiable reads in WG5.

⁴ 68 one genus accounted for an average 50.18 % of all classifiable reads in WG6.

⁵ 81 genera accounted for an average 50.56 % of all classifiable reads in WG7.

Supplementary Table 23. Total number of genera identified in VWM after searching both its metagenomic readsets against the RDP database.

Name of the phylum	Number of genera identified	Names of genera identified
<i>Actinobacteria</i>	5	<i>Actinoplanes, Saccharopolyspora, Thermobispora, Tropheryma, Thermobifida</i>
<i>Aquificae</i>	5	<i>Sulfurihydrogenibium, Venenivibrio, Persephonella, Hydrogenobaculum, Desulfurobacterium</i>
<i>Bacteroidetes</i>	4	<i>Alistipes, Cytophaga, Rhodothermus, Salinibacter</i>
<i>Chloroflexi</i>	5	<i>Chloroflexus, Roseiflexus, Herpetosiphon, Dehalococcoides, Thermomicrobium</i>
<i>Cyanobacteria</i>	2	<i>Synechococcus, Oscillatoria</i>
<i>Deinococcus-Thermus</i>	2	<i>Thermus, Meiothermus</i>
<i>Dictyoglomi</i>	1	<i>Dictyoglomus</i>
<i>Firmicutes</i>	12	<i>Anoxybacillus, Bacillus, Geobacillus, Paenibacillus, Trichococcus, Lactobacillus, Clostridium, Caldicellulosiruptor, Coprothermobacter, Thermodesulfobium, Streptococcus, Carboxydotherrmus</i>
<i>Nitrospirae</i>	1	<i>Thermodesulfovibrio</i>
<i>Proteobacteria</i>	7	<i>Pseudomonas, Blastochloris, Thiobacillus, Acidithiobacillus, Microbulbifer, Campylobacter, Thiohalocapsa</i>
<i>Spirochaetes</i>	1	<i>Treponema</i>
<i>Tenericutes</i>	1	<i>Acholeplasma</i>
<i>Thermodesulfobacteria</i>	2	<i>Thermodesulfobacterium, Thermodesulfatator</i>
<i>Thermotogae</i>	3	<i>Thermotoga, Thermosipho, Fervidobacterium</i>

SupplementaryTable 24. Total number of genera identified in DG3 after searching both its metagenomic readsets against the RDP database.

Name of the phylum	Number of genera identified	Names of genera identified
<i>Acidobacteria</i>	1	<i>Candidatus Solibacter</i>
<i>Actinobacteria</i>	11	<i>Actinoplanes, Atopobium, Propionibacterium, Streptomyces, Frankia, Curtobacterium, Rathayibacter, Renibacterium, Nocardia, Kitasatospora, Thermoleophilum</i>
<i>Aquificae</i>	1	<i>Sulfurihydrogenibium</i>
<i>Bacteroidetes</i>	21	<i>Alistipes, Cytophaga, Flectobacillus, Flexibacter, Hymenobacter, Microscilla, Spirosoma, Flammeovirga, Flexithrix, Capnocytophaga, Croceibacter, Elizabethkingia, Flavobacterium, Gramella, Myroides, Tenacibaculum, Sphingobacterium, Chitinophaga, Prolixibacter, Marinoscillum, Wautersiella</i>
<i>Chlorobi</i>	4	<i>Chlorobaculum, Prosthecochloris, Chlorobium, Chloroherpeton</i>
<i>Chloroflexi</i>	7	<i>Chloroflexus, Roseiflexus, Oscillochloris, Herpetosiphon, Dehalococcoides, Sphaerobacter, Thermomicrobium</i>
<i>Cyanobacteria</i>	22	<i>Cyanothece, Gloeocapsopsis, Microcystis, Synechococcus, Anabaena, Dolichospermum, Nodularia, Calothrix, Scytonema, Geitlerinema, Oscillatoria, Planktothrix, Pseudanabaena, Spirulina, Chroococcidiopsis, Pleurocapsa, Stanieria, Xenococcus, Prochlorothrix, Thermosynechococcus, Leptolyngbya, Aphanizomenon</i>
<i>Deinococcus-Thermus</i>	2	<i>Deinococcus, Thermus</i>
<i>Firmicutes</i>	16	<i>Bacillus, Sporosarcina, Lysinibacillus, Planomicrobium, Kurthia, Faecalibacterium, Listeria, Brevibacillus, Leuconostoc, Oxobacter, Desulfotomaculum, Alicyclobacillus, Laceyella, Clostridium, Ammonifex, Thermodesulfobium</i>
<i>Planctomycetes</i>	1	<i>Isosphaera</i>
<i>Proteobacteria</i>	16	<i>Methylobacterium, Paracoccus, Rubritepida, Bdellovibrio, Desulfomicrobium, Arcobacter, Thiocapsa, Actinobacillus, Acinetobacter, Thiothrix, Helicobacter, Campylobacter, Burkholderia, Desulfocella, Acidithiobacillus, Pseudomonas</i>
<i>Spirochaetes</i>	4	<i>Leptonema, Leptospira, Spirochaeta, Treponema</i>
<i>Tenericutes</i>	1	<i>Mycloplasma</i>
<i>Thermotogae</i>	1	<i>Thermotoga</i>
<i>Verrucomicrobia</i>	4	<i>Diplosphaera, Chthoniobacter, Verrucomicrobium, Methylacidiphilum</i>

SupplementaryTable 25. Total number of genera identified in DG4 after searching both its metagenomic readsets against the RDP database.

Name of the phylum	Number of genera identified	Names of genera identified
<i>Actinobacteria</i>	9	<i>Gordonia, Microbacterium, Rhodococcus, Rathayibacter, Streptomyces, Atopobium, Rubrobacter, Tropheryma</i>
<i>Aquificae</i>	2	<i>Sulfurihydrogenibium, Persephonella</i>
<i>Bacteroidetes</i>	24	<i>Bacteroides, Odoribacter, Parabacteroides, Tannerella, Alistipes, Cytophaga, Flexibacter, Hymenobacter, Spirosoma, Flexithrix, Capnocytophaga, Elizabethkingia, Gramella, Tenacibaculum, Wautersiella, Saprospira, Pedobacter, Chitinophaga, Prolixibacter, Porphyromonas, Cyclobacterium, Flectobacillus, Microscilla, Cellulophaga</i>
<i>Chlorobi</i>	4	<i>Chlorobium, Prosthecochloris, Chlorobaculum, Chloroherpeton</i>
<i>Chloroflexi</i>	8	<i>Roseiflexus, Oscillochloris, Dehalococcoides, Herpetosiphon, Chloroflexus, Thermomicrobium, Sphaerobacter, Ktedonobacter</i>
<i>Cyanobacteria</i>	17	<i>Cyanobacterium, Cyanothece, Gloeocapsopsis, Microcystis, Synechococcus, Calothrix, Scytonema, Geitlerinema, Leptolyngbya, Microcoleus, Oscillatoria, Phormidium, Spirulina, Chroococciopsis, Chlorogloeopsis, Fischerella, Nostoc</i>
<i>Deinococcus-Thermus</i>	3	<i>Deinococcus, Truepera, Thermus</i>
<i>Firmicutes</i>	14	<i>Alicyclobacillus, Bacillus, Laceyella, Exiguobacterium, Leuconostoc, Streptococcus, Clostridium, Anaerococcus, Butyrivibrio, Desulfosporosinus, Ruminococcus, Syntrophomonas, Staphylococcus, Lactococcus</i>
<i>Planctomycetes</i>	1	<i>Isosphaera</i>
<i>Proteobacteria</i>	31	<i>Bradyrhizobium, Alishewanella, Azospirillum, Desulfovibrio, Enterobacter, Escherichia, Kinetoplastibacterium, Kingella, Novosphingobium, Paracoccus, Phyllobacterium, Pseudomonas, Rhodobaca, Rhodobacter, Roseisalinus, Roseococcus, Rubritepida, Shigella, Sphingopyxis, Stenotrophomonas, Thiocapsa, Thiothrix, Xanthomonas, Xylella, Desulfocella, Azotobacter, Helicobacter, Methylococcus, Nitrososphaera, Sorangium, Thiorhodococcus</i>
<i>Spirochaetes</i>	3	<i>Leptospira, Spirochaeta, Treponema</i>
<i>Tenericutes</i>	1	<i>Acholeplasma</i>
<i>Thermodesulfobacteria</i>	1	<i>Thermodesulfobacterium</i>
<i>Thermotogae</i>	1	<i>Fervidobacterium</i>
<i>Verrucomicrobia</i>	2	<i>Pedosphaera, Methylococcus</i>

SupplementaryTable 26. Total number of genera identified in WG3 after searching both its metagenomic readsets against the RDP database.

Name of the phylum	Number of genera identified	Names of genera identified
<i>Actinobacteria</i>	6	<i>Thermobispora, Enterorhabdus, Actinoplanes, Propionibacterium, Kitasatospora, Streptomyces</i>
<i>Aquificae</i>	3	<i>Persephonella, Sulfurihydrogenibium, Venenivibrio</i>
<i>Bacteroidetes</i>	9	<i>Hymenobacter, Rhodothermus, Flexithrix, Bacteroides, Alistipes, Salinibacter, Porphyromonas, Blattabacterium, Flavobacterium</i>
<i>Chlamydiae</i>	2	<i>Chlamydophila, Criblamydia</i>
<i>Chlorobi</i>	4	<i>Prosthecochloris, Chlorobaculum, Chloroherpeton, Chlorobium</i>
<i>Chloroflexi</i>	7	<i>Chloroflexus, Roseiflexus, Oscillochloris, Dehalococcoides, Ktedonobacter, Thermomicrobium, Herpetosiphon</i>
<i>Cyanobacteria</i>	8	<i>Synechococcus, Thermosynechococcus, Dolichospermum, Gloeobacter, Cylandrospermopsis, Nostoc, Planktothrix, Prochlorothrix</i>
<i>Deinococcus-Thermus</i>	2	<i>Thermus, Meiothermus</i>
<i>Firmicutes</i>	11	<i>Alicyclobacillus, Bacillus, Geobacillus, Aneurinibacillus, Paenibacillus, Lactobacillus, Leuconostoc, Clostridium, Butyrivibrio, Caldicellulosiruptor, Brevibacillus</i>
<i>Nitrospirae</i>	1	<i>Thermodesulfovibrio</i>
<i>Proteobacteria</i>	22	<i>Pseudomonas, Xanthomonas, Thiobacillus, Helicobacter, Thiocapsa, Magnetospirillum, Comamonas, Thiomonas, Neisseria, Desulfovibrio, Desulfoglaeba, Thermodesulforhabdus, Microbulbifer, Idiomarina, Halochromatium, Halorhodospira, Thiohalospira, Methylothermus, Xylella, Marichromatium, Campylobacter, Candidatus Liberibacter</i>
<i>Spirochaetes</i>	3	<i>Borrelia, Leptonema, Leptospira</i>
<i>Tenericutes</i>	1	<i>Spiroplasma</i>
<i>Thermodesulfobacteria</i>	2	<i>Thermodesulfobacterium, Thermodesulfatator</i>
<i>Thermotogae</i>	2	<i>Thermotoga, Fervidobacterium</i>
<i>Verrucomicrobia</i>	1	<i>Chthoniobacter</i>

SupplementaryTable 27. Total number of genera identified in WG4 after searching both its metagenomic readsets against the RDP database.

Name of the phylum	Number of genera identified	Names of genera identified
<i>Actinobacteria</i>	18	<i>Corynebacterium, Glycomyces, Clavibacter, Actinoplanes, Nocardia, Rhodococcus, Propionibacterium, Thermobispora, Kitasatospora, Actinomadura, Tropheryma, Bifidobacterium, Atopobium, Eggerthella, Enterorhabdus, Thermoleophilum, Rathayibacter, Streptomyces</i>
<i>Aquificae</i>	5	<i>Hydrogenobacter, Desulfurobacterium, Persephonella, Sulfurihydrogenibium, Venenivibrio</i>
<i>Bacteroidetes</i>	28	<i>Bacteroides, Butyricimonas, Odoribacter, Parabacteroides, Porphyromonas, Tannerella, Prevotella, Alistipes, Rikenella, Cytophaga, Flexibacter, Hymenobacter, Microscilla, Flexithrix, Blattabacterium, Coenonia, Flavobacterium, Leeuwenhoekia, Myroides, Ornithobacterium, Riemeella, Tenacibaculum, Zunongwangia, Rhodothermus, Salinibacter, Prolixibacter, Capnocytophaga, Maribacter</i>
<i>Chlamydiae</i>	2	<i>Criblamydia, Chlamydophila</i>
<i>Chlorobi</i>	4	<i>Chlorobaculum, Chlorobium, Chloroherpeton, Prosthecochloris</i>
<i>Chloroflexi</i>	7	<i>Chloroflexus, Roseiflexus, Oscillochloris, Herpetosiphon, Dehalococcoides, Sphaerobacter, Thermomicrobium</i>
<i>Cyanobacteria</i>	21	<i>Gloeobacter, Acaryochloris, Microcystis, Synechococcus, Thermosynechococcus, Anabaena, Anabaenopsis, Dolichospermum, Nodularia, Nostoc, Calothrix, Geitlerinema, Leptolyngbya, Lyngbya, Pseudanabaena, Spirulina, Chroococcidiopsis, Prochlorothrix, Arthrospira, Oscillatoria, Planktothrix</i>
<i>Deferribacteres</i>	2	<i>Deferribacter, Flexistipes</i>
<i>Deinococcus-Thermus</i>	2	<i>Meiothermus, Thermus</i>
<i>Dictyoglomi</i>	1	<i>Dictyoglomus</i>
<i>Firmicutes</i>	22	<i>Alicyclobacillus, Bacillus, Blautia, Brevibacillus, Caldicellulosiruptor, Caloramator, Clostridium, Desulfitobacterium, Geobacillus, Halothermothrix, Lactobacillus, Leuconostoc, Staphylococcus, Streptococcus, Sulfobacillus, Syntrophomonas, Veillonella, Weissella, Mechercharimyces, Paenibacillus, Sporanaerobacter, Ammonifex</i>
<i>Fusobacteria</i>	1	<i>Ilyobacter</i>
<i>Nitrospirae</i>	2	<i>Leptospirillum, Thermodesulfobivrio</i>
<i>Planctomycetes</i>	1	<i>Isosphaera</i>
<i>Proteobacteria</i>	33	<i>Candidatus Liberibacter, Acetobacter, Rubritepida, Rhodovibrio, Ehrlichia, Ralstonia, Nitrospira, Desulfosarcina, Desulfomicrobium, Desulfobivrio, Desulfocaldus, Campylobacter, Helicobacter, Acidithiobacillus, Pseudoalteromonas, Marichromatium, Thiocapsa, Halorhodospira, Thioalkalivibrio, Methylohalobius,</i>

		<i>Methylothermus, Acinetobacter, Pseudomonas, Stenotrophomonas, Xanthomonas, Xylella, Francisella, Magnetospirillum, Burkholderia, Methylobacillus, Thauera, Desulfonauticus, Allochromatium</i>
<i>Spirochaetes</i>	5	<i>Leptonema, Leptospira, Borrelia, Spirochaeta, Treponema</i>
<i>Synergistetes</i>	1	<i>Aminobacterium</i>
<i>Tenericutes</i>	1	<i>Spiroplasma</i>
<i>Thermodesulfobacteria</i>	2	<i>Thermodesulfatator, Thermodesulfobacterium</i>
<i>Thermotogae</i>	3	<i>Fervidobacterium, Thermosipho, Thermotoga</i>
<i>Verrucomicrobia</i>	1	<i>Chthoniobacter</i>

SupplementaryTable 28. Total number of genera identified in WG5 after searching both its metagenomic readsets against the RDP database.

Name of the phylum	Number of genera identified	Names of genera identified
<i>Actinobacteria</i>	4	<i>Streptomyces, Bifidobacterium, Acidithiobacillum, Rhodococcus</i>
<i>Bacteroidetes</i>	17	<i>Cytophaga, Flexibacter, Hymenobacter, Microscilla, Spirosoma, Flammeovirga, Flexithrix, Blattabacterium, Capnocytophaga, Flavobacterium, Wautersiella, Prolixibacter, Prevotella, Flectobacillus, Elizabethkingia, Saprospira, Chitinophaga</i>
<i>Chlorobi</i>	4	<i>Chlorobaculum, Chloroherpeton, Prosthecochloris, Chlorobium</i>
<i>Chloroflexi</i>	7	<i>Chloroflexus, Roseiflexus, Oscillochloris, Herpetosiphon, Dehalococcoides, Sphaerobacter, Thermomicrobium</i>
<i>Cyanobacteria</i>	13	<i>Microcystis, Synechococcus, Anabaena, Nostoc, Calothrix, Geitlerinema, Leptolyngbya, Oscillatoria, Pseudanabaena, Chroococcidiopsis, Stanieria, Xenococcus, Prochlorothrix</i>
<i>Firmicutes</i>	10	<i>Alicyclobacillus, Leuconostoc, Oxobacter, Tissierella, Butyrivibrio, Ammonifex, Caldanaerobius, Bacillus, Lactobacillus, Clostridium</i>
<i>Proteobacteria</i>	10	<i>Methylobacterium, Bdellovibrio, Desulfocella, Desulfomicrobium, Helicobacter, Thiocapsa, Pseudomonas, Acinetobacter, Thiothrix, Desulfovibrio</i>
<i>Spirochaetes</i>	3	<i>Leptospira, Spirochaeta, Treponema</i>
<i>Tenericutes</i>	1	<i>Candidatus Phytoplasma</i>
<i>Thermotogae</i>	1	<i>Thermotoga</i>
<i>Verrucomicrobia</i>	2	<i>Chthoniobacter, Methylacidiphilum</i>

SupplementaryTable 29. Total number of genera identified in WG6 after searching both its metagenomic readsets against the RDP database.

Name of the phylum	Number of genera identified	Names of genera identified
<i>Acidobacteria</i>	1	<i>Candidatus Solibacter</i>
<i>Actinobacteria</i>	13	<i>Actinomyces, Kytococcus, Gordonia, Arthrobacter, Nocardia, Rhodococcus, Streptomyces, Alloscardovia, Stackebrandtia, Microbacterium, Kocuria, Bifidobacterium, Atopobium</i>
<i>Aquificae</i>	3	<i>Hydrogenobaculum, Persephonella, Sulfurihydrogenibium</i>
<i>Bacteroidetes</i>	45	<i>Marinilabilia, Arenibacter, Butyricimonas, Candidatus Amoebophilus, Candidatus Azobacteroides, Candidatus Hemobacterium, Capnocytophaga, Cellulophaga Chitinophaga, Chryseobacterium, Coenonia, Cyclobacterium, Cytophaga, Dokdonia, Elizabethkingia, Flammeovirga, Flavobacterium, Flectobacillus, Flexibacter, Flexithrix, Gramella, Hymenobacter, Leeuwenhoekella, Microscilla, Myroides, Odoribacter, Ornithobacterium, Parabacteroides, Pedobacter, Persicobacter, Polaribacter, Porphyromonas, Prevotella, Prolixibacter, Rhodothermus, Riemerella, Salinibacter, Saprospira, Sphingobacterium, Tenacibaculum, Terrimonas, Zunongwangia, Wautersiella, Bacteroides, Alistipes</i>
<i>Chlamydiae</i>	4	<i>Criblamydia, Candidatus Protochlamydia, Neochlamydia, Parachlamydia</i>
<i>Chlorobi</i>	4	<i>Chlorobaculum, Chlorobium, Chloroherpeton, Prosthecochloris</i>
<i>Chloroflexi</i>	7	<i>Chloroflexus, Roseiflexus, Oscillochloris, Herpetosiphon, Dehalococcoides, Sphaerobacter, Thermomicrobium</i>
<i>Cyanobacteria</i>	16	<i>Acaryochloris, Gloeocapsopsis, Microcystis, Synechococcus, Anabaena, Dolichospermum, Calothrix, Lyngbya, Oscillatoria, Pseudanabaena, Stanieria, Prochlorothrix, Xenococcus, Symploca, Planktothrix, Arthrospira</i>
<i>Deinococcus-Thermus</i>	3	<i>Deinococcus, Truepera, Thermus</i>
<i>Firmicutes</i>	25	<i>Alicyclobacillus, Ammonifex, Bacillus, Brevibacillus, Clostridium, Desulfosporosinus, Erysipelothrix, Jeotgalibacillus, Laceyella, Lactobacillus, Lactococcus, Leuconostoc, Lysinibacillus, Megasphaera, Pelotomaculum, Planomicrobium, Ruminococcus, Selenomonas, Sporosarcina, Staphylococcus, Aeribacillus, Carnobacterium, Desulfotomaculum, Geobacillus, Phascolarctobacterium</i>
<i>Planctomycetes</i>	4	<i>Blastopirellula, Isosphaera, Pirellula, Planctomyces</i>
<i>Proteobacteria</i>	62	<i>Asticcacaulis, Acetobacter, Acidiphilium, Acinetobacter,</i>

		<i>Alcaligenes, Anaplasma, Bdellovibrio, Blastomonas, Bradyrhizobium, Burkholderia, Candidatus Neoehrlichia, Desulfobacterium, Desulfocella, Desulfomicrobium, Desulfovibrio, Desulfuromonas, Erythrobacter, Escherichia, Geobacter, Gluconacetobacter, Gluconobacter, Helicobacter, Holospora, Hyphomonas, Jannaschia, Kinetoplastibacterium, Klebsiella, Legionella, Loktanella, Mesorhizobium, Methylobacterium, Methylophaga, Nitrosococcus, Nitrosomonas, Ochrobactrum, Paracoccus, Phaeobacter, Porphyrobacter, Pseudomonas, Pseudoruegeria, Rhizobium, Rhodobacter, Rhodobium, Rhodospirillum, Rhodothalassium, Rhodovibrio, Rhodovulum, Roseisalinus, Roseobacter, Roseococcus, Roseospira, Rubritepida, Sorangium, Sphingobium, Sphingomonas, Sphingopyxis, Stenotrophomonas, Thermodesulfurhabdus, Thioclava, Thiothrix, Xanthomonas, Xylella</i>
<i>Spirochaetes</i>	3	<i>Leptospira, Borrelia, Treponema</i>
<i>Tenericutes</i>	2	<i>Acholeplasma, Candidatus Phytoplasma</i>
<i>Thermotogae</i>	1	<i>Thermotoga</i>
<i>Verrucomicrobia</i>	7	<i>Diplosphaera, Chthoniobacter, Pedosphaera, Akkermansia, Prosthecobacter, Rubritalea, Methylacidiphilum</i>

SupplementaryTable 30. Total number of genera identified in WG7 after searching both its metagenomic readsets against the RDP database.

Name of the phylum	Number of genera identified	Names of genera identified
<i>Euryarchaeota</i>	1	<i>Methanocella</i>
<i>Acidobacteria</i>	1	<i>Candidatus Solibacter</i>
<i>Actinobacteria</i>	19	<i>Acidithiomicrobium</i> , <i>Brevibacterium</i> , <i>Corynebacterium</i> , <i>Microbacterium</i> , <i>Arthrobacter</i> , <i>Nesterenkonia</i> , <i>Nocardia</i> , <i>Rhodococcus</i> , <i>Nocardioides</i> , <i>Thermobifida</i> , <i>Propionibacterium</i> , <i>Amycolatopsis</i> , <i>Kitasatospora</i> , <i>Streptomyces</i> , <i>Actinomadura</i> , <i>Atopobium</i> , <i>Eggerthella</i> , <i>Actinocorallia</i> , <i>Thermoleophilum</i>
<i>Aquificae</i>	1	<i>Sulfurihydrogenibium</i>
<i>Bacteroidetes</i>	45	<i>Bacteroides</i> , <i>Alistipes</i> , <i>Butyricimonas</i> , <i>Candidatus Amoebophilus</i> , <i>Candidatus Azobacteroides</i> , <i>Capnocytophaga</i> , <i>Cellulophaga</i> , <i>Chitinophaga</i> , <i>Coenonia</i> , <i>Cyclobacterium</i> , <i>Cytophaga</i> , <i>Dokdonia</i> , <i>Elizabethkingia</i> , <i>Flammeovirga</i> , <i>Flavobacterium</i> , <i>Flectobacillus</i> , <i>Flexibacter</i> , <i>Flexithrix</i> , <i>Gramella</i> , <i>Hymenobacter</i> , <i>Leeuwenhoekiiella</i> , <i>Microscilla</i> , <i>Myroides</i> , <i>Odoribacter</i> , <i>Ornithobacterium</i> , <i>Parabacteroides</i> , <i>Pedobacter</i> , <i>Persicobacter</i> , <i>Porphyromonas</i> , <i>Prevotella</i> , <i>Prolixibacter</i> , <i>Rhodothermus</i> , <i>Riemerella</i> , <i>Rikenella</i> , <i>Salinibacter</i> , <i>Saprosira</i> , <i>Sphingobacterium</i> , <i>Tannerella</i> , <i>Tenacibaculum</i> , <i>Terrimonas</i> , <i>Wautersiella</i> , <i>Zobellia</i> , <i>Marinilabilia</i> , <i>Chryseobacterium</i> , <i>Barnesiella</i>
<i>Chlamydiae</i>	5	<i>Criblamydia</i> , <i>Candidatus Protochlamydia</i> , <i>Waddlia</i> , <i>Parachlamydia</i> , <i>Chlamydophila</i>
<i>Chlorobi</i>	5	<i>Chlorobaculum</i> , <i>Chlorobium</i> , <i>Chloroherpeton</i> , <i>Prosthecochloris</i> , <i>Pelodictyon</i>
<i>Chloroflexi</i>	7	<i>Chloroflexus</i> , <i>Roseiflexus</i> , <i>Oscillochloris</i> , <i>Herpetosiphon</i> , <i>Dehalococcoides</i> , <i>Sphaerobacter</i> , <i>Thermomicrobium</i>
<i>Cyanobacteria</i>	32	<i>Acaryochloris</i> , <i>Anabaena</i> , <i>Calothrix</i> , <i>Chlorogloeopsis</i> , <i>Chroococciopsis</i> , <i>Cuspidothrix</i> , <i>Cyanothece</i> , <i>Dolichospermum</i> , <i>Fischerella</i> , <i>Geitlerinema</i> , <i>Gloeocapsopsis</i> , <i>Leptolyngbya</i> , <i>Lynngbya</i> , <i>Microcystis</i> , <i>Nodularia</i> , <i>Nostoc</i> , <i>Oscillatoria</i> , <i>Phormidium</i> , <i>Planktothrix</i> , <i>Prochlorococcus</i> , <i>Prochlorothrix</i> , <i>Pseudanabaena</i> , <i>Spirulina</i> , <i>Stanieria</i> , <i>Symploca</i> , <i>Synechococcus</i> , <i>Thermosynechococcus</i> , <i>Xenococcus</i> , <i>Synechocystis</i> , <i>Scytonema</i> , <i>Anabaenopsis</i> , <i>Cyanobacterium</i>
<i>Deferribacteres</i>	2	<i>Denitrovibrio</i> , <i>Flexistipes</i>
<i>Deinococcus-Thermus</i>	4	<i>Deinococcus</i> , <i>Truepera</i> , <i>Meiothermus</i> , <i>Thermus</i>
<i>Firmicutes</i>	39	<i>Alicyclobacillus</i> , <i>Ammonifex</i> , <i>Bacillus</i> , <i>Butyricoccus</i> , <i>Butyrivibrio</i> , <i>Caldicellulosiruptor</i> , <i>Candidatus Desulfurudis</i> , <i>Clostridium</i> , <i>Desulfitibacter</i> , <i>Desulfitobacterium</i> , <i>Desulfonispora</i> , <i>Desulfotomaculum</i> , <i>Dialister</i> , <i>Faecalibacterium</i> , <i>Geobacillus</i> , <i>Halothermothrix</i> , <i>Kurthia</i> , <i>Laceyella</i> , <i>Lactobacillus</i> , <i>Leuconostoc</i> , <i>Phascolarctobacterium</i> ,

		<i>Ruminococcus, Sporanaerobacter, Staphylococcus, Streptococcus, Sulfobacillus, Symbiobacterium, Syntrophomonas, Tissierella, Acetivibrio, Desulfosporosinus, Eubacterium, Lachnospira, Moorella, Oenococcus, Selenomonas, Tepidimicrobium, Thermodesulfobium, Veillonella</i>
<i>Fusobacteria</i>	1	<i>Fusobacterium</i>
<i>Nitrospirae</i>	2	<i>Leptospirillum, Nitrospira</i>
<i>Planctomycetes</i>	6	<i>Candidatus Kuenenia, Blastopirellula, Pirellula, Planctomyces, Rhodopirellula, Isosphaera</i>
<i>Proteobacteria</i>	89	<i>Hyphomicrobium, Acetobacter, Acidiphilium, Acidovorax, Afifella, Alcaligenes, Alkalispirillum, Aquabacterium, Azoarcus, Azospira, Azospirillum, Bdellovibrio, Bordetella, Burkholderia, Caedibacter, Campylobacter, Candidatus Liberibacter, Candidatus Tremblaya, Chondromyces, Chromobacterium, Corallococcus, Dechloromonas, Derrxia, Desulfobacter, Desulfocaldus, Desulfocella, Desulfococcus, Desulfohalobium, Desulfomicrobium, Desulfomonile, Desulfonatronovibrio, Desulfonatrum, Desulfonema, Desulforhabdus, Desulfovibrio, Erythrobacter, Escherichia, Francisella, Gluconobacter, Helicobacter, Hydrogenimonas, Hyphomonas, Kinetoplastibacterium, Kozakia, Legionella, Magnetospirillum, Maricaulis, Marinosulfonomonas, Methylobacillus, Methylobacterium, Methylohalomonas, Methylosinus, Myxococcus, Nitrococcus, Nitrosomonas, Nitrospira, Nitrosovibrio, Novosphingobium, Oxalobacter, Pannonibacter, Paracoccus, Pasteurella, Phaeospirillum, Plesiocystis, Porphyrobacter, Pseudomonas, Ralstonia, Rhodobaca, Rhodobacter, Rhodovulum, Rickettsia, Rubritepida, Rubrivivax, Sorangium, Sphingobium, Sphingopyxis, Syntrophomonas, Syntrophobacter, Thermodesulforhabdus, Thioalkalivibrio, Thiobacter, Thiocapsa, Thiococcus, Thiorhodococcus, Thiorhodospira, Thiothrix, Wolbachia, Xanthomonas, Xylella</i>
<i>Spirochaetes</i>	4	<i>Leptospira, Borrelia, Spirochaeta, Treponema</i>
<i>Tenericutes</i>	4	<i>Acholeplasma, Spiroplasma, Mycoplasma, Candidatus Phytoplasma</i>
<i>Thermotogae</i>	3	<i>Petrotoga, Thermosipho, Thermotoga</i>
<i>Verrucomicrobia</i>	8	<i>Opitutus, Chthoniobacter, Pedosphaera, Akkermansia, Prosthecobacter, Rubritalea, Methylocacidiphilum, Verrucomicrobium</i>

Supplementary Table 31. Microbial genera that were detected¹ in all the three mat communities of the progressively-drying thermal gradient.

Phylum affiliation	VWM	DG3	DG4
Actinobacteria	<u>Thermobispora</u> (0.009%) <u>Thermobifida</u> (0.01%) <u>Tropheryma</u> (0.001%) <u>Saccharopolyspora</u> (0.01%)	<u>Thermobispora</u> (0.02%) <u>Thermobifida</u> (0.04%) <u>Tropheryma</u> (0.004%) <u>Saccharopolyspora</u> (0.04%)	<u>Thermobispora</u> (0.07%) <u>Thermobifida</u> (0.09%) <u>Tropheryma</u> (0.01%) <u>Saccharopolyspora</u> (0.09%)
Aquificae	<u>Sulfurihydrogenibium</u> (21.57%) <u>Persephonella</u> (0.27%)	<u>Sulfurihydrogenibium</u> (0.12%) <u>Persephonella</u> (0.02%)	<u>Sulfurihydrogenibium</u> (0.06%) <u>Persephonella</u> (0.02%)
Bacteroidetes	<u>Alistipes</u> (0.009%) <u>Cytophaga</u> (0.02%)	<u>Alistipes</u> (0.03%) <u>Cytophaga</u> (0.25%)	<u>Alistipes</u> (0.03%) <u>Cytophaga</u> (0.25%)
Chloroflexi	<u>Chloroflexus</u> (0.4%) <u>Roseiflexus</u> (0.89%) <u>Herpetosiphon</u> (0.02%) <u>Dehalococcoides</u> (0.05%) <u>Thermomicrobium</u> (0.02%)	<u>Chloroflexus</u> (4.56%) <u>Roseiflexus</u> (14.73%) <u>Herpetosiphon</u> (0.96%) <u>Dehalococcoides</u> (0.1%) <u>Thermomicrobium</u> (0.13%)	<u>Chloroflexus</u> (7.22%) <u>Roseiflexus</u> (13.62%) <u>Herpetosiphon</u> (2.1%) <u>Dehalococcoides</u> (0.28%) <u>Thermomicrobium</u> (0.35%)
Cyanobacteria	<u>Synechococcus</u> (0.17%) <u>Oscillatoria</u> (0.01%)	<u>Synechococcus</u> (3.09%) <u>Oscillatoria</u> (0.48%)	<u>Synechococcus</u> (1.08%) <u>Oscillatoria</u> (0.18%)
Deinococcus-Thermus	<u>Thermus</u> (50.64%)	<u>Thermus</u> (1.03%)	<u>Thermus</u> (0.44%)
Firmicutes	<u>Bacillus</u> (0.18%) <u>Clostridium</u> (0.27%) <u>Streptococcus</u> (0.03%)	<u>Bacillus</u> (0.525%) <u>Clostridium</u> (0.32%) <u>Streptococcus</u> (0.06%)	<u>Bacillus</u> (0.88%) <u>Clostridium</u> (0.56%) <u>Streptococcus</u> (0.11%)
Proteobacteria	<u>Pseudomonas</u> (0.07%) <u>Thiobacillus</u> (0.02%) <u>Acidithiobacillus</u> (0.01%) <u>Campylobacter</u> (0.08%)	<u>Pseudomonas</u> (0.215%) <u>Thiobacillus</u> (0.04%) <u>Acidithiobacillus</u> (0.03%) <u>Campylobacter</u> (0.04%)	<u>Pseudomonas</u> (1.36%) <u>Thiobacillus</u> (0.05%) <u>Acidithiobacillus</u> (0.05%) <u>Campylobacter</u> (0.05%)
Spirochaetes	<u>Treponema</u> (0.02%)	<u>Treponema</u> (0.1%)	<u>Treponema</u> (0.1%)
Thermotogae	<u>Thermotoga</u> (0.8%) <u>Fervidobacterium</u> (0.16%)	<u>Thermotoga</u> (0.09%) <u>Fervidobacterium</u> (0.03%)	<u>Thermotoga</u> (0.14%) <u>Fervidobacterium</u> (0.04%)

¹ Genera which were identified upon searching the respective metagenomes against the RDP as well as the *nr* protein database have their names underlined; those identified only upon searching against the *nr* protein database (and were not detectable in the RDP search) are not underlined. Mean percentage of all annotable metagenomic reads of the community ascribable to a genus (upon searching against the *nr* protein database) is given in parenthesis after the name of the genus.

Supplementary Table 32. Microbial genera that were detected¹ in all the six mat communities of the wet thermal gradient

	VWM	WG3	WG4	WG5	WG6	WG7
Actinobacteria	<i>Kitasatospora</i> (0.008%)	<i>Kitasatospora</i> (0.009%)	<i>Kitasatospora</i> (0.008%)	<i>Kitasatospora</i> (0.01%)	<i>Kitasatospora</i> (0.01%)	<i>Kitasatospora</i> (0.01%)
	<i>Thermobispora</i> (0.009%)	<i>Thermobispora</i> (0.01%)	<i>Thermobispora</i> (0.02%)	<i>Thermobispora</i> (0.03%)	<i>Thermobispora</i> (0.02%)	<i>Thermobispora</i> (0.03%)
	<i>Thermobifida</i> (0.01%)	<i>Thermobifida</i> (0.02%)	<i>Thermobifida</i> (0.03%)	<i>Thermobifida</i> (0.06%)	<i>Thermobifida</i> (0.04%)	<i>Thermobifida</i> (0.04%)
	<i>Streptomyces</i> (0.03%)	<i>Streptomyces</i> (0.13%)	<i>Streptomyces</i> (0.16%)	<i>Streptomyces</i> (0.27%)	<i>Streptomyces</i> (0.21%)	<i>Streptomyces</i> (0.28%)
	<i>Tropheryma</i> (0.001%)	<i>Tropheryma</i> (0.004%)	<i>Tropheryma</i> (0.003%)	<i>Tropheryma</i> (0.002%)	<i>Tropheryma</i> (0.004%)	<i>Tropheryma</i> (0.004%)
	<i>Propionibacterium</i> (0.01%)	<i>Propionibacterium</i> (0.02%)	<i>Propionibacterium</i> (0.03%)	<i>Propionibacterium</i> (0.03%)	<i>Propionibacterium</i> (0.06%)	<i>Propionibacterium</i> (0.06%)
	<i>Saccharopolyspora</i> (0.01%)	<i>Saccharopolyspora</i> (0.03%)	<i>Saccharopolyspora</i> (0.03%)	<i>Saccharopolyspora</i> (0.05%)	<i>Saccharopolyspora</i> (0.05%)	<i>Saccharopolyspora</i> (0.05%)
Aquificae	<i>Sulfurihydrogenibium</i> (21.57%)	<i>Sulfurihydrogenibium</i> (7.31%)	<i>Sulfurihydrogenibium</i> (6.33%)	<i>Sulfurihydrogenibium</i> (0.04%)	<i>Sulfurihydrogenibium</i> (0.04%)	<i>Sulfurihydrogenibium</i> (0.08%)
	<i>Persephonella</i> (0.27%)	<i>Persephonella</i> (0.1%)	<i>Persephonella</i> (0.1%)	<i>Persephonella</i> (0.01%)	<i>Persephonella</i> (0.02%)	<i>Persephonella</i> (0.03%)
	<i>Hydrogenobaculum</i> (0.28%)	<i>Hydrogenobaculum</i> (0.09%)	<i>Hydrogenobaculum</i> (0.1%)	<i>Hydrogenobaculum</i> (0.01%)	<i>Hydrogenobaculum</i> (0.01%)	<i>Hydrogenobaculum</i> (0.02%)
Bacteroidetes	<i>Alistipes</i> (0.009%)	<i>Alistipes</i> (0.04%)	<i>Alistipes</i> (0.09%)	<i>Alistipes</i> (0.03%)	<i>Alistipes</i> (0.22%)	<i>Alistipes</i> (0.21%)
	<i>Cytophaga</i> (0.02%)	<i>Cytophaga</i> (0.13%)	<i>Cytophaga</i> (0.26%)	<i>Cytophaga</i> (0.2%)	<i>Cytophaga</i> (1.38%)	<i>Cytophaga</i> (0.77%)
	<i>Rhodothermus</i> (0.08%)	<i>Rhodothermus</i> (0.29%)	<i>Rhodothermus</i> (0.36%)	<i>Rhodothermus</i> (0.19%)	<i>Rhodothermus</i> (0.33%)	<i>Rhodothermus</i> (0.43%)
	<i>Salinibacter</i> (0.05%)	<i>Salinibacter</i> (0.17%)	<i>Salinibacter</i> (0.24%)	<i>Salinibacter</i> (0.17%)	<i>Salinibacter</i> (0.26%)	<i>Salinibacter</i> (0.34%)
Chloroflexi	<i>Chloroflexus</i> (0.4%)	<i>Chloroflexus</i> (3.09%)	<i>Chloroflexus</i> (3.5%)	<i>Chloroflexus</i> (6.97%)	<i>Chloroflexus</i> (1.87%)	<i>Chloroflexus</i> (1.26%)
	<i>Roseiflexus</i> (0.89%)	<i>Roseiflexus</i> (20.39%)	<i>Roseiflexus</i> (12.7%)	<i>Roseiflexus</i> (9.86%)	<i>Roseiflexus</i> (2.53%)	<i>Roseiflexus</i> (2.12%)
	<i>Herpetosiphon</i> (0.02%)	<i>Herpetosiphon</i> (0.34%)	<i>Herpetosiphon</i> (0.4%)	<i>Herpetosiphon</i> (1.66%)	<i>Herpetosiphon</i> (0.57%)	<i>Herpetosiphon</i> (0.48%)
	<i>Dehalococcoides</i> (0.05%)	<i>Dehalococcoides</i> (0.08%)	<i>Dehalococcoides</i> (0.1%)	<i>Dehalococcoides</i> (0.13%)	<i>Dehalococcoides</i> (0.08%)	<i>Dehalococcoides</i> (0.11%)
	<i>Thermomicrobium</i> (0.02%)	<i>Thermomicrobium</i> (0.1%)	<i>Thermomicrobium</i> (0.11%)	<i>Thermomicrobium</i> (0.17%)	<i>Thermomicrobium</i> (0.09%)	<i>Thermomicrobium</i> (0.1%)
Cyanobacteria	<i>Synechococcus</i> (0.17%)	<i>Synechococcus</i> (5.09%)	<i>Synechococcus</i> (8%)	<i>Synechococcus</i> (4.74%)	<i>Synechococcus</i> (0.48%)	<i>Synechococcus</i> (1.98%)
	<i>Oscillatoria</i> (0.01%)	<i>Oscillatoria</i> (0.07%)	<i>Oscillatoria</i> (0.12%)	<i>Oscillatoria</i> (0.82%)	<i>Oscillatoria</i> (0.06%)	<i>Oscillatoria</i> (0.32%)
Deinococcus	<i>Thermus</i> (50.64%)	<i>Thermus</i> (7.8%)	<i>Thermus</i> (5.38%)	<i>Thermus</i> (0.23%)	<i>Thermus</i> (0.11%)	<i>Thermus</i> (0.17%)

- Thermus	<u>Meiothermus</u> (2.16%) <u>Deinococcus</u> (0.34%)	<u>Meiothermus</u> (0.57%) <u>Deinococcus</u> (0.17%)	<u>Meiothermus</u> (0.44%) <u>Deinococcus</u> (0.18%)	<u>Meiothermus</u> (0.24%) <u>Deinococcus</u> (0.26%)	<u>Meiothermus</u> (0.13%) <u>Deinococcus</u> (0.16%)	<u>Meiothermus</u> (0.17%) <u>Deinococcus</u> (0.2%)
Firmicutes	<u>Anoxybacillus</u> (0.01%) <u>Alicyclobacillus</u> (0.03%) <u>Bacillus</u> (0.18%) <u>Geobacillus</u> (0.06%) <u>Paenibacillus</u> (0.03%) <u>Lactobacillus</u> (0.05%) <u>Clostridium</u> (0.27%) <u>Leuconostoc</u> (0.01%) <u>Streptococcus</u> (0.03%) <u>Coprothermobacter</u> (0.01%)	<u>Anoxybacillus</u> (0.02%) <u>Alicyclobacillus</u> (0.04%) <u>Bacillus</u> (0.31%) <u>Geobacillus</u> (0.13%) <u>Paenibacillus</u> (0.07%) <u>Lactobacillus</u> (0.06%) <u>Clostridium</u> (0.23%) <u>Leuconostoc</u> (0.01%) <u>Streptococcus</u> (0.05%) <u>Coprothermobacter</u> (0.02%)	<u>Anoxybacillus</u> (0.03%) <u>Alicyclobacillus</u> (0.05%) <u>Bacillus</u> (0.41%) <u>Geobacillus</u> (0.16%) <u>Paenibacillus</u> (0.11%) <u>Lactobacillus</u> (0.08%) <u>Clostridium</u> (0.47%) <u>Leuconostoc</u> (0.01%) <u>Streptococcus</u> (0.06%) <u>Coprothermobacter</u> (0.02%)	<u>Anoxybacillus</u> (0.03%) <u>Alicyclobacillus</u> (0.06%) <u>Bacillus</u> (0.5%) <u>Geobacillus</u> (0.19%) <u>Paenibacillus</u> (0.14%) <u>Lactobacillus</u> (0.08%) <u>Clostridium</u> (0.33%) <u>Leuconostoc</u> (0.01%) <u>Streptococcus</u> (0.07%) <u>Coprothermobacter</u> (0.01%)	<u>Anoxybacillus</u> (0.03%) <u>Alicyclobacillus</u> (0.04%) <u>Bacillus</u> (0.69%) <u>Geobacillus</u> (0.18%) <u>Paenibacillus</u> (0.15%) <u>Lactobacillus</u> (0.09%) <u>Clostridium</u> (0.36%) <u>Leuconostoc</u> (0.01%) <u>Streptococcus</u> (0.08%) <u>Coprothermobacter</u> (0.01%)	<u>Anoxybacillus</u> (0.04%) <u>Alicyclobacillus</u> (0.07%) <u>Bacillus</u> (0.61%) <u>Geobacillus</u> (0.2%) <u>Paenibacillus</u> (0.2%) <u>Lactobacillus</u> (0.1%) <u>Clostridium</u> (0.88%) <u>Leuconostoc</u> (0.01%) <u>Streptococcus</u> (0.09%) <u>Coprothermobacter</u> (0.02%)
Proteobacteria	<u>Pseudomonas</u> (0.07%) <u>Thiobacillus</u> (0.02%) <u>Acidithiobacillus</u> (0.01%) <u>Campylobacter</u> (0.08%)	<u>Pseudomonas</u> (0.67%) <u>Thiobacillus</u> (0.43%) <u>Acidithiobacillus</u> (0.03%) <u>Campylobacter</u> (0.06%)	<u>Pseudomonas</u> (0.19%) <u>Thiobacillus</u> (0.05%) <u>Acidithiobacillus</u> (0.03%) <u>Campylobacter</u> (0.07%)	<u>Pseudomonas</u> (0.3%) <u>Thiobacillus</u> (0.04%) <u>Acidithiobacillus</u> (0.04%) <u>Campylobacter</u> (0.04%)	<u>Pseudomonas</u> (0.35%) <u>Thiobacillus</u> (0.08%) <u>Acidithiobacillus</u> (0.04%) <u>Campylobacter</u> (0.08%)	<u>Pseudomonas</u> (0.53%) <u>Thiobacillus</u> (0.25%) <u>Acidithiobacillus</u> (0.08%) <u>Campylobacter</u> (0.07%)
Spirochaetes	<u>Treponema</u> (0.02%) <u>Borrelia</u> (0.01%)	<u>Treponema</u> (0.06%) <u>Borrelia</u> (0.01%)	<u>Treponema</u> (0.08%) <u>Borrelia</u> (0.03%)	<u>Treponema</u> (0.14%) <u>Borrelia</u> (0.04%)	<u>Treponema</u> (0.05%) <u>Borrelia</u> (0.02%)	<u>Treponema</u> (0.4%) <u>Borrelia</u> (0.05%)
Thermotogae	<u>Thermotoga</u> (0.8%) <u>Thermosiphon</u> (0.12%) <u>Fervidobacterium</u> (0.16%) <u>Petrogona</u> (0.08%)	<u>Thermotoga</u> (0.23%) <u>Thermosiphon</u> (0.06%) <u>Fervidobacterium</u> (0.07%) <u>Petrogona</u> (0.05%)	<u>Thermotoga</u> (0.84%) <u>Thermosiphon</u> (0.14%) <u>Fervidobacterium</u> (0.29%) <u>Petrogona</u> (0.07%)	<u>Thermotoga</u> (0.08%) <u>Thermosiphon</u> (0.03%) <u>Fervidobacterium</u> (0.02%) <u>Petrogona</u> (0.02%)	<u>Thermotoga</u> (0.06%) <u>Thermosiphon</u> (0.03%) <u>Fervidobacterium</u> (0.02%) <u>Petrogona</u> (0.02%)	<u>Thermotoga</u> (0.13%) <u>Thermosiphon</u> (0.06%) <u>Fervidobacterium</u> (0.05%) <u>Petrogona</u> (0.04%)

¹ Genera identified upon searching the metagenomes against RDP as well as nr protein database have their names underlined; those identified only upon searching against the nr protein database (and were not detectable in the RDP search) are not underlined. Mean percentage of all annotable metagenomic reads of the community ascribable to a genus (upon searching against nr protein database) is given in parenthesis after the genus name.

Supplementary Table 33. Microbial genera* comprised primarily of thermophilic species but present even at low-temperature (33-46°C) sites of *Shivlinga*'s thermal gradients.

Phyla	Genera	Temp. range for laboratory growth	References [#]	VWM (66°C)	DG3 (52°C)	DG4 (41°C)	WG3 (56°C)	WG4 (46°C)	WG5 (38°C)	WG6 (36°C)	WG7 (33°C)
<i>Aquificae</i>	<i>Sulfurihydrogenibium</i>	70–40°C	(Takai <i>et al.</i> , 2003)	+	+	+	+	+	–	+	+
	<i>Persephonella</i>	80–55°C	(Gotz <i>et al.</i> , 2002; Nakagawa <i>et al.</i> , 2003)	+	–	+	+	+	–	+	–
	<i>Hydrogenobaculum</i>	80–45°C	(Stohr <i>et al.</i> , 2001)	+	–	–	–	–	–	+	–
<i>Deinococcus–Thermus</i>	<i>Thermus</i>	80–40°C	(Vajna <i>et al.</i> , 2012)	+	+	+	+	+	–	+	+
	<i>Meiothermus</i>	70–35°C	(Chen <i>et al.</i> , 2002; Mori <i>et al.</i> , 2012)	+	–	–	+	+	–	–	+
<i>Dictyoglomi</i>	<i>Dictyoglomus</i>	80–50°C	(Saiki <i>et al.</i> , 1985)	+	–	–	–	+	–	–	–
<i>Thermodesulfobacteria</i>	<i>Thermodesulfobacterium</i>	80–50°C	(Jeanthon <i>et al.</i> , 2002)	+	–	+	+	+	–	–	–
	<i>Thermodesulfatator</i>	80–55°C	(Alain <i>et al.</i> , 2010; Moussard <i>et al.</i> , 2004)	+	–	–	+	+	–	–	–
<i>Thermotogae</i>	<i>Thermotoga</i>	90–55 °C	(Huber <i>et al.</i> , 1986)	+	+	–	+	+	+	+	+
	<i>Thermosipho</i>	80–37°C	(Podosokorskaya <i>et al.</i> , 2011; Urios <i>et al.</i> , 2004)	+	–	–	–	+	–	–	+
	<i>Petrotoga</i>	65–40°C	(Lien <i>et al.</i> , 1998)	–	–	–	–	–	–	–	+

* Identified in RDP searches of the metagenomes. [#] References used in this table have been given in Supplementary references.

Supplementary Table 34. Phylum- or class-level percentage distribution of the total bacterial metagenomic reads¹ identified in the mat samples of the drying thermal gradient.

	VWM 1 st sample	VWM 2 nd sample	VWM average	DG3 1 st sample	DG3 2 nd sample	DG3 average	DG4 1 st sample	DG4 2 nd sample	DG4 average
<i>Acidobacteria</i>	0.12	0.17	0.145	0.84	0.68	0.76	1.16	1.16	1.16
<i>Actinobacteria</i>	0.36	0.42	0.39	1.9	2.41	2.155	5.03	5.02	5.025
<i>Alphaproteobacteria</i>	0.46	0.62	0.54	2.3	2.82	2.56	7.26	7.58	7.42
<i>Aquificae</i>	21.7	33.3	27.5	0.48	0.2	0.34	0.31	0.29	0.3
<i>Bacteroidetes</i>	0.3	0.49	0.395	5.92	3.61	4.765	4.16	4.26	4.21
<i>Betaproteobacteria</i>	0.38	0.52	0.45	1.56	1.82	1.69	2.9	2.71	2.805
<i>Chlamydiae</i>	0.02	0.03	0.025	0.07	0.08	0.075	0.12	0.13	0.125
<i>Chlorobi</i>	0.21	0.36	0.285	16.44	3.42	9.93	4.13	4.01	4.07
<i>Chloroflexi</i>	1.96	1.61	1.785	34.72	30.97	32.845	40.93	40.8	40.865
<i>Cyanobacteria</i>	0.93	0.9	0.915	18.96	38.5	28.73	7.29	8.19	7.74
<i>Deferribacteres</i>	0.08	0.18	0.13	0.1	0.07	0.085	0.11	0.1	0.105
<i>Deinococcus-Thermus</i>	67.4	51.53	59.465	3.34	1.1	2.22	2.61	2.57	2.59
<i>Deltaproteobacteria</i>	1.27	2.48	1.875	2.54	2.72	2.63	3.99	3.97	3.98
<i>Dictyoglomi</i>	0.07	0.15	0.11	0.07	0.05	0.06	0.1	0.11	0.105
<i>Epsilonproteobacteria</i>	0.48	1.00	0.74	0.2	0.22	0.21	0.24	0.25	0.245
<i>Firmicutes</i>	1.7	2.74	2.22	4.9	4.48	4.69	8.23	8.37	8.3
<i>Fusobacteria</i>	0.04	0.08	0.06	0.1	0.09	0.095	0.14	0.15	0.145
<i>Gammaproteobacteria</i>	0.74	1.03	0.885	2.39	3.25	2.82	7.18	6.23	6.705
<i>Gemmatimonadetes</i>	0.01	0.01	0.01	0.11	0.07	0.09	0.12	0.11	0.115
<i>Nitrospirae</i>	0.18	0.4	0.29	0.16	0.12	0.14	0.18	0.17	0.175
<i>Planctomycetes</i>	0.06	0.09	0.075	0.47	0.56	0.515	0.9	0.92	0.91
<i>Spirochaetes</i>	0.07	0.11	0.09	0.42	1.06	0.74	0.54	0.53	0.535

<i>Synergistetes</i>	0.05	0.07	0.06	0.13	0.1	0.115	0.18	0.18	0.18
<i>Tenericutes</i>	0.03	0.03	0.03	0.04	0.03	0.035	0.06	0.07	0.065
<i>Thermotogae</i>	1.17	1.45	1.31	0.27	0.21	0.24	0.39	0.4	0.395
<i>Verrucomicrobia</i>	0.07	0.09	0.08	1.06	0.75	0.91	0.69	0.68	0.69
<i>UnclassifiedBacteria</i>	0.08	0.1	0.09	0.36	0.38	0.37	0.81	0.81	0.81
<i>UnclassifiedProteobacteria</i>	0.03	0.05	0.04	0.04	0.09	0.07	0.1	0.1	0.1
Others², as shown in Fig.5A									
<i>Thermodesulfobacteria</i>	0.01	0.01	0.01	0	0	0	0	0	0
<i>Elusimicrobia</i>	0.01	0.01	0.01	0.02	0.02	0.02	0.02	0.02	0.02
<i>Chrysiogenetes</i>	0.01	0.01	0.01	0.02	0.02	0.02	0.03	0.03	0.03
<i>Lentisphaerae</i>	0	0.01	0.005	0.03	0.03	0.03	0.04	0.04	0.04
<i>Fibrobacteres</i>	0	0.02	0.01	0.02	0.02	0.02	0.02	0.02	0.02
<i>Poribacteria</i>	0	0	0	0.01	0.01	0.01	0.02	0.02	0.02
<i>Zetaproteobacteria</i>	0	0.01	0.005	0.01	0.01	0.01	0.02	0.02	0.02

¹Reads were searched by BlastX against the *nr* protein database with minimum alignment length of 45 bp (15 amino acids) and minimum identity cutoff of 60%.

²Other include bacterial phyla or proteobacterial classes contributing <0.1% reads in all the six metagenomic datasets.

Supplementary Table 35. Phylum- or class-level percentage distribution of the total bacterial metagenomic reads¹ identified in the mat samples of the wet thermal gradient.

	WG3 1 st sample	WG3 2 nd sample	WG3 Avg.	WG4 1 st sample	WG4 2 nd sample	WG4 Avg.	WG5 1 st sample	WG5 2 nd sample	WG5 Avg.	WG6 1 st sample	WG6 2 nd sample	WG6 Avg.	WG7 1 st sample	WG7 2 nd sample	WG7 Avg.
<i>Acidobacteria</i>	0.61	0.74	0.675	0.68	0.71	0.695	0.77	0.7	0.74	0.82	0.9	0.86	2.98	2.49	2.74
<i>Actinobacteria</i>	1.31	1.46	1.385	1.74	1.63	1.685	2.7	2.64	2.67	2.09	2.3	2.195	2.76	2.46	2.61
<i>Alphaproteobacteria</i>	1.53	1.75	1.64	1.77	1.79	1.78	3	2.9	2.95	8.55	10.87	9.71	11.89	8.8	10.35
<i>Aquificae</i>	9.54	13.35	11.445	8.95	10.48	9.715	0.2	0.19	0.2	0.2	0.19	0.2	0.31	0.35	0.33
<i>Bacteroidetes</i>	2.68	3.73	3.205	4.87	6.22	5.545	3	3.65	3.33	52.3	47.66	49.98	14.97	18.39	16.68
<i>Betaproteobacteria</i>	2.31	2.46	2.385	1.47	1.45	1.46	1.9	1.83	1.87	3.19	3.6	3.4	10.06	6.89	8.48
<i>Chlamydiae</i>	0.06	0.08	0.07	0.08	0.09	0.085	0.09	0.08	0.09	0.13	0.14	0.14	0.16	0.18	0.17
<i>Chlorobi</i>	3.36	4.12	3.74	7.57	8.82	8.195	2.99	3.5	3.25	2.41	2.41	2.41	6.44	7.7	7.07
<i>Chloroflexi</i>	39.06	33.38	36.22	30.19	22.5	26.345	34.28	31.51	32.9	8.98	8.92	8.95	8.07	6.78	7.43
<i>Cyanobacteria</i>	13.27	12.05	12.66	18.84	19.71	19.275	35.02	37.09	36.06	3.17	3.58	3.38	13.4	17.73	15.57
<i>Deferribacteres</i>	0.11	0.17	0.14	0.27	0.43	0.35	0.07	0.07	0.07	0.1	0.1	0.1	0.16	0.17	0.17
<i>Deinococcus-Thermus</i>	13.01	10.64	11.825	7.94	8.05	7.995	1.28	1.25	1.27	0.7	0.7	0.7	0.97	0.87	0.92
<i>Deltaproteobacteria</i>	2.36	3.08	2.72	2.97	3.53	3.25	2.86	2.83	2.85	2.69	2.84	2.77	6.54	6.13	6.34
<i>Dictyoglomi</i>	0.07	0.1	0.085	0.22	0.35	0.285	0.06	0.06	0.06	0.05	0.04	0.05	0.08	0.09	0.09
<i>Epsilonproteobacteria</i>	0.38	0.55	0.465	0.42	0.57	0.495	0.2	0.2	0.2	0.39	0.41	0.4	0.36	0.41	0.39
<i>Firmicutes</i>	3.34	4.34	3.84	4.64	5.34	4.99	4.88	4.58	4.73	4.54	4.64	4.59	6.46	6.87	6.67
<i>Fusobacteria</i>	0.09	0.11	0.1	0.11	0.17	0.14	0.08	0.09	0.09	0.16	0.16	0.16	0.18	0.21	0.2
<i>Gammaproteobacteria</i>	3.77	4.04	3.905	2.85	2.83	2.84	3.22	3.28	3.25	5.33	5.73	5.53	7.04	6.52	6.78
<i>Gemmatimonadetes</i>	0.07	0.07	0.07	0.08	0.08	0.08	0.08	0.06	0.07	0.09	0.08	0.09	0.18	0.16	0.17
<i>Nitrospirae</i>	0.17	0.24	0.205	0.37	0.58	0.475	0.14	0.12	0.13	0.11	0.13	0.12	0.22	0.22	0.22
<i>Planctomycetes</i>	0.34	0.42	0.38	0.39	0.41	0.4	0.56	0.56	0.56	1.4	1.67	1.54	2.03	1.82	1.93
<i>Spirochaetes</i>	0.34	0.45	0.395	0.54	0.76	0.65	0.93	1.09	1.01	0.39	0.4	0.4	1.59	1.69	1.64
<i>Synergistetes</i>	0.1	0.12	0.11	0.14	0.17	0.155	0.11	0.1	0.105	0.09	0.1	0.1	0.23	0.22	0.23
<i>Tenericutes</i>	0.03	0.05	0.04	0.05	0.06	0.055	0.04	0.03	0.035	0.06	0.06	0.06	0.05	0.06	0.06
<i>Thermotogae</i>	0.48	0.66	0.57	1.58	2	1.79	0.22	0.23	0.225	0.18	0.18	0.18	0.35	0.38	0.37
<i>Verrucomicrobia</i>	1.16	1.3	1.23	0.72	0.68	0.7	0.7	0.75	0.725	1.14	1.42	1.28	1.54	1.5	1.52
<i>unclassified Bacteria</i>	0.28	0.33	0.305	0.35	0.35	0.35	0.43	0.4	0.415	0.47	0.47	0.47	0.55	0.51	0.53
<i>unclassified Proteobacteria</i>	0.05	0.06	0.055	0.05	0.06	0.055	0.09	0.09	0.09	0.07	0.07	0.07	0.13	0.12	0.125

Others², as shown in Fig.5B															
<i>Thermodesulfobacteria</i>	0	0	0	0	0	0	0	0	0	0	0	0	0	0	0
<i>Elusimicrobia</i>	0.02	0.03	0.025	0.04	0.06	0.05	0.02	0.01	0.015	0.02	0.03	0.025	0.04	0.04	0.04
<i>Chrysiogenetes</i>	0.02	0.03	0.025	0.03	0.03	0.03	0.02	0.02	0.02	0.02	0.02	0.02	0.05	0.05	0.05
<i>Lentisphaerae</i>	0.02	0.03	0.025	0.03	0.03	0.03	0.04	0.03	0.035	0.08	0.09	0.085	0.11	0.1	0.105
<i>Zetaproteobacteria</i>	0.01	0.02	0.015	0.01	0.02	0.015	0.02	0.01	0.015	0.02	0.02	0.02	0.04	0.04	0.04
<i>Fibrobacteres</i>	0.01	0.02	0.015	0.02	0.02	0.02	0.02	0.02	0.02	0.03	0.02	0.025	0.04	0.04	0.04
<i>Poribacteria</i>	0.01	0.01	0.01	0.01	0.01	0.01	0.02	0.02	0.02	0.02	0.02	0.02	0.02	0.02	0.02

¹ Reads were searched by BlastX against the *nr* protein database with minimum alignment length of 45 bp (15 amino acids) and minimum identity cutoff of 60%.

² Other include bacterial phyla or proteobacterial classes contributing <0.1% reads in all the ten metagenomic datasets.

Supplementary Table 36. The contingency table that was used to determine by Chi-square test whether individual COG-counts under different metabolic/functional categories¹ across the eight communities were significantly high or low.

Functional categories	VWM	DG3	DG4	WG3	WG4	WG5	WG6	WG7
J	7.7	7.4	7.0	7.8	8.9	7.0	7.6	7.7
K	4.1	4.0	4.5	3.6	4.1	4.0	4.3	4.7
L	10.1	8.3	7.6	10.3	7.7	7.8	9.9	7.8
D	1.4	1.2	1.2	1.5	1.4	1.3	1.3	1.4
V	2.9	2.8	2.9	2.6	2.3	2.9	3.1	2.8
T	7.3	9.8	10.3	7.2	7.5	10.8	7.8	8.3
M	9.6	10.2	10.2	9.6	10.5	9.9	9.5	10.2
N	1.0	0.6	0.6	0.9	1.5	0.4	0.7	1.0
U	1.9	1.8	1.7	1.9	2.0	1.7	2.1	2.1
O	5.9	6.2	6.1	6.2	6.4	6.1	6.0	6.3
C	9.5	9.1	8.7	10.0	9.6	8.9	8.5	9.4
G	7.4	7.5	7.3	7.1	7.5	8.1	7.1	6.9
E	10.3	10.0	10.1	10.3	9.9	10.0	10.5	9.8
F	3.9	3.6	3.3	3.9	3.8	3.4	3.5	3.5
H	4.6	4.9	4.5	4.9	4.8	4.6	4.2	4.4
I	3.7	3.7	3.8	3.6	3.7	3.4	3.8	3.8
P	7.1	7.1	8.0	7.1	6.7	7.4	7.7	7.9
Q	1.7	1.9	2.3	1.6	1.5	2.1	2.2	2.0

¹ **One-letter codes used to indicate the various metabolic/functional categories:** **J**, Translation; ribosomal structure and biogenesis; **K**, Transcription; **L**, Replication; recombination and repair; **D**, Cell cycle control; cell division; chromosome partitioning; **V**, Defense mechanisms; **T**, Signal transduction mechanisms; **M**, Cell wall/membrane/envelope biogenesis; **N**, Cell motility; **U**, Intracellular trafficking; secretion; and vesicular transport; **O**, Posttranslational modification; protein turnover; chaperones; **C**, Energy production and conversion; **G**, Carbohydrate transport and metabolism; **E**, Amino acid transport and metabolism; **F**, Nucleotide transport and metabolism; **H**, Coenzyme transport and metabolism; **I**, Lipid transport and metabolism; **P**, Inorganic ion transport and metabolism; **Q**, Secondary metabolites biosynthesis; transport and catabolism.

Supplementary References

Supplementary references used in Table 2 of the main text and the Supplementary Table 33.

Alain K, Postec A, Grinsard E, Lesongeur F, Prieur D, Godfroy A. *Thermodesulfatator atlanticus* sp. nov., a thermophilic, chemolithoautotrophic, sulfate-reducing bacterium isolated from a Mid-Atlantic Ridge hydrothermal vent. *Int J Syst Evol Microbiol.* 2010;60:33-38.

Kumar P, Srinivas TN, Thiel V, Tank M, Sasikala C, Ramana Ch V, et al. *Thiohalocapsa marina* sp. nov., from an Indian marine aquaculture pond. *Int J Syst Evol Microbiol.* 2009;59:2333-2338.

Bernardet JF, Bowman JP. Flavobacterium. *Bergey's Manual of Systematics of Archaea and Bacteria.* John Wiley and Sons: Chichester, UK. 2015.

Briand JF, Leboulanger C, Humbert JF, Bernard C, Dufour P. *Cylindrospermopsis raciborskii* (cyanobacteria) invasion at mid-latitudes: selection, wide physiological tolerance, orglobalwarming. *J Phycol.* 2004;40:231-238.

Brinkhoff T, Muyzer G, Wirsén CO, Kuever J. *Thiomicrospira chilensis* sp. nov., a mesophilic obligately chemolithoautotrophic sulfuroxidizing bacterium isolated from a Thioploca mat. *Int J Syst Bacteriol.* 1999;49:875-879.

Castenholz RW. Phylum BX. Cyanobacteria. In: Boone DR, Castenholz RW (eds). *Bergey's Manual of Systematic Bacteriology.* Springer: New York. 2001;473-599.

Chang YH, Han JI, Chun J, Lee KC, Rhee MS, Kim YB, et al. *Comamonas koreensis* sp. nov., a non-motile species from wetland in Woopo, Korea. *Int J Syst Evol Microbiol.* 2002;52:377-381.

Chen MY, Lin GH, Lin YT, Tsay SS. *Meiothermus taiwanensis* sp. nov., a novel filamentous, thermophilic species isolated in Taiwan. *Int J Syst Evol Microbiol.* 2002;52:1647-1654.

Christensen P. Description and Taxonomic Status of *Cytophaga heparina* (Payza and Korn) comb. nov. (Basionym: *Flavobacterium heparinum* Payza and Korn 1956). *Int J Syst Bacteriol.* 1980;30:473-475.

Clavel T, Duck W, Charrier C, Wenning M, Elson C, Haller D. *Enterorhabdus caecimuris* sp. nov., a member of the family Coriobacteriaceae isolated from a mouse model of spontaneous colitis, and emended description of the genus *Enterorhabdus* Clavel *et al.* 2009. *Int J Syst Evol Microbiol.* 2010;60:1527-1531.

- Evans NJ, Brown JM, Demirkan I, Murray RD, Birtles RJ, Hart CA, et al. *Treponema pedis* sp. nov., a spirochaete isolated from bovine digital dermatitis lesions. *Int J Syst Evol Microbiol.* 2009;59:987-991.
- Gotz D, Banta A, Beveridge TJ, Rushdi AI, Simoneit BR, Reysenbach AL. *Persephonella marina* gen. nov., sp. nov. and *Persephonella guaymasensis* sp. nov., two novel, thermophilic, hydrogen-oxidizing microaerophiles from deep-sea hydrothermal vents. *Int J Syst Evol Microbiol.* 2002;52:1349-1359.
- Han X, Zheng J, Xin D, Xin Y, Wei X, Zhang J. *Streptomyces albiflavescens* sp. nov., an actinomycete isolated from soil. *Int J Syst Evol Microbiol.* 2015;65:1467-1473.
- Hatamoto M, Kaneshige M, Nakamura A, Yamaguchi T. *Bacteroides luti* sp. nov., an anaerobic, cellulolytic and xylanolytic bacterium isolated from methanogenic sludge. *Int J Syst Evol Microbiol.* 2014;64:1770-1774.
- Hirschler-Rea A, Matheron R, Riffaud C, Moune S, Eatock C, Herbert RA, et al. Isolation and characterization of spirilloid purple phototrophic bacteria forming red layers in microbial mats of Mediterranean salterns: description of *Halorhodospira neutriphila* sp. nov. and emendation of the genus *Halorhodospira*. *Int J Syst Evol Microbiol.* 2003;53:153-163.
- Hosoya S, Yokota A. Reclassification of *Flexibacter aggregans* (Lewin 1969) Leadbetter 1974 as a later heterotypic synonym of *Flexithrix dorothae* Lewin 1970. *Int J Syst Evol Microbiol.* 2007;57:1086-1088.
- Huber R, Langworthy T, König H, Thomm M, Woese C, Sleytr U, et al. *Thermotoga maritima* sp. nov. represents a new genus of unique extremely thermophilic eubacteria growing up to 90°C. *Arch Microbiol.* 1986;144:324-333.
- Imelfort M, Parks D, Woodcroft BJ, Dennis P, Hugenholtz P, Tyson GW. GroopM: an automated tool for the recovery of population genomes from related metagenomes. *Peer J.* 2014;2:e603.
- Imhoff JF, Suling J, Petri R. Phylogenetic relationships among the Chromatiaceae, their taxonomic reclassification and description of the new genera *Allochromatium*, *Halochromatium*, *Isochromatium*, *Marichromatium*, *Thiococcus*, *Thiohalocapsa* and *Thermochromatium*. *Int J Syst Bacteriol.* 1998;48:1129-1143.
- Jeanthon C, L'Haridon S, Cueff V, Banta A, Reysenbach AL, Prieur D. *Thermodesulfobacteriumhydrogeniphilum* sp. nov., a thermophilic, chemolithoautotrophic, sulfate-reducing bacterium isolated from a deep-sea hydrothermal vent at Guaymas Basin, and emendation of the genus *Thermodesulfobacterium*. *Int J Syst Evol Microbiol.* 2002;52:765-772.

- Kang DD, Froula J, Egan R, Wang Z. MetaBAT, an efficient tool for accurately reconstructing single genomes from complex microbial communities. *PeerJ*. 2015;3:e1165.
- Kelly DP, Wood AP. Reclassification of some species of *Thiobacillus* to the newly designated genera *Acidithiobacillus* gen. nov., *Halothiobacillus* gen. nov. and *Thermithiobacillus* gen. nov. *Int J Syst Evol Microbiol*. 2000;50:511-516.
- Kim YO, Kong HJ, Park S, Kang SJ, Kim KK, Moon DY, et al. *Paracoccusfistulariae* sp. nov., a lipolytic bacterium isolated from bluespotted cornetfish, *Fistularia commersonii*. *Int J Syst Evol Microbiol*. 2010;60:2908-2912.
- Koussemon M, Combet-Blanc Y, Patel BK, Cayol JL, Thomas P, Garcia JL, et al. *Propionibacteriummicroaerophilum* sp. nov., a microaerophilic bacterium isolated from olive mill wastewater. *Int J Syst Evol Microbiol*. 2001;51:1373-1382.
- Koziel M, O'Doherty P, Vandamme P, Corcoran GD, Sleator RD, Lucey B. *Campylobactercorcagiensis* sp. nov., isolated from faeces of captive lion-tailed macaques (*Macaca silenus*). *Int J Syst Evol Microbiol*. 2014;64:2878-2883.
- Li H, Durbin R. Fast and accurate short read alignment with Burrows-Wheeler transform. *Bioinformatics* (Oxford, England) . 2009;25:1754-1760.
- Li H, Handsaker B, Wysoker A, Fennell T, Ruan J, Homer N, et al. The Sequence Alignment/Map format and SAMtools. *Bioinformatics* (Oxford, England). 2009;25:2078-2079.
- Lien T, Madsen M, Rainey FA, Birkeland NK. *Petrotogamobilis* sp. nov., from a North Sea oil-production well. *Int J Syst Bacteriol*. 1998;48:1007-1013.
- Mori K, Iino T, Ishibashi J, Kimura H, Hamada M, Suzuki K. *Meiothermushypogaeus* sp. nov., a moderately thermophilic bacterium isolated from a hot spring. *Int J Syst Evol Microbiol*. 2012;62:112-117.
- Moussard H, L'Haridon S, Tindall BJ, Banta A, Schumann P, Stackebrandt E, et al. *Thermodesulfatatorindicus* gen. nov., sp. nov., a novel thermophilic chemolithoautotrophic sulfate-reducing bacterium isolated from the Central Indian Ridge. *Int J Syst Evol Microbiol*. 2004;54:227-233.
- Nakagawa S, Takai K, Horikoshi K, Sako Y. *Persephonellahydrogeniphila* sp. nov., a novel thermophilic, hydrogen-oxidizing bacterium from a deep-sea hydrothermal vent chimney. *Int J Syst Evol Microbiol*. 2003;53:863-869.
- Parks DH, Imelfort M, Skennerton CT, Hugenholtz P, Tyson GW. CheckM: assessing the quality of microbial genomes recovered from isolates, single cells, and metagenomes. *Genome Res*. 2015;25:1043-1055.

- Podosokorskaya OA, Kublanov IV, Reysenbach AL, Kolganova TV, Bonch-Osmolovskaya EA. *Thermosiphon affectus* sp. nov., a thermophilic, anaerobic, cellulolytic bacterium isolated from a Mid-Atlantic Ridge hydrothermal vent. *Int J Syst Evol Microbiol.* 2011;61:1160-1164.
- Rautio M, Eerola E, Vaisanen-Tunkelrott ML, Molitoris D, Lawson P, Collins MD, et al. Reclassification of *Bacteroides putredinis* (Weinberg *et al.*, 1937) in a new genus *Alistipes* gen. nov., as *Alistipes putredinis* comb. nov., and description of *Alistipes finegoldii* sp. nov., from human sources. *Syst Appl Microbiol.* 2003;26:182-188.
- Rooney AP, Dunlap CA, Flor-Weiler LB. *Acinetobacter lactuca* sp. nov., isolated from iceberg lettuce (Asteraceae: *Lactuca sativa*). *Int J Syst Evol Microbiol.* 2016;66:3566-3572.
- Saiki T, Kobayashi Y, Kawagoe K, Beppu T. *Dictyoglomus thermophilum* gen. nov., sp. nov., a Chemoorganotrophic, Anaerobic, Thermophilic Bacterium. *Int J Syst Bacteriol.* 1985;35:253-259.
- Schleifer KH, Schüler D, Spring S, Weizenegger M, Amann R, Ludwig W, et al. The Genus *Magnetospirillum* gen. nov. Description of *Magnetospirillum gryphiswaldense* sp. nov. and Transfer of *Aquaspirillum magnetotacticum* to *Magnetospirillum magnetotacticum* comb. nov. *Syst Appl Microbiol.* 1991;14:379-385.
- Shah HN, Collins MD. Proposal for Reclassification of *Bacteroides asaccharolyticus*, *Bacteroides gingivalis*, and *Bacteroides endodontalis* in a New Genus, *Porphyromonas*. *Int J Syst Evol Microbiol.* 1988;38:128-131.
- Sherman JM, Stark P. Streptococci which grow at high temperatures. *J. Bacteriol.* 1931;22:275-285.
- Shida O, Takagi H, Kadowaki K, Nakamura LK, Komagata K. Transfer of *Bacillus alginolyticus*, *Bacillus chondroitinus*, *Bacillus curdolanolyticus*, *Bacillus glucanolyticus*, *Bacillus kobensis*, and *Bacillus thiaminolyticus* to the genus *Paenibacillus* and emended description of the genus *Paenibacillus*. *Int J Syst Bacteriol.* 1997;47:289-98.
- Smythe L, Adler B, Hartskeerl RA, Galloway RL, Turenne CY, Levett PN, et al. Classification of *Leptospiragenomospecies* 1, 3, 4 and 5 as *Leptospira alstonii* sp. nov., *Leptospira vanthielii* sp. nov., *Leptospira terpstrae* sp. nov. and *Leptospira yanagawae* sp. nov., respectively. *Int J Syst Evol Microbiol.* 2013;63:1859-1862.
- Sorokin DY, Tourova TP, Muyzer G, Kuenen GJ. *Thiohalospirahalophila* gen. nov., sp. nov. and *Thiohalospira alkaliphila* sp. nov., novel obligately chemolithoautotrophic, halophilic, sulfur-oxidizing gammaproteobacteria from hypersaline habitats. *Int J Syst Evol Microbiol.* 2008;58:1685-1692.

Stohr R, Waberski A, Volker H, Tindall BJ, Thomm M. *Hydrogenothermusmarinus* gen. nov., sp. nov., a novel thermophilic hydrogen-oxidizing bacterium, recognition of *Calderobacteriumhydrogenophilum* as a member of the genus *Hydrogenobacter* and proposal of the reclassification of *Hydrogenobacteracidophilus* as *Hydrogenobaculumacidophilum* gen. nov., comb. nov., in the phylum 'Hydrogenobacter/Aquifex'. Int J Syst Evol Microbiol. 2001;51:1853-1862.

Subhash Y, Sasikala C, Ramana Ch V. *Hymenobacterroseus* sp. nov., isolated from sand. Int J Syst Evol Microbiol. 2014;64:4129-4133.

Sucharita K, Kumar ES, Sasikala C, Panda BB, Takaichi S, Ramana Ch V. *Marichromatiumfluminis* sp. nov., a slightly alkaliphilic, phototrophic gammaproteobacterium isolated from river sediment. Int J Syst Evol Microbiol. 2010;60:1103-1107.

Sun W, Dong GX, Zhang YQ, Wei YZ, Li QP, Yu LY, et al. *Actinoplanes sichuanensis* sp. nov. and *Actinoplanes xinjiangensis* sp. nov. Int J Syst Evol Microbiol. 2009;59:2763-2768.

Takai K, Kobayashi H, Neelson KH, Horikoshi K. *Sulfurihydrogenibium subterraneum* gen. nov., sp. nov., from a subsurface hot aquifer. Int J Syst Evol Microbiol. 2003;53:823-827.

Tully JG, Whitcomb RF, Rose DL, Bove JM, Carle P, Somerson NL, et al. *Acholeplasmabrassicae* sp. nov. and *Acholeplasmapalmae* sp. nov., two non-sterol-requiring mollicutes from plant surfaces. Int J Syst Bacteriol. 1994;44:680-684.

Urios L, Cueff-Gauchard V, Pignet P, Postec A, Fardeau ML, Ollivier B, et al. *Thermosiphonatlanticus* sp. nov., a novel member of the *Thermotogales* isolated from a Mid-Atlantic Ridge hydrothermal vent. Int J Syst Evol Microbiol. 2004;54:1953-1957.

Vajna B, Kanizsai S, Keki Z, Marialigeti K, Schumann P, Toth EM. *Thermuscomposti* sp. nov., isolated from oyster mushroom compost. Int J Syst Evol Microbiol. 2012;62:1486-1490.

Wang MQ, Sun L. *Pseudomonas oceani* sp. nov., isolated from deep seawater. Int J Syst Evol Microbiol. 2016;66:4250-4255.

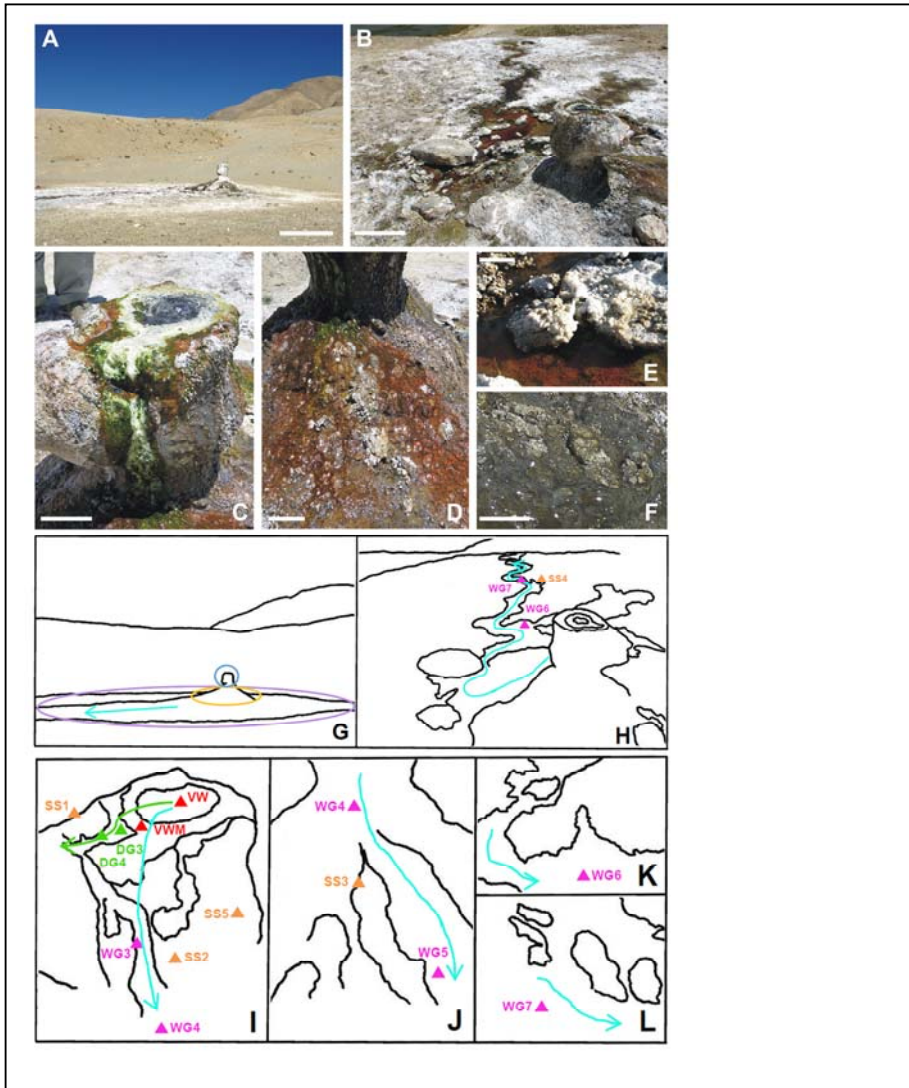
Wells JM, Raju BC, Hung HY, Weisburg WG, Mandelco-Paul L, Brenner DJ. *Xylellafastidiosa* gen. nov., sp. nov.: Gram-Negative, Xylem-Limited, Fastidious Plant Bacteria Related to *Xanthomonas* spp. Int J Syst Evol Microbiol. 1987;37:136-143.

Wolfgang WJ, Carpenter AN, Cole JA, Gronow S, Habura A, Jose S, et al. *Neisseriawadsworthii* sp. nov. and *Neisseriashayeganii* sp. nov., isolated from clinical specimens. Int J Syst Evol Microbiol. 2011;61:91-98.

Wood AP, Kelly DP, McDonald IR, Jordan SL, Morgan TD, Khan S, et al. A novel pink-pigmented facultative methylotroph, *Methylobacteriumthiocyanatum* sp. nov., capable of growth on thiocyanate or cyanate as sole nitrogen sources. Arch Microbiol. 1998;169:148-158.

Zhang Z, Wang Y, Ruan J. A proposal to revive the genus *Kitasatospora* (Omura, Takahashi, Iwai, and Tanaka 1982). Int J Syst Bacteriol. 1997;47:1048-1054.

Figure 1



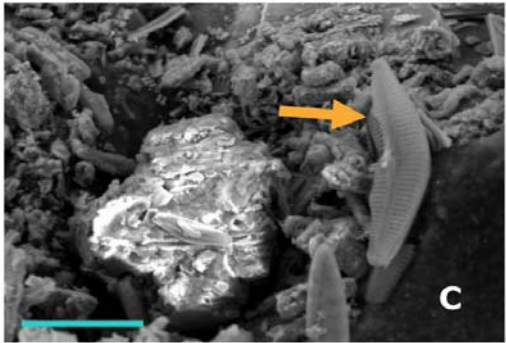
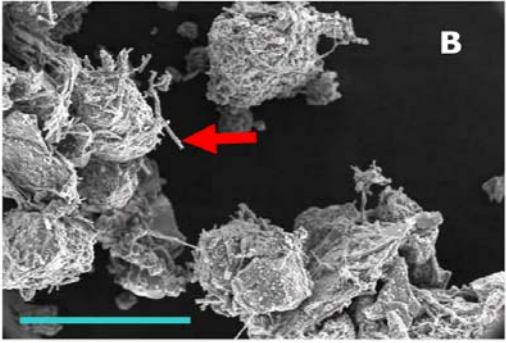
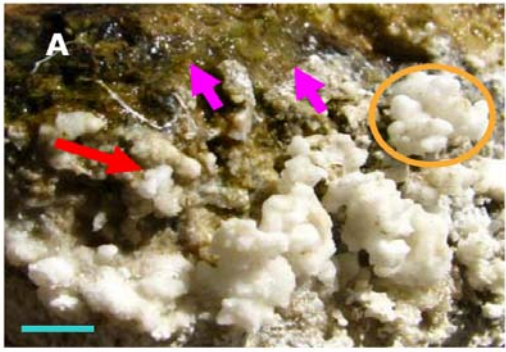


Figure 2

Figure 3

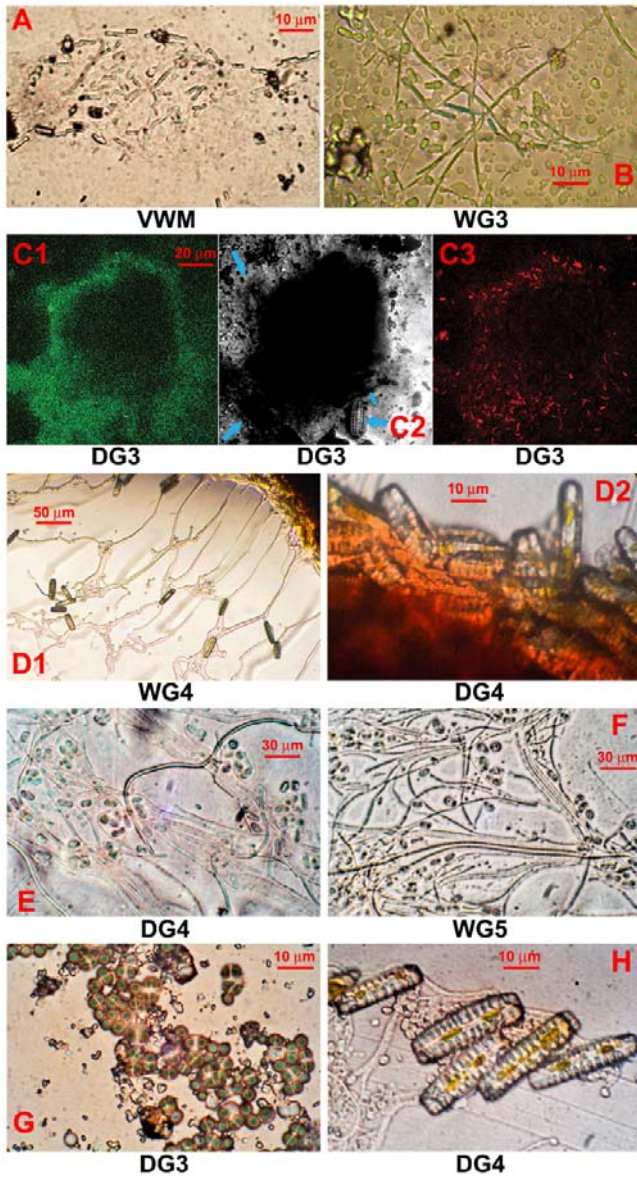


Figure 4

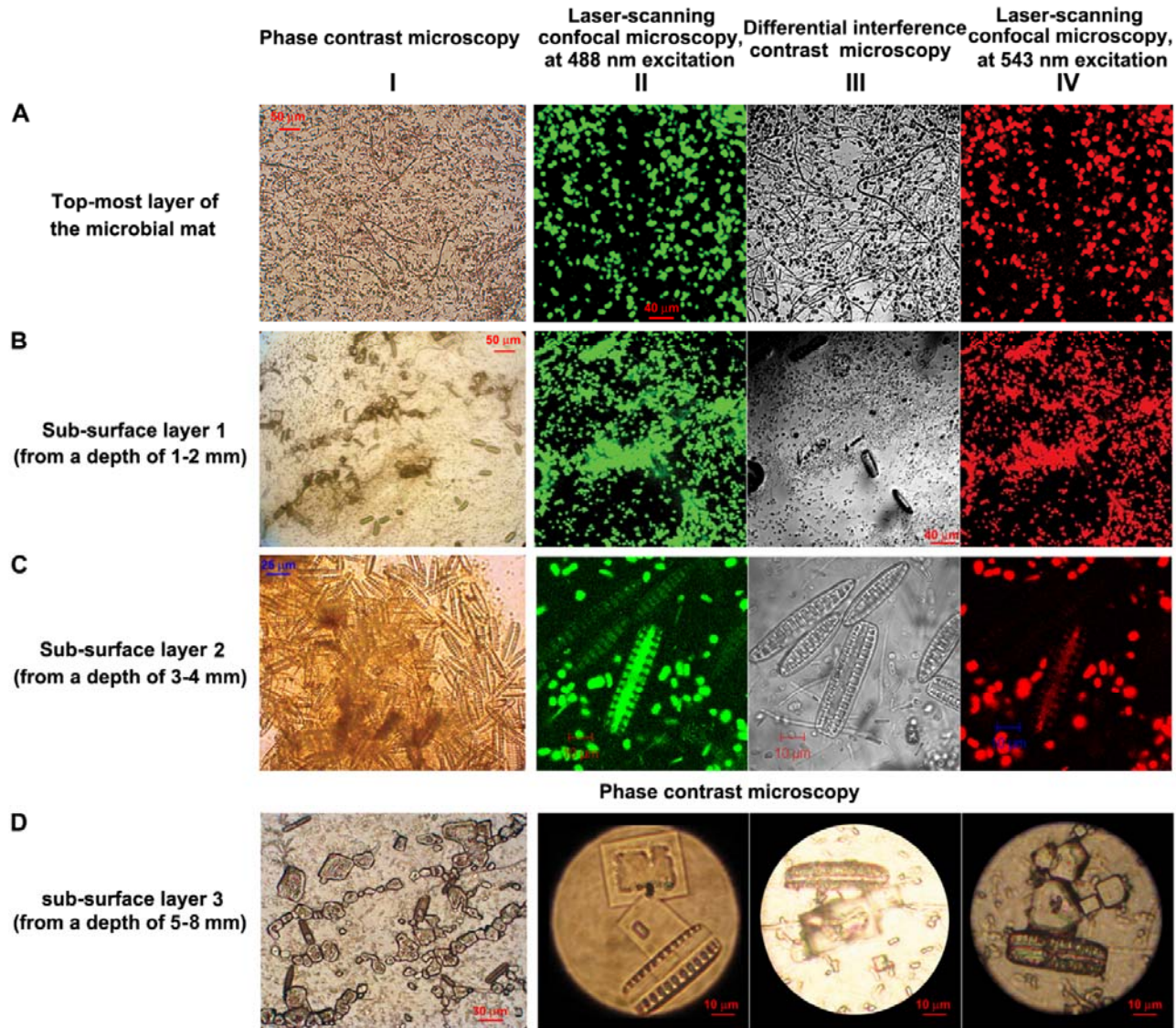
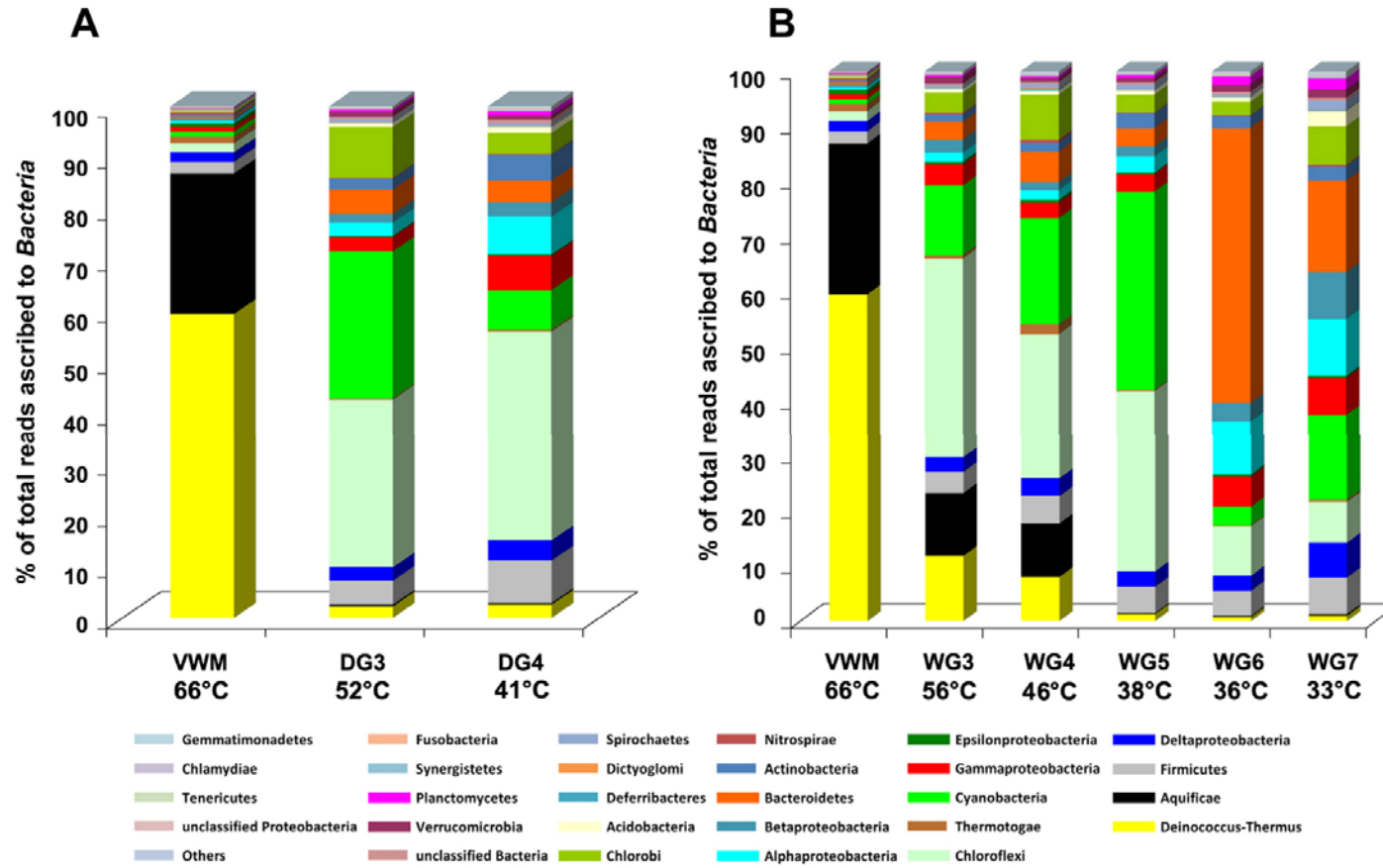


Figure 5



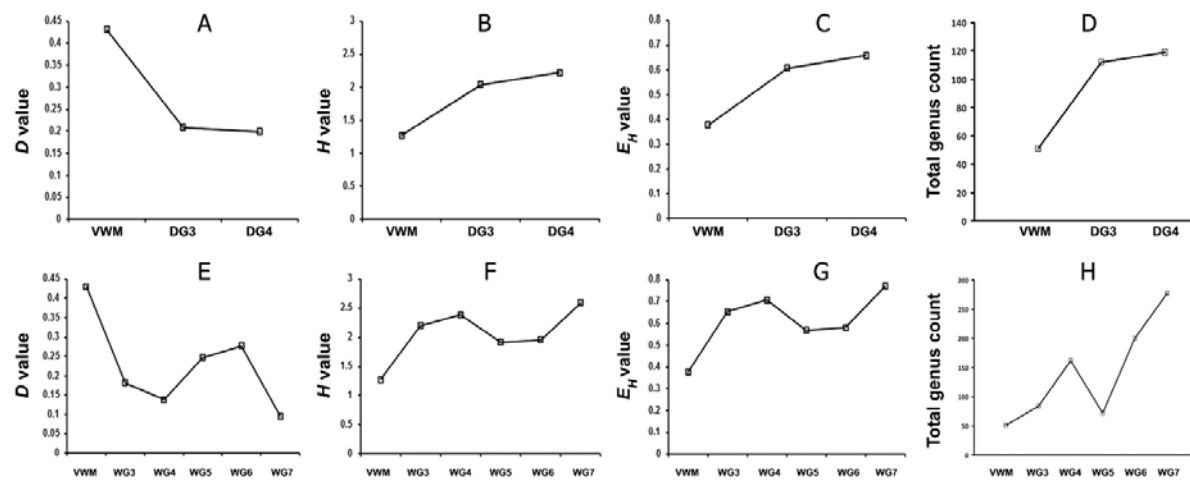


Figure 6

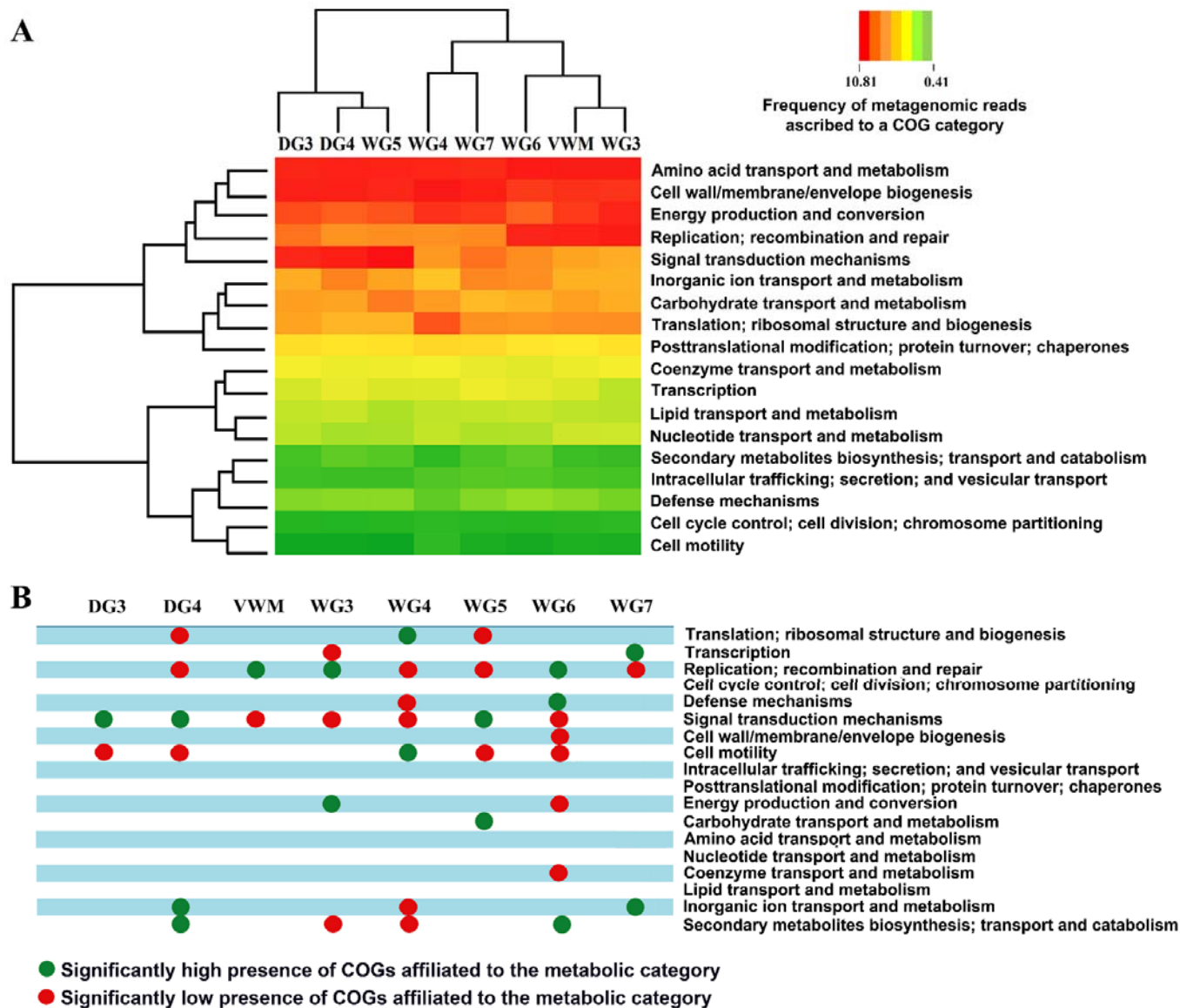


Figure 7